ALMA MATER STUDIORUM - UNIVERSITÀ DI BOLOGNA

SCUOLA DI INGEGNERIA ED ARCHITETTURA

DIPARTIMENTO DI INGEGNERIA DELL'ENERGIA ELETTRICA E DELL'INFORMAZIONE "GUGLIELMO MARCONI" - DEI

CORSO DI LAUREA IN INGEGNERIA DELL'ENERGIA ELETTRICA LM

TESI DI LAUREA

in

Tecnologie Elettriche Innovative M

Dielectric Spectroscopy as a condition monitoring diagnostic technique for thermally aged PVC/EPR nuclear power plant cables

CANDIDATO:
Mario Vincenzo Imperatore

RELATORE:
Prof. Davide Fabiani

CORRELATORI:
Prof. Nicola Bowler
Prof. Andrea Cavallini

Anno Accademico 2015/2016
Sessione III

Alla mia famiglia
ovunque essa sia.

Abstract in lingua italiana

I cavi in bassa tensione costituiscono il *sistema nervoso* di una centrale nucleare, avendo ruolo fondamentale nel garantire l'operazione in sicurezza di essa. Questi, infatti, hanno il compito, durante tutta la vita, di sopportare quelle sollecitazioni comunemente presenti negli ambienti nucleari, come elevate temperature, elevati livelli di radiazione, presenza di umidità e di particelle contaminanti, sollecitazioni meccaniche. Queste sollecitazioni causano degradazione dei materiali.

In particolare sono isolamenti e guaine a subire maggiormente questo effetto, diventando sempre meno elastici e sempre meno in grado di funzionare con affidabilità in sicurezza.

A causa delle catastrofiche conseguenze di un eventuale incidente nucleare, e soprattutto nella recente intenzione di prolungare la vita di una centrale nucleare da 40 fino a 60-80 anni, diverse tecniche diagnostiche vengono studiate ed applicate a questi sistemi. I gestori, infatti, hanno l'obbligo di dimostrare che i componenti siano ancora in grado di assolvere le proprie funzioni, e numerosi studi hanno come obbiettivo la valutazione delle effettive condizioni di questi.

Metodi basati sull'analisi di proprietà meccaniche come l'allungamento a rottura (EaB) vengono comunemente utilizzati per questo scopo, ma questa tecnica richiede la rimozione e la successiva distruzione della sezione di cavo sotto esame.

Per questo motivo, altre tecniche non distruttive sono oggetto di studi. Tecniche come l'analisi termogravimetrica (TGA), la spettroscopia in trasfor-

mata di Fourier (FTIR), la misura di carica spaziale, e la spettroscopia dielettrica, stanno diventando sempre più diffuse in questo campo.

Fra queste, la spettroscopia dielettrica si è dimostrata essere un'ottima tecnica diagnostica per valutare lo stato di cavi in bassa tensione per centrali nucleari. Questa tesi, quindi, mira a contribuire agli studi sulla spettroscopia dielettrica come metodo diagnostico, con particolare attenzione all'aspetto non distruttivo.

Infatti questo lavoro di tesi, svolto presso l'Iowa State University (USA), mostrerà come sia possibile misurare le proprietà dielettriche di cavi multipolari (tre conduttori) isolati in EPR e ricoperti da una guaina in PVC, senza che essi debbano essere distrutti; e come queste proprietà mostrino un'effettiva variazione con le condizioni di invecchiamento.

I punti focali di questo lavoro saranno tre: i) il *background* teorico, che mostra come e perchè la spettroscopia dielettrica possa essere ottimo indicatore diagnostico; ii) la ricerca, tramite simulazioni numeriche, della migliore connessione al provino, visto come un condensatore costituito da quattro elettrodi e da tre dielettrici; iii) l'analisi dei risultati sperimentali, che mostreranno come capacità e fattore di dissipazione aumentino con il tempo di invecchiamento, e come questo aumento preceda la riduzione dell'allungamento a rottura.

Grazie alla non invasività della tecnica, che richiede l'asportazione di pochi millimetri di materiale dai provini, i cavi in esame potranno, ipoteticamente, essere reinseriti nella propria ubicazione originale. Un ulteriore sviluppo di questo lavoro potrebbe essere, con appositi giunti ed appositi strumenti di misura, l'estensione di questa tecnica a misure su cavi in funzione così che non sia necessaria la disconnessione del cavo, ma sia possibile effettuare queste misure a distanza, ad intervalli regolari per avere un quadro generale delle condizioni dei cavi elettrici del sistema.

Summary

A typical boiling water reactor (BWR) requires approximately 95 km of power cables, 80 km of control cables, and 400 km of instrument cables. In the containment building of a pressurized water reactor (PWR) almost 1600 km of cables could be installed.

This amount typically consists in low-voltage, unshielded, multi-polar cables. Function of these is wide: for power transmission, control of equipment, control of instrumentation, communication of signals and data.

Low voltage cables are the *nervous system* of a Nuclear Power Plant (NPP), having a crucial role in granting its safe operation. These have the task, during the whole service life, to withstand stresses commonly present in the harsh environment of the NPPs, which consists in a wide range of environmental conditions and stresses involving temperature, radiation, contaminants, humidity and bending; moreover a particularly grave environment can be found inside the containment area. High temperatures lead to thermal oxidation in the presence of oxygen, as a result of chain scission or cross-linking. Gamma radiation, the most relevant among radiation stresses, causes oxidative degradation.

Among all the sub-components, insulation and jacket materials effectively exhibit the most significant degradation. Degradation mechanisms cause polymers to become more and more brittle thus no more useful as cable electrical isolation, requiring good thermal, mechanical, and electrical properties.

The relatively low-level radiation and elevated operating temperatures

suggest to focus on the temperature-induced degradation.

Because of the catastrophic consequences of a nuclear accident, Condition Monitoring diagnostics has always been held in high regard. In the recent expectation of extending NPP service life from 40 up to 60-80 years, utilities must show that the components can still perform their safety function(s), and many studies are dedicated to the assessment of the NPP cables state. In addition, proper assessment is needed because replacing the whole quantity of cables would be a severe cost burden.

Effectively, methods based on tensile tests such as Elongation at Break or Young's Modulus, are widely used to assess integrity and function, and typically NPP cables are changed every 40 years. Mechanical properties are intrusive and destructive diagnostic methods, i.e. they require the removal and the destruction of the cable section from its original position to perform the diagnostic measurement.

The advantage in using EaB and other mechanical properties lies in their effective correlation with ageing. Nevertheless, the disadvantage presented by the use of destructive techniques, is driving to search for other properties which can play the role of ageing markers.

For this reason, other techniques, Destructive or Non-Destructive, are becoming widely studied also. These techniques include Thermogravimetric Analysis (TGA), Fourier Transform Infrared Spectroscopy (FTIR) as well as electrical techniques such as voltage withstand measurement, space charge measurement, and dielectric spectroscopy.

Among these, dielectric spectroscopy has proven itself an excellent diagnostic technique to assess the state of low-voltage NPP cables but literature regarding the effect of ageing on electrical properties of low-voltage insulation is still lacking an the long term relation between physical/chemical degradation mechanism and electrical property variations have not been studied in detail for low-voltage cable materials. Especially for intact, multi-polar cables.

Therefore this thesis aims at contributing to the studies about the impact

of ageing on cable electrical parameters, in order to understand the evolution of these with cable degradation.

This thesis work, conducted at the Iowa State University in Ames, USA, in particular, has the purpose to perform dielectric spectroscopy measurements on thermally-aged, whole, intact, three-polar, low voltage cable samples.

With a special consideration to the Non-Destructive aspect, philosophy of this method is that the assessment of cable state can be carried out without the need to destroy the cable section during the measurement, as it happens for techniques like EaB, so that it can be put back in its original position after the measurement. According to this philosophy, furthermore, a potential continuation in this subject could be the extension of this method to on-line measurements, with proper methods, which would mean also loosing the need to interrupt NPP service to assess cable state.

Contents

Chapter 1

Introduction on nuclear power plant cable ageing management

Aim of this thesis is to contribute to Condition Monitoring diagnostics on low-voltage electric cables, extensively used for several functions inside nuclear power plants (NPPs).

These cables are exposed to a wide range of environmental conditions and stresses: temperature, radiation, humidity, contaminants, mechanical bending, responsible of material degradation. This is particularly true for those cables inside the containment area; these aspects will be extensively faced in this chapter.

A large fraction of these cables is safety-related and its functions often consist in directly supporting the safe operation of the NPP.

The nuclear safety-related cables have a lead role in granting the safe operation of the NPP: they have to be able to support the function of safety-related equipment during normal operating conditions, anticipated operational occurrences, and design basis accidents[1] (DBA), namely accidents in-

[1]A Design-basis accident is defined as a "A postulated accident that a nuclear facility must be designed and built to withstand without loss to the systems, structures, and components necessary to ensure public health and safety." [5].

cluding loss-of-coolant accident (LOCA[2]), main steam line break (MSLB[3]), and high energy line break (HELB[4]), for the entire time they are in service.

Therefore the life assessment of cable systems is a crucial matter, above all in the expectation of extending NPP service life from 40 up to 60-80 years.

This, together with the lack of literature regarding the effect of ageing on electrical properties of low-voltage insulation, justifies the reason to focus on NPP cables as potentially means to improve safety inside NPPs.

Additional cable system components such as connectors can also cause problems in ageing nuclear power plants, causing erratic signals, noise, measurement errors, spikes, or other anomalies that can interfere with the safe and efficient plant operation. These components will not be object of this work.

To begin this task, the types of cables commonly present inside NPPs will be now extensively exposed, together with the description of the common stresses and ageing mechanisms they activate in the polymeric materials composing the cables.

[2]Loss of coolant accident (LOCA) is the postulated accident that result in a loss of reactor coolant at a rate in excess of the capability of the reactor makeup system from breaks in the reactor coolant pressure boundary, up to and including a break equivalent in size to the double-ended rupture of the largest pipe of the reactor coolant system [5].

[3]Main steam line break (MSLB) may occurr after the rupture of one steam line upstream of the main steam isolation valves, it is characterised by significant space-time effects in the core caused by asymmetric cooling and an assumed stuck-out control rod after the reactor trip [7].

[4]High energy line break (HELB) is a sudden break in the high energy pipelines which, during normal conditions, are at 95 °C (maximum) and 1,900 kPa (maximum). It may cause jet impingement on surrounding targets, waterhammer and environmental effects such as flooding and spray wetting.

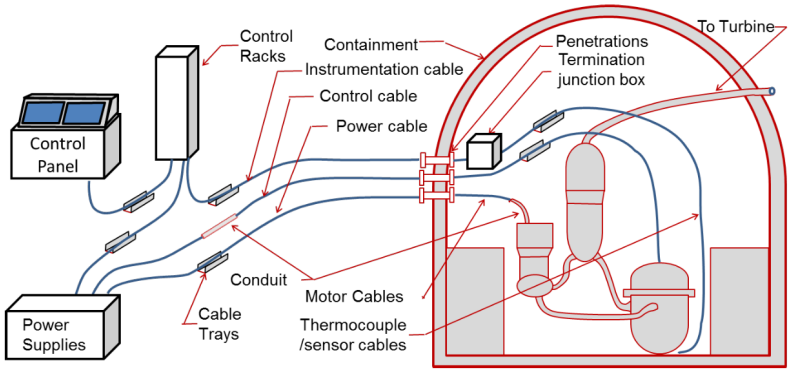

Figure 1.1: Typical cable layout in a NPP electric system [11].

1.1 Overview on nuclear power plant cables

Cables in nuclear power plants can be sorted according to:

Application: power, control of equipment, instrumentation, thermocouple, communication, speciality configuration, safety related, or non-safety related;

Voltage: low ($\leqslant$ 2 kV), medium ($\leqslant$ 2-46 kV), or high ($>$ 46 kV);

Environment: normal operating temperature (60 °C), high temperature (75-100 °C), fire/flame retardant, high radiation, submerged/water, or aggressive solvents;

Design: single/multi-conductor, triplex, thermocouple alloys, coaxial, shielded/unshielded, special jacket, conductor/shield material, or insulation/jacket material.

Typically, the total length of the whole cable amount is between 757 km, in a boiling water reactor (BWR) NPP, and 1600 km, in the containment building of a pressurized water reactor (PWR) NPP. A BWR typically requires 95 km of power cables, 80 km of control cables, 400 km of instrument cables.

Design and materials depend on the specific application of the cable, these

may overlap but interchanging different types for different applications is not normally permitted.

Although some special cable constructions (coaxial, triaxial, mineral-insulated) are used in nuclear power plants, the predominant type is a low-voltage, unshielded, multi-conductor cable.

Cables are normally contained in raceway not sealed from the environment, making them exposed to the environment.

Low voltage power cables supply power to low voltage auxiliary devices commonly composing a NPP such as motors, motor control centers, heaters, and small transformers. These are usually unshielded and may be single conductor or multi-conductor, from four to eight. Power cables conductor diameters are usually 2 mm and larger, these carry continuous or intermittent currents, and voltages up to 600 volts. The auxiliaries they connect operate at nominal voltages of 600, 480 and 208 volts (three phase), or 277, 240 and 120 volts (single phase); or in addition 250 and 125 volts (DC). Medium voltage power cables have different ageing mechanisms and ageing issues [4], and will not be object of the study.

Control cables are commonly used to interconnect the control components of a system, such as solenoid operated valves, relays, limit switches and control switches. These typically provide the feed-back signal path for component status and carry low voltage and low currents. These are often made by multi-conductors cables and include shielding for application near high voltage systems, which could easily distort the low signal control cables are carrying.

Control cables conductor diameters are typically from 1.6 to 2 mm, at 120-240 volts (AC) or 125 volts (DC); low-voltage digit signals are used also. Nominal voltage of control circuit is generally 120 volts (AC) or 125/250 volts (DC), occasionally 24/48 volts (DC) also [9].

There is no significant distinction between power and control cables: the design and materials used for these two overlap, although current levels in control cables applications are much lower than in power cables: below few

amperes.

Instrumentation cables normally carry low voltage and low current analogue or digital signals. Typical instrumentation cables connect resistance temperature detectors (RTDs), pressure transmitters, thermocouples. Cables for this function are normally composed of twisted pairs and are shielded. In addition, radiation detection and neutron monitoring circuits may use coaxial or triaxial shielded configurations. The common need is to improve their electro-magnetic immunity (EMI). Instrumentation cables conductors are typically 1.6 mm or lower, nominal currents are in the range between microampere and milliampere.

As explained in section 3.1, cables object of the study are suitable for power and control circuits.

The typical components of NPP low voltage cables, in particular for LV power cables and I&C (instrument and control), are described below.

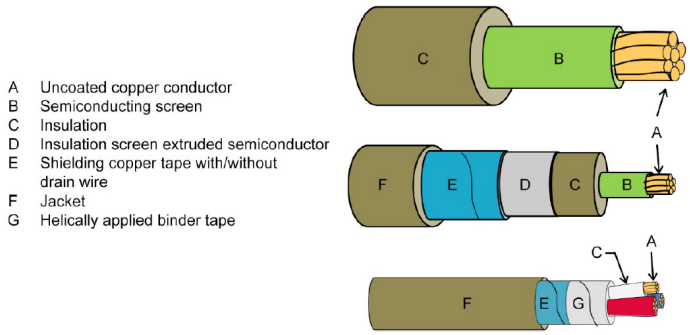

Figure 1.2: Configurations of cable designs typically used in NPPs [11].

1.1.1 Conductors

Conductors are normally made of copper and aluminium. Particularly annealed copper is the most used due to its relatively high and thermal conductivity, good ductility and malleability, reasonable cost and strength. Copper is often coated with tin, tin-lead alloy, pure lead, nickel, or silver

coating thick up to 1.3 micrometers. This is to minimize oxidation, enhance solderability and allow operation at higher conductor temperatures. Tinned copper is favoured for ease of making connections. Cable conductors are normally made of stranded wires, when flexibility is needed, or of solid wires, when strength is needed. Inside the contemplated environment, metallic conductors are relatively insensitive to ageing and related degradation.

1.1.2 Electrical insulation

Cable conductors are typically insulated with a material with high electrical resistivity and high dielectric breakdown voltage. Furthermore, it should be resistant to water, chemicals, abrasion and heat, in order to be safely compatible with NPP environments. To fulfil this, materials are not pure, but they're enhanced with additives such as fillers, plasticizers, accelerators and vulcanizing agents to enhance their electrical and physical properties. Role of fillers will be deepened in subsection 1.1.5.

A wide range of organic polymeric materials, amorphous or semi-crystalline ones, is used for cable insulation, this include:

- polyethylene (PE);
- silicone rubber (SiR);
- ethylene-propylene copolymer (EPR) and terpolymer (EPDM);
- ethylene-vinyl acetate (EVA);

and relative blends.

Speciality cables may user use other insulation materials such as polyether ether ketone (PEEK). Where both temperature and radation are high, inorganic mineral insulation (MI) or polymide film (Kapton) is typically used (Kapton whistands temperature and radiation above 262 °C and 100 GGy

[9]).

Organic polymers are among the "weak links" so far as ageing is concerned, especially in an oxygen environment where oxidative degradation can be induced.

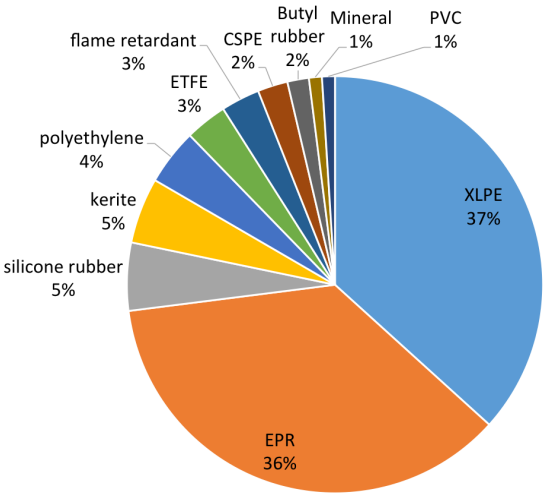

Figure 1.3: Main insulation materials used inside U.S. nuclear power plants [7].

These insulation materials, except silicon rubber, are rated for 90 °C for continuous temperature, 130 °C for emergency temperature, and 250 °C for short-circuit maximum temperature. Silicon rubber compounds are the predominant insulating materials used in high temperature environments and they are rated for continuous operation at 125 - 125 °C [9].

1.1.3 Jacket

A jacket (or sheath) is added to cover cables and provide physical protection and mechanical strength. Jacket material is usually selected based on the environment in which the cable is to be used and, as for insulation, materials used for jackets are not pure but enriched with additives, also selected on the basis of the expected environment.

Typically, cable jackets are made of similar materials used as cable insulation but, in addition, other materials such as chlorosulfonated polyethylene (CSPE, also known as Hypalon), polychloroprene (CR, also known as Neoprene) or polyvinylchloride (PVC) are used as well. In order to minimize the release of halogens in the event of fire, PVC jackets are becoming infrequently used in the design of cables for NPPs. Hypalon has slightly better characteristics than Neoprene and shows good stability and excellent resistance to moisture. In some cables, particularly control and low voltage power cables, a jacketing layer over the insulation of the individual conductors, is provided for fire retardancy.

While installed cables with intact insulation may well be able to continue to provide safe operation with degraded jacket material, the tendency of jacketing materials to degrade more readily than insulation materials enables their use as lead indicators for local stress prior to insulation degradation and failure.

1.1.4 Shielding

Shielding may be used in cables to provide increased immunity to noise and electromagnetic/radio frequency interferences (EMI/RFI). This is particularly necessary for cables carrying small signal informations. Shielding reduces information crosstalk between adjacent circuits also.

These cables may have foil shielding and/or braided shielding. Foil shields are typically thin layers of aluminium bonded to polyester films (e.g. Mylar). A drain wire is sometimes used in conjunction with the foil shield to connect the shield to the ground (fig. 1.2). Braided shields are usually made of copper or aluminium.

This shield also constitutes a tape barrier between cable's inner conductor(s) and jacket: it may prevent cracks in the jacket from propagating into and through the conductor insulation, contributing to the mechanical strength of the whole cable.

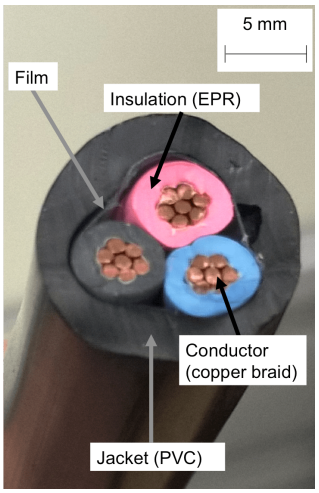

Figure 1.4: Section of the cable object of this work.

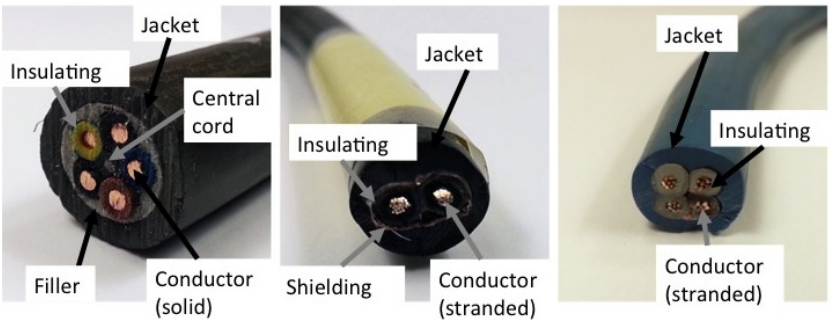

Figure 1.5: Exampls of nuclear power plant cable design [8].

1.1.5 Polymers additives

Task of additives, such as fillers, plasticizers, accelerators and vulcanizing agents, is to enhance their electrical and physical properties, namely to enhance cables resistance to environmental stresses [8]. Flame retardants are the most abundant additives and can constitute more than 50% of the material weight. Due to the hygroscopic nature of these, they may significantly affect electrical properties, and due to their abundance this modification should be taken into account.

Flame retardant cable materials can be divided into non-halogen and halogen-containing flame retardants. In general:

- inorganic flame retardants, such as metal hydroxides, like aluminium hydroxide (ATH) and magnesium hydroxide. Other compounds like zinc borate are used as well;
- phosphorous based flame retardants comprise mainly organic and inorganic phosphorus compounds with different oxidation states;
- nitrogen-based flame retardants are typically melamine and melamine derivatives used in combination with phosphorus-based flame retardants.

Antioxidants are compounds that can act at different stages of the oxidation process. A combination of two types of antioxidants, playing the role of radical trap and hydroperoxide decomposer, is commonly used to inhibit the oxidative process at more than one step. Hindred amines and phenols are examples of alkoxy and peroxy radical trap antioxidants. During ageing, antioxidants get consumed and no longer protect the polymer. Combinations of phenolic antioxidants with phosphites and thiosynergists are often used. The phosphite antioxidant reacting with hydroperoxide becomes oxidized to phosphate while the peroxide is reduced to alcohol or other harmless functional group. In addition, peroxide decomposing antioxidants are thought to be capable of reacting with the consumed phenolic antioxidant to regenerate its protective action.

This explains how a combination of two antioxidants can improve antioxidant effectiveness and provide longer service lifetimes.

Antioxidants improve thermal and radiation stability, but their effect is not linear: even if the stabilization against radiation ageing increases at large doses as the amount of antioxidant is increased, a minimum concentration of oxidation is required to have a significant protection. Furthermore, this effect saturates: an excess content of antioxidant does not contribute to reducing more the degradation rate.

Lubricants are composed by metal stearates, fatty acids, acid esters or alcohols, esters, paraffin waxes, amides or a combination of these. They are

added to reduce the shear rate during the manufacture process, particularly if inorganic fillers are present.

Plasticizers are added to improve flexibility and softness of wires and cables. They are chemically and thermally stable; their addition also enhances the material stability and reduces the degradation rate of the host polymer.

The colour of wires and cables is given by organic or inorganic pigments; dyes are available in the form of powder, liquid, as well as concentrate resins. Usually, a mixture of several dyes is required, comprising titanium dioxide or iron oxide.

In addition to the above specified components, other additives are also used, like stabilizers, initiators, curing agents, etc. Effectively, most of the technically relevant polymers need appropriate stabilization by additives since damaging effects through the impact of heath, shear and ultraviolet light occur during high temperature processing in the melt and service of polymers later on. Specific stabilizers and stabilizer combinations are therefore required to inhibit, or at least retard, a variety of undesired effects such as oxidation, chain scission, uncontrolled recombination, and cross-linking reactions.

Among the total amount of polymer additives -excluding fillers and pigments- less than 10% is dedicated to polymer stabilizers, which are commonly used in concentration from some parts per million to about 1% of the related polymer. Except polyvinylchloride (PVC), roughly 80% of the polymer stabilizers are used with polyolefins.

Sufficient compatibility of stabilizers in polymer matrices is highly an important factor for their applicability and determines significantly their performance.

Stabilizers typically consists of antioxidants and acid scavengers. Additives are added to the polymer melt directly in the reactor or later during the compounding step by feeding into the extruder. Organo(III) phosphites and organo(III) phosphonites are widely used and act during polymer processing in the melt as hydroperoxide-decomposing agents and fall under the

definition "secondary antioxidants". These additives help to maintain basic physical properties such as molecular weight and color during processing. Such so-called "secondary antioxidants" are usually added in combination (blends) with other additives like sterically hindered phenols and acid scavengers [10].

Summarizing, the chemical composition of insulation and sheath comprises a lot of constituents of various nature and concentrations. The composition of insulation and sheath materials usually remains trade secret and is undisclosed by cable manufacturers [8].

The influence of additives should never be neglected: the plastics industry is continuously developing new polymeric materials and indispensable properties of plastic materials can only be achieved by optimal adjustment of the additive package to the specified requirements.

There are approximately three dozen manufacturers in the United States who have supplied safety-related electric cables to nuclear power plants. While the materials used in cables from these different manufacturers may be of the same generic polymer, those can have very different ageing characteristics due to variations in the manufacturing process used. These variations can occur not only among manufacturers, but also among cables from the same manufacturer. Variations can be caused by differences in the chemical composition of materials supplied to the manufacturer, or by differences in the curing process used in manufacturing the material. They can also be caused by the use of different additives in the material formulation.

Therefore one should effectively expect a different behaviour to the one investigated on the pristine polymer. This different behaviour is expected also among the three insulators, made with the same material but with different dyes.

Importance given to additive package, and its unknown composition, should suggest to take into account Condition Monitoring diagnostics when dealing with insulating polymers.

1.2 Stressing agents inside NPP

Stressing agents constituting the typical environment inside a nuclear power plant can generally be divided into three groups [11]:

Environmental: radiation, heat, moisture, contaminating chemicals, etc;

Operational: high voltage, electrical transients, ohmic heating, flexing/vibration, mechanical damage, etc;

Error-induced damage from inappropriate design/selection for the given environment or operational stressors above, and manufacturing or maintenance deficiencies.

One of the factor the intensity of these agents typically depends from, is position. For instance, regarding dose rate distribution, radiation zone maps are established when a plant is constructed, but for older plant this is not always available. Furthermore, the dose rate distribution may change during the operation years of the NPP.

It is possible to discriminate between three different environments within nuclear power plants [9] and three corresponding environmental conditions:

- service conditions: 2 MGy and 60 °C. Actually most service conditions are between 35 and 60 °C, and between 0.2 and 1 MGy;
- high temperature conditions: 2 MGy and 75-100 °C. Typical examples are the zone in the vicinity of pressurized electric heaters in a PWR and in certain high elevations in the drywell of a BWR, for components such as continuously energized solenoids;
- high radiation-high temperature: 2,000 MGy and 75-125 °C. It is the typical condition in the immediately adjacency to the reactor vessel. Typical instruments exposed to these conditions are neutron detectors, reactor head cabling, and other reactor instrumentation.

Stress factors are usually continuous in time, but may vary in intensity depending on external events, such as climate changes, plant events, hazards.

Generally these combined stressors act synergistically and lead to material degradation. This increases the probability of cracking under mechanical stresses and the inability of the cable to fulfil its safety tasks.

The principal concerns for adverse environments experienced by polymers-insulated/jacketed electrical cables in the NPPs are the elevated temperatures, the gamma radiation exposure, and the presence of moisture or other chemical environmental stresses, such as contact with lubricants. For many of the polymers of interest in cables, oxidation is the main degradation mechanism. The initiation of the phenomenon can either be temperature or radiation, but the combination of both acts in synergy.

1.2.1 Temperature

Thermal ageing is caused by ambient room temperature, localized high temperature (hot spots) or radiant heat, and ohmic heating. The main effect is material embrittlement (fig. 3.5c). Although the ambient room in most the power plant leads to a very slow degradation of cable, relatively rapidly severe damage can be produced by localized elevated temperature or radiant heat from sources such as adjacent process lines or inadequate ventilation (dead air spaces). Other hot spots can be constituted by steam pipes or high temperature equipment such as heaters, energized solenoid valves.

Hot spots effects are often located in circumscribed zones of the cable. Nevertheless, within hot spots, because the rate of material degradation is higher than everywhere else, localized embrittlement can lead to localized cracking, which might expand to the whole cable.

Temperature ageing is further emphasized when ohmic losses add, and when cables are sprayed with flame retardant solutions, preventing cables from dissipating internal heat (self heating). Ohmic losses have to be contemplated only when dealing with power cables, the higher is the current,

the greater is the rate of heat generation[5]. Typically ohmic losses effects the entire length of a cable run but can be more severe in proximity of circumscribed bad connections (constituting hot spots).

1.2.2 Radiation

There are four radiation types in a nuclear power plant: alpha, beta, gamma, and neutron. While cables in general may be exposed to any combination of these inside reactor containment, gamma is the principal type that has to be accounted [9].

The radiation tolerance of an individual material will vary depending on chemical structure of it, including the additive package. Usually Hypalon, XLPE and EPR can withstand a significantly higher total dose than PVC, which begins to exhibit degradation when subjected to a total dose of 10^4 Gy. In general, cable materials exposed to a total gamma dose of less than approximately 10^3 Gy will experience little or no radiation ageing effects. The most common effect of radiation is hardening, but butyl rubber softens instead [12].

1.2.3 Mechanical and chemical stresses

Sometimes cable bending effects cannot be neglected for as the cable is bent, the outer edge is subject to tensile stresses whereas the inner section is under compressive stress. If the bend is of a sufficiently small radius, the elongation capability of the aged material can be exceeded and cracks can be initiated to rapidly propagate to the overall cable.

This stressor is particularly severe for terminations/connections, during maintenance or testing, but negligible for the residual sections, never disturbed after installation.

[5]The rate of heat generation follows Joule's law $P = RI_{rms}^2 \quad [W]$.

Ozone chemical-attacks significantly affect only polymers containing high proportions of double bonds in the molecular chains. Among the polymers commonly used in cables insulation and jacket (subsections 1.1.2 and 1.1.3), only some of the EPR materials diene-containing terpolymers (such as EPDM), are likely to be exposed to ozone [8].

Moisture is particularly significant for BWR systems. Typically relative humidity in PWR systems is between 10 % and 100 %, 80 % on average. In BWR systems relative humidity is between 20% and 90 %, 45 % on average. The main effect of moisture is the acceleration of the degradation rate [9].

Moisture within cable insulation has a significant effect on the electrical properties of the cable, which becomes more conductive and thus dielectric losses increase. Little is known of its effect on changes in the mechanical properties [8]. A severe effect of moisture is the formation of conductive paths between conductor and ground, or conductor or conductor, encouraged by the presence of conducting contaminants. This leads to surface discharges, causing surface hot spots and surface degradation.

1.3 Degradation mechanisms

Material ageing is the irreversible, often slow, change of at least one of the properties of a material submitted to its environment during its operational life, which can lead to the functional failure of the material itself. One should highlight the irreversibility of the mentioned changes, for ageing has to be distinguished from the transient changes due to a temporary external stress. This properties irreversible change is the macroscopic consequence of ageing.

Typically one observes:

a) a decrease in the tensile elongation of the material, often associated with a decrease in tensile strength;

b) an increase in the hardness or Young's modulus, particularly for materials used for jackets;

c) increase in the density;

d) changes in the electrical properties, such as increases in dielectric losses.

Typically changes in electrical properties are not large and loss of cable functionality is usually determined by the changes in mechanical properties. But, for example, PVC may fail electrically during a DBE test before becoming severe embrittled [13].

Ageing of polymeric material depends on three basis factors [13]:

- the polymer system itself;
- the pre-service and service environmental conditions on this system;
- the time scale (generally long periods).

Electrical cable materials for NPPs, as explained, include organic compounds, made of a polymeric or co-polymeric matrix and a set of additives. Those materials are exposed to various environmental conditions, usually for long times (40-50 years).

According to the mentioned scheme the three basic factors for ageing are present and they will cause ageing of the polymeric materials.

The macroscopic property changes are always the manifestation of changes in the physic-chemical structure of the materials. The ageing mechanisms may include various elementary mechanisms which may have cumulative, competitive, synergistic and/or antagonistic effects. Two large categories of ageing mechanisms are usually distinguished: the chemical degradation due to changes in the chemical structure, and the physical changes such as changes in composition due to the diffusion of low-molecular-weight components (such as plasticizers or water) out of the amorphous regions.

1.3.1 Chemical changes

The main chemical degradation mechanisms are:

- scission of macromolecular chains: two shorter chains are created by the breaking of a larger one. In the commonly used materials it is usually a scission of alkoxy or peroxide groups. This results in the mechanical weakening of the material;

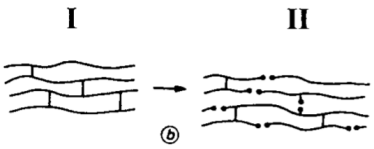

Figure 1.6: A schematic scission of macromolecular chains [13].

- cross-linking reactions, corresponding to the formation of a covalent link between two adjacent macromolecules. The increment of crosslink density creates a new three-dimensional network. This typically causes material stiffness to increase. But prolonged cross-linking may cause embrittlement;

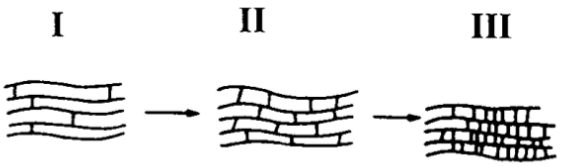

Figure 1.7: A schematic cross-linking reaction [13].

- oxidation. It is the main cause of degradation in ambient atmosphere and it is accelerated by high temperatures and ionizing radiations, having the effect of producing more free radicals. Without these agents, the rate of oxidation at ambient temperature is small, because of the almost

absence of free radicals. Because of its relevance, oxidation process will be examined in depth below.

The typical reaction scheme of oxidation is:

a) initiation step: formation of free radicals on polymer chain, by thermal or radiation energy;

b) propagation step: formation of peroxy radicals and hydroperoxide;

c) chain branching step: decomposition of hydroperoxide;

d) termination step: deactivation of radicals in inert products such as alcohol or acids.

In detail, the chemical reactions in a polymer enriched with antioxidants, during thermal or radiation activated oxidation, are [8, 14]:

a) Initiation: radical formation on polymer chain by thermal or radiation energy;

$$R-H(\text{polymer}) \rightarrow R\bullet\,(\text{free radical in polymer}) + H\bullet\,(\text{proton}) \quad (1.1)$$

b) Propagation: the radical reacts with oxygen to form peroxy radical;

$$R\bullet + O_2 \rightarrow R-O-O\bullet\,(\text{peroxy radical}) \quad (1.2)$$

peroxy radical abstracts hydrogen from the neighbour polymer to form hydro-peroxide together with the same radical of (1.1) on neighbour polymer;

$$R-O-O\bullet + R-H \rightarrow R-O-OH(\text{hydro-peroxide}) + R\bullet \quad (1.3)$$

c) Chain branching: hydro peroxide decomposes to poly-oxy radical and hydro-oxy radical;

$$R-O-OH \rightarrow R-O\bullet\,(\text{poly-oxy radical}) + \bullet OH(\text{hydro-oxy radical}) \quad (1.4)$$

d) Termination: poly-oxy radical decomposes to chain scission and oxidation products (carbonyl groups C=O, alcohols);

$$R - O\bullet \rightarrow \text{Chain scission} \tag{1.5}$$

for example this may be:

$$R - O\bullet \rightarrow R\bullet + -CO- \tag{1.6}$$

Finally the antioxidant reacts with radicals to terminate the oxidation reactions.

$$R-O-O\bullet(RO\bullet) + AX(\text{antioxidant}) \rightarrow R-O-OX(R-OX) + AY \tag{1.7}$$

Antioxidant stops the chain reaction by the quench of free radicals.

The combination of (1.2) and (1.3) produces the cycle reaction, namely the chain reaction of oxidation until the radicals are recombined (fig. 1.8).

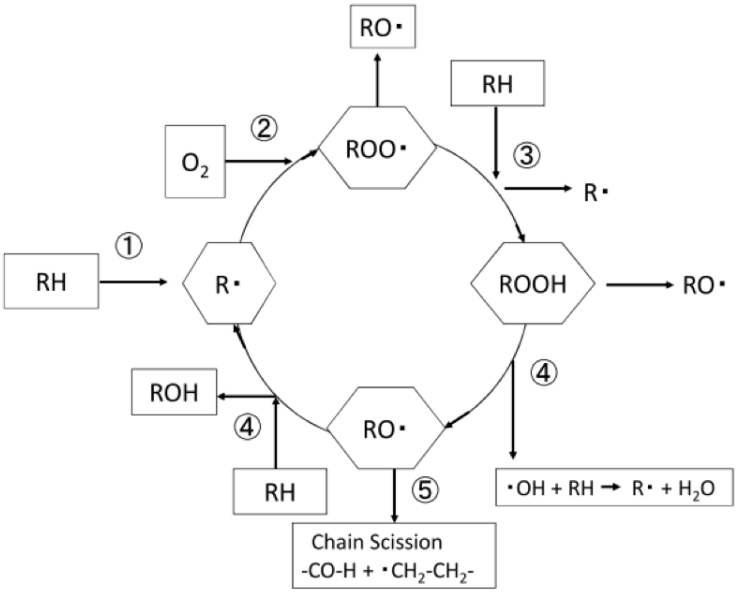

Figure 1.8: Chemical reactions involved in polymer oxidation [8].

Oxidation leads to both chain scission and cross-linking, depending on the detailed kinetics of the individual steps in the oxidation chain reaction. These kinetics strongly depend on the additive package.

Effects of scission and cross-linking combined with oxidation vary according to several factors, such as the type of polymer, the use of additives, and the environment [9, 3]. These effects are not easily predicted.

Chain scission without oxidation results in a net decrease in polymer molecular weight, and is evidenced by reduced tensile strength, hardness and Young's modulus (increased elasticity).

Crosslinking without oxidation typically results in increased tensile strength, hardness and Young's modulus.

Oxidation generally reduces the molecular weight of the polymers and introduces oxygen containing functional groups, with a lower density. It is often characterized by brittleness and cracking. Usually oxidation followed by chain scission does not leave free radical sites.

1.3.2 Physical changes

The main physical degradation mechanisms are:

Evaporation of plasticizers: plasticizers evaporate at the surface of the material, while, simultaneously, surface is replenished by the plasticizer diffusion from the core (fig. 1.9). There can be competition between the two kinetic regimes evaporation and diffusion, depending on temperature. This mechanism is of particular concern in materials with a high plasticizer content, such as PVC.

Migration of plasticizers: this phenomenon appears in multilayer systems composed by plasticized materials. The migration of plasticizers from one layer to another occurs until it is reached the equilibrium, corresponding to a uniform distribution of each plasticizer in each material.

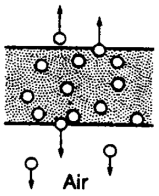

Figure 1.9: Schematic evaporation of plasticizers mechanism [13].

For thermal ageing at temperatures below 70-80 °C, in the absence of radiation, the main ageing mechanism for plasticized PVC is the evaporation of plasticizers from the surface of the external sheath of the cable. At higher temperatures, over 80 °C, and under irradiation, this mechanism is in competition with the intramolecular elimination of the hydrochloric acid (HCl) from the macromolecular chains [13].

During radiation ageing, radicals are generated uniformly throughout both crystalline and amorphous regions [15]. At temperatures well below the crystalline melting point, these species are trapped in the crystalline regions and unable to react to form oxidative products because of low chain mobility and low oxygen diffusion rate. Therefore degradation proceeds primarily through oxidative scission reactions in the amorphous regions, where both chain mobility and oxygen diffusion rates are higher. Because the amorphous regions bind together and produce load transfer between the crystalline blocks, chain scission in there regions has a marked effect on the mechanical properties of the system.

If radiation ageing occurs at slightly higher temperatures, nearer to the melting region for the crystalline portion, then chain mobility is high enough for the trapped species to react to form covalent chemical cross-links rather than scission. In addition, the enhanced mobility enables some recrystallization to occur, which can reform molecular bonds that were broken by oxidative scission in the amorphous regions. Combination of these effects is to effectively "heal" some of the damage created by radiation ageing. The overall macroscopic effect is a reduced rate of radiation degradation at higher

temperatures (inverse temperature effect).

Finally tab. 1.1 summarizes typical ageing mechanisms, degradation and potential effects for each of the common stressors present in the NPP environment.

Applicable stressors	**Ageing mechanisms**	**Degradation**	**Potential effects**
Heat, oxygen	Thermal and thermo-oxidative degradation from ambient and ohmic heating	Embrittlement, cracking, melting, discolouration	Reduced insulation resistance (IR); electrical failure; increased vulnerability to failure
Radiation, oxygen	Chemical decomposition of organics; radiation-induced oxidation	Embrittlement, cracking, discolouration, swelling	Reduced IR, electrical failure
External mechanical stresses	Wear resulting from work in area, personnel traffic or poor support practices	Cuts, cracking, abrasion, tearing	Reduced IR, electrical failure

Table 1.1: Summary of stressors, significating and observed aging mechanisms, degradation, and potential effects [12].

1.3.3 Synergistic effects of temperature and radiation

Temperature and radiation have synergistic effects on the degradation of materials. Depending on the conditions, there will be a predominant degradation process which will characterize the ageing behaviour of the material. For this purpose a predominance chart (fig. 1.10), showing the dominant process as function of the dose rate and temperature, can be used. In this chart it is possible to discriminate four zones:

Zone I: Thermo-oxidation controlled by oxygen diffusion;

Zone II: Thermo-oxidation non-controlled by oxygen diffusion;

Zone III: Radio-oxidation non-controlled by oxygen diffusion;

Zone IV: Radio-oxidation controlled by oxygen diffusion.

Oxidation kinetics are governed by the diffusion of oxygen when the free radical initiation rate is faster than the rate of dissolved oxygen diffusion in the material. This may happen both in thermal and radiation ageing.

When this happens, an heterogeneous degradation (diffusion limited oxidation, DLO, see section 3.2) is conceived: the outer layer of the material, facing the environment, is more oxidized than the inner one. Oxygen diffusion controlled processes depend on the oxygen permeability of the polymer, on the temperature and the radiation dose rate, and on the sample thickness.

While planning an accelerated ageing, using chart of fig. 1.10 it is possible, theoretically, to forecast if homogeneous (II or III) or non homogeneous (I or IV) ageing is achieved; and to forecast if temperature or radiation ageing is predominant in that environment. It is furthermore possible to determine the critical values of dose rate and temperature after which oxidation is no more homogeneous.

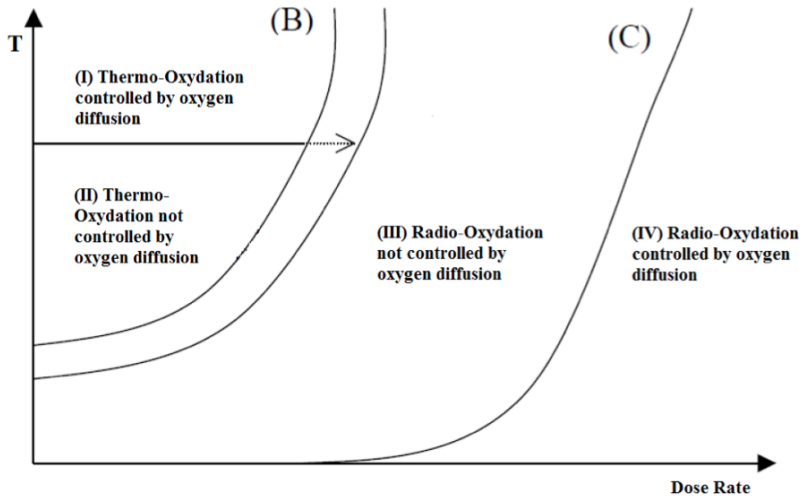

Figure 1.10: Predominance diagram for the mechanisms of degradation during thermal and radiation ageing [8]. Lines (B) and (C), respectively, separate zone (II) and (III), and (III) and (IV).

As an example for DLO, next figures (1.11a, 1.11b and 1.11c) show experimental results of Fourier Transform Infrared Spectroscopy on EPR-based samples, in the wavelength range 500 - 4000 cm^{-1}, from [14]. For this study FTIR was performed on slices 0.17 ± 0.01 mm thick from a sheet 1.05 ± 0.05 mm thick. These samples contains various additives, such as fire retardants, fillers, pigments and the antioxidant Nocrac-MB.

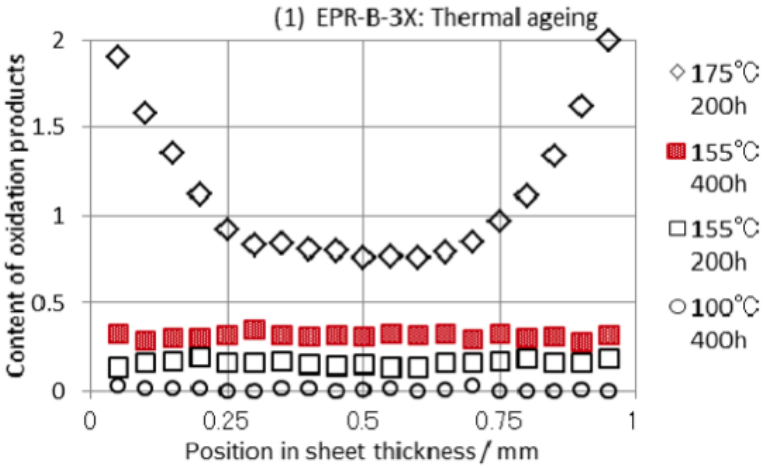

(a) Only thermal ageing: 200-400 h at 100-175 °C.

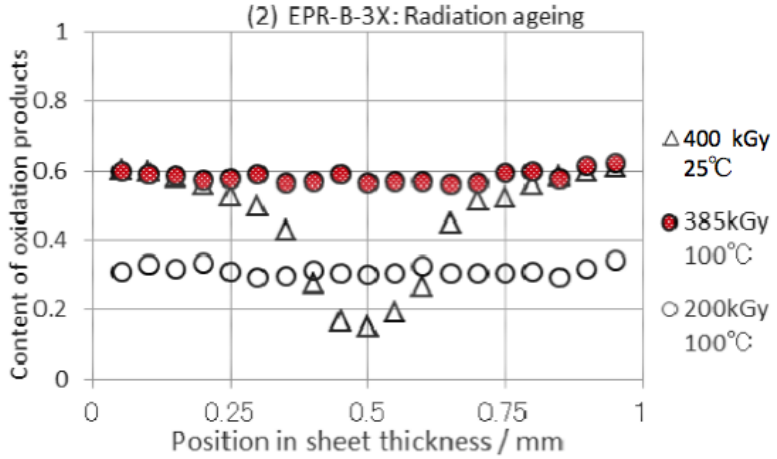

(b) Radiation ageing: 400 kGy at room temperature (25 °C) with 1 kGy/h of dose rate, and 200-385 kGy at 100 °C, with 1.00 kGy/h of dose rate.

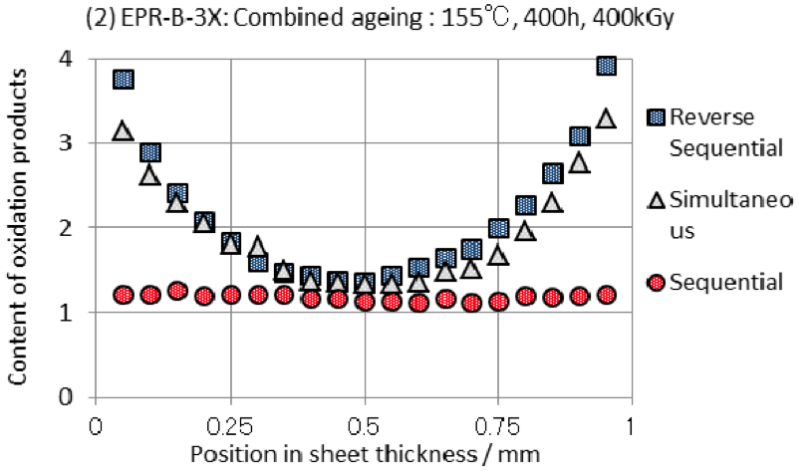

(c) Various techniques of combined ageing: sequential (first thermal at 155 °C, then radiation at 100 °C and 400 kGy for 400 h), reverse sequential (first radiation, then thermal), or simultaneous (radiation during thermal).

Figure 1.11: Content of oxidation products vs. position in sheet thickness for EPR based samples [14].

In these results it is possible to observe the apparition of inhomogeneous ageing, namely the presence of a more oxidized external layer, responsible of a curvature in the content of oxidation products curve along the sample thickness.

In fig. 1.11a (only thermal ageing), a pronounced curvature appears for samples aged at 175 °C for 200 h (it is absent for samples aged for 400 h at lower temperatures): the relative content of oxidation products is about 0.8 at the middle of the sample and 2 at the exterior layers, more than two times higher. DLO also appears in fig. 1.11b (only radiation ageing) for samples aged at 400 kGy for 400 h but it is less pronounced: the more oxidized zone is less wide and less deep. In fig. 1.11c (combined ageing) DLO appears for both simultaneous and reverse sequential ageing. One should note how the different techniques of simultaneous accelerated ageing can be very different: in particular sequential ageing leads to very different results from simultane-

ous and reverse sequential, which cause are almost overlapping effects in this study.

Chapter 2

Diagnostics for aged NPP cables

It is concern of the nuclear industry, in the intent of proving if the cable infrastructure is still capable of operating in safety, to assess the actual conditions of the cable systems.

Stressors mentioned in section 1.2 modify polymer chemistry according to the mechanisms mentioned in section 1.3 and result in changes in mechanical, physical, and electrical performance of the materials, namely in the macroscopical properties of the material. These properties are measurable and can constitute a window inside the structural changes of the material. The various techniques rely on several different physical phenomena and can be better or worse significant for diagnostics. The industry has widely accepted mechanical tests such as indenter modulus as a key indicator and elongation at break (EaB) as a measure of cable remaining life. But innovative techniques are trying to dethrone these traditional techniques. Scope of this chapter is to deepen this subject, with particular attention to dielectric spectroscopy.

2.1 Why condition monitoring diagnostics

In response to the mentioned needs, a number of condition monitoring (CM) diagnostic techniques has been developed. Condition monitoring diagnostics relies on the idea that to know the real state of a system it is possible, and needed, to measure its macroscopic properties, expression of its structure in opposition to the theoretical models for degradation and life prediction.

Why is CM diagnostics particularly recommended for the electrical systems inside a nuclear power plant? Why diagnostic models are not completely reliable when dealing with electrical insulation?

Electrical and thermal stress conditions in modern electrical systems are becoming much more challenging than in the past. The presence of voltage transient and harmonic distortion is stressing insulation systems in a not-conventional and often not-predictable way. The real stresses experienced in the field by materials can be different from those considered for the design: e.g. over-voltages, electrical transients and non-sinusoidal waveforms, that generally cause different thermal ageing, sometimes accelerated. This is very much the case at present, and will become a cumbersome problem in the future, due to the increasing presence of power electronics [16]. Unpredictable stress conditions make inapplicable the model failure probability, often modelled for different environmental conditions, and not considering the synergistic effects usually happening inside a NPP environment.

Furthermore, as seen in section 1.1.5, polymers used for insulation and jacket of cables in NPP are strongly enriched with additives, to make them safely compatible to their function, in the NPP environment. Manufactures may keep researching for newer and newer additives, which composition may be remain trade secret. Even starting from a known base, the complete chemical composition of the polymeric materials used for NPP cables is not completely known, it is different from manufacturer to manufacturer, and, above all, different from the one of the pure polymer.

But diagnostic studies aimed to find ageing models may be performed on pure polymers, or on enriched polymers which composition may be unique

and very different from other polymers with the same base and same application.

Because of this uncertainty, condition monitoring becomes a must: it is the only chance to allow ageing, reliability, availability, that is, conditions, of an electrical apparatus to be surveyed.

In addition, when dealing with suddenly changing conditions, diagnostic devices permanently installed on (or close to) the electrical apparatus can provide a dynamic health index, a summarizing quantity describing macroscopically the insulation condition.

The advantage of Condition Monitoring diagnostics is that the best technical-economical conditions for asset maintenance plans can be reached, which will allow the proper maintenance time, action and cost to be established given a reliability level for the asset.

It is important to highlight that a single technique cannot measure degradation, but to provide an indication of degradation, a combination of techniques is needed [25].

2.2 Main condition monitoring techniques for NPP cables

Available CM techniques can be classified as either non-destructive or destructive. The first one have no deleterious effect on the cable under test, allowing its hypothetical future reinsertion in its original position. With destructive techniques, a section of cable or its polymer layers must be removed from service and tested. Early destructive tests required large section of cables (such as 152 mm or more) per test, and, if insufficient slack existed in the cable to allow retermination, replacement of the cable would be required [12]. But cable replacement due to test is expensive and it is unacceptable unless that cable is representative of a large population. Because many of the destructive tests are highly useful for condition assessing, methods using

very small specimens, in the range of the milligrams, have been developed as well.

Table 2.1 summarizes this aspect for the principal CM techniques.

Method	Destructive	Non - destructive	Small specimen
Mechanical properties			
Tensile testing	✓		
Indenter method		✓	
Chemical properties			
Oxidation Induction Time (OIT)			✓
Oxidation Induction Temperature (OITp)			✓
Thermogravimetric Analysis (TGA)			✓
Gel content [1]			✓
Density			✓
Fourier Transform Infrared spectroscopy (FTIR)			✓
Nuclear Magnetic Resonance (NMR)			✓
Plasticizer content (PVC only)			✓
UV spectroscopy			✓
Electrical properties			
Voltage withstand	✓		

[1] But accuracy increases with larger specimens.

Insulation resistance (IR)		✓	
Impedance/ Capacitance		✓	
Dissipation factor (Tan delta)		✓	
Insulation power factor (PF)		✓	
Time Domain Reflectometry TDR)		✓	

Table 2.1: Main CM methods for low voltage NPP cables, with emphasis on the non-destructive aspect. The "Small specimen" class can be considered as a subclass of the "Non-destructive" class.

As possible to see observe from table 2.1, non-destructive are the majority and tensile testing (elongation at break, strength at break, Young's modulus) requires the destruction of the sample. Elongation at break is widely used as a diagnostic marker for NPP cables.

Reviewing prior literature [15], it is possible to identify how popularly specific properties have been used as key indicator of ageing-related degradations.

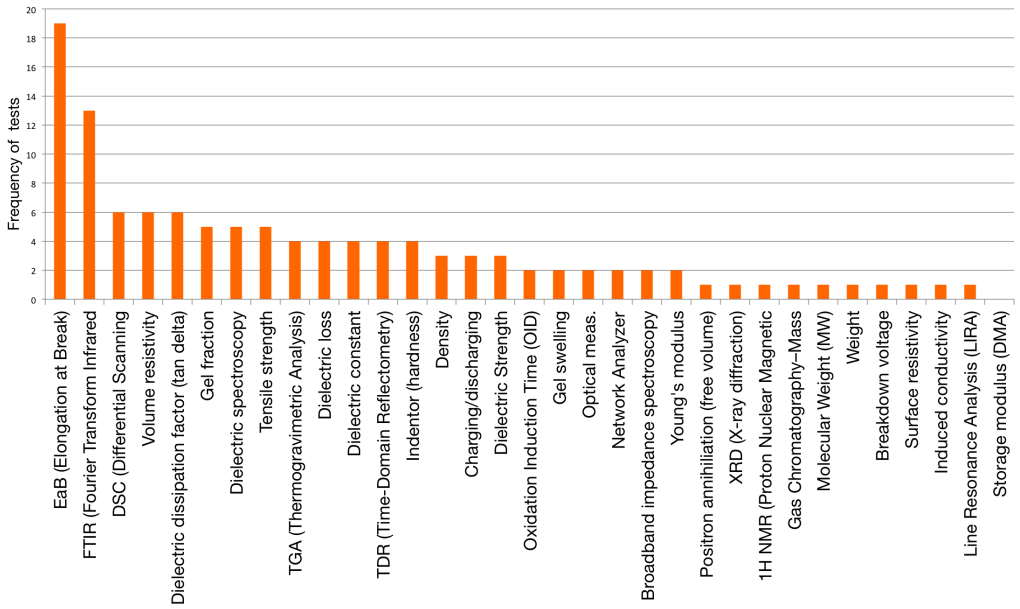

Figure 2.1: Literature review on the frequency of cable ageing tests [15].

The desirable attributes a Condition Monitoring technique should have can be listed as follows [25, 15, 18]:

a) sensitive and reliable with ageing: property shows a monotonic trend with ageing, so that it is possible to indicate an end-of-life criterion;

b) non-intrusive and non-destructive, i.e. not requiring the cable to be disturbed or damaged;

c) simple to use under field conditions;

d) capable of being used during normal operation (*in situ* measurements);

e) not requiring disconnection of equipment (on-line measurements);

f) property should be correlated with an accomplished failure criterion, such as elongation at break;

g) capable of identifying localized degradation;

h) providing reproducible results that are not affected by, or can be corrected for the test environment (temperature, humidity, radiation);

i) less expensive to implement than cable replacement;

j) potential for developing measurement techniques that can interrogate the cable condition over long distances;

k) measurement equipment available.

Furthermore, it is desiderable to link the measured indicators with an independent parameter, such as time or cycles, in order to identify trends in the condition of the cable to guide the engineer's decision to effectively manage the ageing and degradation state of the cable in issue [18].

2.2.1 Techniques using mechanical properties

Tensile testing

Tensile testing relies on the idea that chemical changes can be revealed through the measurement of mechanical properties of the material such as elongation at break, strength at break, and stiffness (Young's modulus, the ratio E between the tensile stress σ and the extensional strain ε). Tensile testing is performed by stretching the sample until it breaks, while recording load and extension. To let this, cable must be stripped down to its individual components so that jacket and insulation can be cut into suitable dimensions.

Embrittlement and variations in structural integrity are consequences of polymer degradation due to ageing, therefore mechanical properties are correlated to ageing. Typically, a value of 50 % absolute elongation at break has defined the end-of-life condition. This value was determined by considering a conservative estimate of cable ageing that defines the ability of an aged cable to survive DBA conditions.

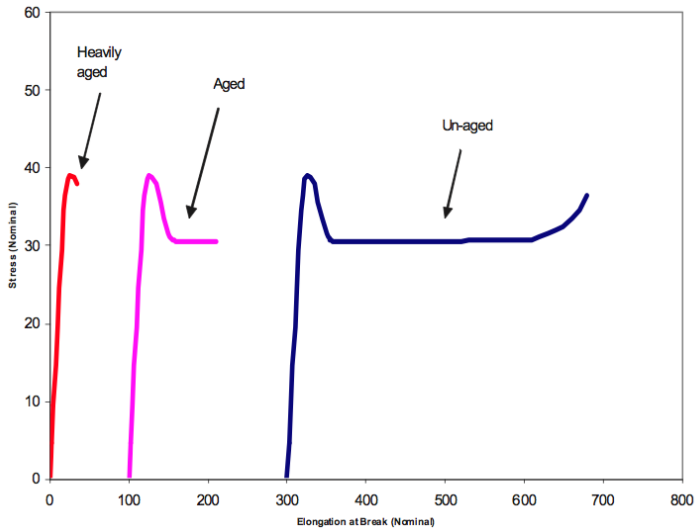

Figure 2.2: A typical set of degradation EaB curves for a thermoplastic material [3].

Tensile testing generates optimum data for cable condition assessment: EaB decreases gradually with the amount of induced degradation for most polymeric materials. However it is impractical to be used as a routine CM method because:

1. it is an intrusive and destructive method, requiring large samples;

2. it requires a large downtime associated with the cable removal and replacement;

3. for cross-linked polyolefins EaB is not a good indicator because its trend remains quite constant over a long period of time and then rapidly decreases to its end-of-life value;

4. EaB measurements may not be possible, or not be representative, if the material consists of a composite based of fibre reinforced polymers or two bonded inseparable layers.

Indenter method

For this method, a small-diameter probe (indenter) is pressed against the cable sample, while measuring the applied compressive force F and corresponding deformation X. The ratio between those two is the indenter modulus (IM):

$$IM = \frac{\Delta F}{\Delta X} \tag{2.1}$$

This modulus is an indicator of cable ageing, it can be plotted at each point in time when a measurement is taken, providing a representation of cable ageing over time. Studies indicate that this modulus generally increases during thermal ageing [15].

This is a non-destructive and non-intrusive test because the probe penetrates the surface of the materials only a few hundred micrometers [3]. This method measures localized degradation and is applicable only for accessible cables.

Good correlation data between IM and degradation have been demonstrated for elastomeric materials and thermally aged PVC. But little or no correlation ahs been observed for irradiated PVC and semi-crystalline polymeric materials such as polyethylene [3].

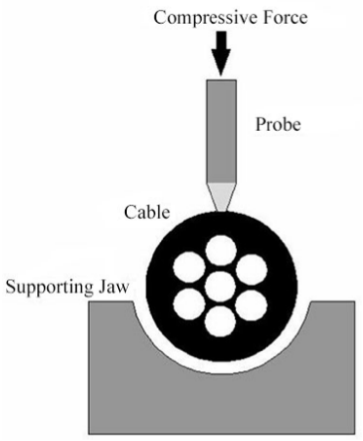

Figure 2.3: Schematic indenter test on a cable sample [15].

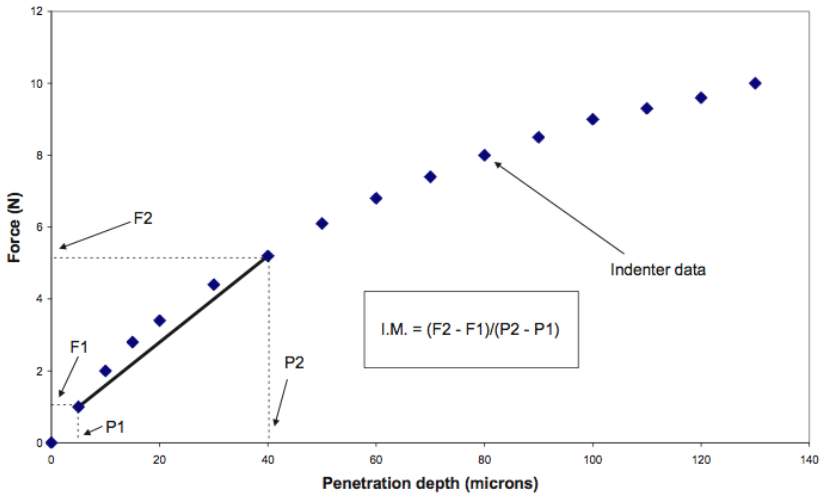

Figure 2.4: Plot of indenter force versus deformation [3].

2.2.2 Techniques using chemical properties

Oxidation Induction Time and Temperature

As mentioned, sometimes significant reductions in elongation at break are only seen in the last quarter of total life (e.g. cross-linked polyolefins). For this reason, although EaB is used as the main indicator of degradation, other parameters which could show more pronounced changes in the earlier stages of degradation are useful. Example of these parameters are oxidation induction time and oxidation induction temperature.

Oxidation induction time (OIT) tests are carried out on small polymer samples weighing 1 - 10 mg. The average of 3 or more tests is desiderable. Sample is placed on the sample pan of a differential scanning calorimeter (DSC) and heated quickly to a predetermined temperature (usually 200 °C), in an inert atmosphere (usually nitrogen). Once the heat flow has stabilized, the inert gas is replaced by oxygen. After an induction period, the sample begins to oxidise. The time at which this occurs can be measured thanks to the exothermic heat flow associated with the oxidation process.

A typical OIT thermogram is shown in Fig. 2.5. The OIT is defined as the time at which a particular heat flow threshold relative to the baseline

(usually 0.1 W/g) is exceeded, and reading off the point at which the tangent intersects the baseline.

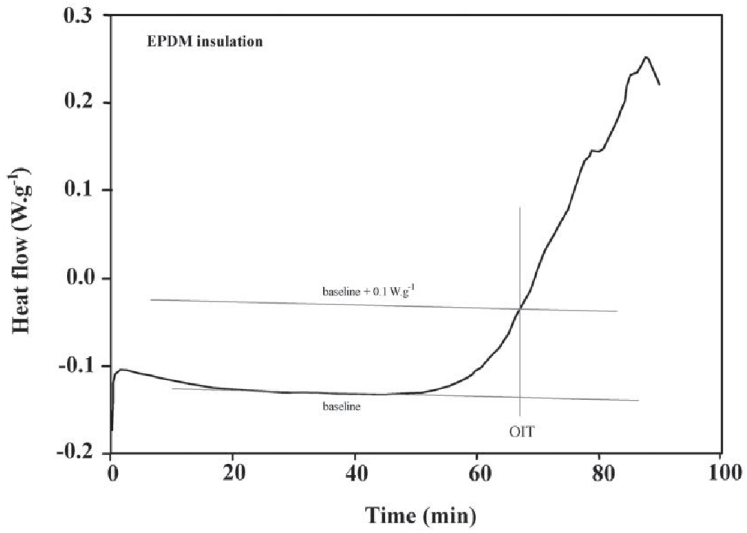

Figure 2.5: Thermogram for EPDM with a heat flow of 0.1 W/g [3].

A long OIT may denote a sample with high levels of antioxidant and a low degree of degradation, a shorter OIT, measured at the same temperature, is likely to denote low levels of antioxidant and a potentially heavily aged sample[2]. Therefore OIT becomes shorter as ageing continues.

OIT method has been standardized and has been shown to correlate well with the degradation of PE, EPR, CSPE and PCP [3].

To determine the oxidation induction temperature (OITp), sample preparation as well as the instrumentation needed is identical to that for OIT. The only difference is that, in this case, the sample is heated at a slow ramp rate (usually 10 °C/min) in flowing oxygen. The oxidation in the sample, as seen, is characterized by an increase in the exothermic heat flow, which accelerates as the temperature increases. The value of OITp is read from the temperature at which a threshold relative to the baseline (usually 0.5 W/g) is exceeded.

[2]As mentioned in section 1.1.5, antioxidants are consumed during polymer life.

As the level of ageing increases, the OITp usually decreases, and this trend can be correlated to EaB for certain polymers [3].

Unlike the OIT tests, physical transitions such as glass transition and melting point may appear on the thermogram, as an endothermic process (see fig. 2.6).

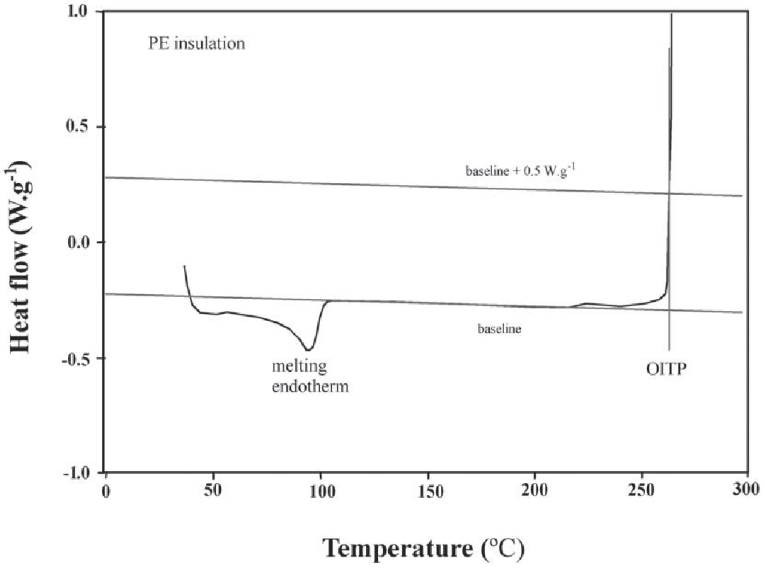

Figure 2.6: A typical thermogram for PE indicating the measuring point for OITp [3].

Since both OIT and OITp are related to the content of antioxidants, they can be suitable parameters for monitoring cable insulation degradation. OIT measurement does not give an absolute indication of the cable degradation: the end-of-life criterion is undefined. Therefore, to assess the residual service lifetime, the OIT values are correlated to the EaB, through the use of correlation curves (crossplots) [8].

Thermogravimetric Analysis

Thermogravimetric analysis (TGA) is carried out using sample sizes similar to those used for OIT/OITp. Sample weight is monitored as the sample is

heated in a chamber at a constant rate. Volatile components such as absorbed moisture, residual solvents or low molecular additives usually evaporate beween 25 °C and 300 °C. The temperature at which the sample weight has decreased to 95% of its original value is usually taken as the reference point. The value of this temperature depends on the level of ageing in the polymer and will decrease with increased ageing levels. Tests can be carried out in air or oxygen purge through the sample chamber, but the nature of the purge will affect the TGA temperature. TGA can give information about the chemical structure of the polymeric macromolecules and additives thermal stability, especially for flame retardants [8]. TGA test is cost effective, quick and simple to use.

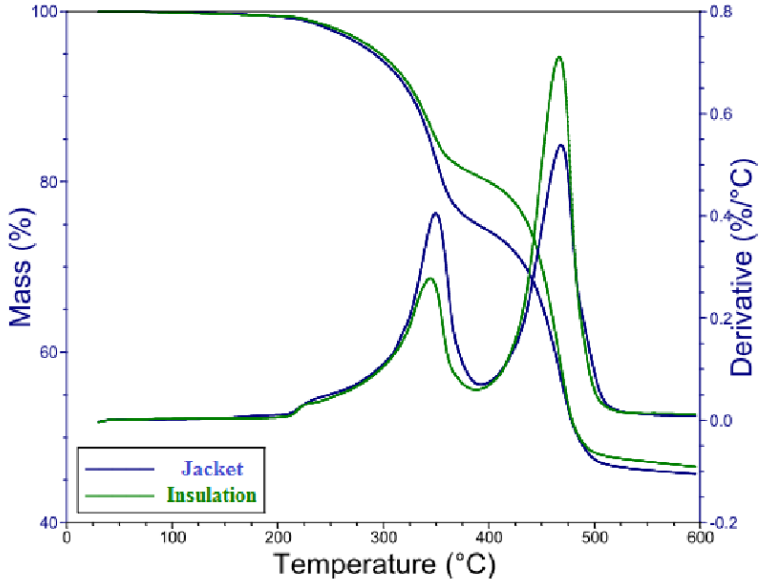

Figure 2.7: TGA trace, showing mass loss versus temperature, and its rate for EVA-based insulation and jacket. It is possible to note two great variations in mass, corresponding to two peaks in the mass loss rate [8].

Typically in the TGA trace four regions of the material decomposition can be identified:

1. release of low molecular weight products and water: 200 - 300 °C;

2. decomposition of pendant groups, emission of water and low molecular weight additives: 300 - 420 °C;

3. degradation of hydrocarbon backbone: 420 °C - plateau;

4. residuals.

Swell/gel

Swell and gel tests can be used to assess ageing by evaluating the degree to which polymers swell or dissolve when heated in solution. The degree of swelling and residual gel is related to the cross-linking of the polymers during ageing and as cross-linking progresses with ageing, the materials swell less or have more residual material.

These tests require a reasonable amount of material (typically 200 mg) and they are not difficult to perform. But tests are lengthy due to the length of time required for heating the material in solution [12].

Density

If a polymer is aged in air, oxidation is normally the predominant degradation mechanism and it leads to both crosslinking and chain scission, together with the formation of oxidation products and the release of gases (s. 1.3). As many polymers have high-density fillers, the release of degradation products from the comparatively low-density polymer chain leads to a higher density through a decrease in the polmer to filler ratio. Shrinkage from a tightening of the polymer chains is often a result from crosslinking, and this also is a cause of an increase in density [8].

Summarizing, the higher the level of ageing, the greater the concentration of oxidation products, the higher the density. This method is considered non-destructive because small quantity of sample is required (1-10 mg). Commonly, to perform measurement with small samples, two methods are used [3]:

a) Archimedes' approach A sample, typically weighing tens of milligrams, is weighed in air and then in a liquid of known density ρ_{liquid}. The density of the polymer is determined as:

$$\rho_{polymer} = \left(\frac{W_{air}}{W_{air} - W_{liquid}} \right) \rho_{liquid} \tag{2.2}$$

where W_{air} and W_{liquid} are the measured weight of the sample respectively in air and in the liquid.

b) Density gradient column A more convenient method, using very small samples (e.g. scrapings of insulation and jacket materials) consists of using a graduated glass tube of about 1 m in length suspended vertically in a water bath held at constant temperature (20-25 °C). The column is filled using two miscible liquids of different densities so that a linear density gradient is obtained decreasing from the bottom to the top of the column. The column is calibrated by carefully introducing specially prepared glass beads inside, their equilibrium position defines the density at that point. Samples are then introduced into the column and, once reached their equilibrium, their position indicates the density. An accuracy of 5 10^{-4} g/cm^{-3} can be achieved with this method [3].

Density measurements are relatively quick and provide satisfactory informations for many materials, such as XLPE, CSPE, EVA, EPR, and PVC. However, in many cases, with PVC and LDPE, density increase is slow at the beginning of ageing, with an increase at later stages (induction time-effect) [8]. As for OIT and OITp, measurements have to be correlated to a property such as EaB.

Fourier Transform Infrared Spectroscopy

Fourier Transform Infrared Spectroscopy (FTIR) is performed using a spectroscope, in which a small material sample is exposed to infrared radiation. Usually 10 milligrams of sample is required, if focusing on the carbonyl

region [8]. The absorbance or transmittance of this radiation by the material at various wavelength is then measured and plotted.

Infrared spectroscopy is an informative method for investigating molecular structure and chemical bond content arising from polymer degradation. As radiation passes through, atoms absorb radiation energy and begin to vibrate. For a particular chemical bond, maximum vibration occurs for a specific wavelength, resulting in specific peaks on the spectra. By irradiating the sample with a continuous of infrared radiation, the obtained spectrum is composed by several peaks in the absorbance/trasmittance, indicating specific chemical bonds. By comparison with the known characteristics of the chemical bonds available from literature it is possible to identify the chemical bonds behind those peaks. For example the carbonyl (C=O) peak is around 1720 cm^{-1} and belongs to ketones, carboxylic acid and aldehydes. Another useful peak is around 2900 cm^{-1} and it represents the C-H stretching of the -CH_2 bond, part of the polymer's backbone structure [8].

The magnitudes of the peaks in the spectrum reflect the changes in the polymer molecular structure, since oxidation is characterized by an increasing presence of carbonyl bonds and decreasing number of -CH_2 bonds. A practical index to quantify the extent of oxidation can be defined as the ratio of the area of the carbonyl absorption to the area of the -CH_2 stretch absorption peak.

FTIR spectroscopy has been used successfully to characterize ageing degradation for XLPE and EPR cable insulation and CSPE jacket material, but it is difficult to run on black (e.g. carbon-black filled) materials or materials, such as EVA, with peaks already present in the carbonyl region before ageing. Furthermore, for many materials, the growth in the carbonyl region is often extremely slow until just before the end-of-life condition. For these FTIR little warnings of imminent end-of-life [8].

Applying this technique on thin slices, coming from different depths of a cable insulation/jacket, it is eventually possible to evaluate the spatial distribution of the oxidation contents and evaluate the diffusion limited oxidation.

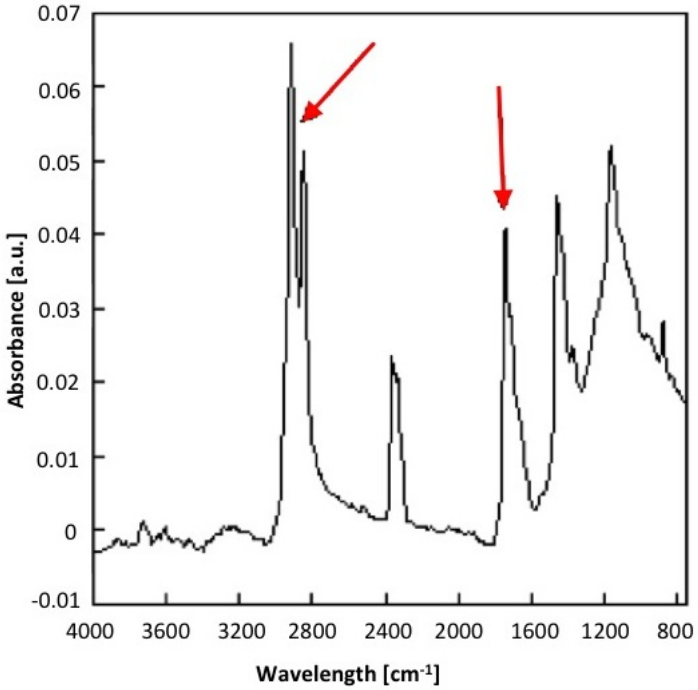

Figure 2.8: Example of a FTIR result: absorbance (in absorbance units) versus wavelength. The carbonyl peak (around 1720 cm^{-1}) and the -CH_2 stretch peak (around 2900 cm^{-1}) are marked by the two red arrows [8].

2.2.3 Traditional techniques using electrical properties

As electrical conductivity is proportional to the product of charge mobility and charge carrier concentration, the conductivity of polymers used in cable and jacket insulation varies with change in charge carrier density in the material. As cables age, multiple processes combine to increase the number of carriers in the polymer insulation material, thereby increasing the conduction and ultimately leading to dielectric breakdown. Increase in the ionic (charge-bearing) content of polymer material over time may result from ingress of moisture or other impurities, departure of additives initially present in the material, creation of charged moieties through bond scission from oxidation or photo-cleavage, or infiltration of surface charges within the material. In addition, changes in spatial distribution of heterogeneities in ad-

ditives and fillers, and rearrangement of polymer structure such as evolution of crystalline phases over time can alter material electrical properties [15].

Voltage withstand

Voltage withstand tests are performed by applying a given voltage, above the normal operating voltage, to the insulation, for a given time, typically 1-5 minutes. The principle behind this is that if defects (local or global) are present in the cable, which increase the conduction because of the increased number of carriers, the high voltage will force it them fail (breakdown). This method is intrusive and destructive, because it requires the disconnection of the cable, which is no more usable after test. Furthermore it requires a laboratory equipped for high voltages.

Insulation resistance

For IR tests, a DC voltage (typically 500 V) is applied to the cable for a short period in which the current is measured (conduction and leakage phenomena). The IR is given by the ratio between the applied voltage and the measured current. Also this method requires cable disconnection but it may be non-destructive, if the applied voltage is compatible with the cable rating.

It is useful to gather information from IR trend (fig. 2.9), and moreover from the ratio $IR(t_2)/IR(t_1)$ between IR measured at two different times t_1 and t_2.

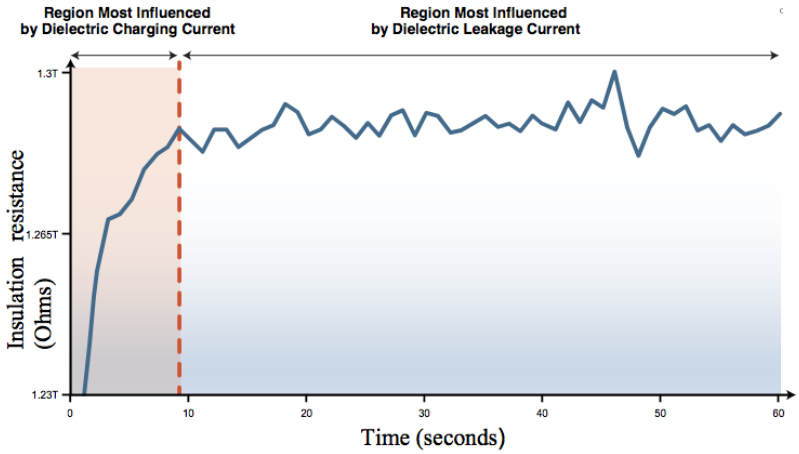

Figure 2.9: Insulation resistance curve for a CRDM cable in NPP [4].

Depending on the values of those two times, three different parameters are defined:

$$\text{dielectric absorbance ratio}: \quad DAR = \frac{IR(t_2 = 60s)}{IR(t_1 = 30s)} \tag{2.3}$$

$$\text{polarization ratio}: \quad PR = \frac{IR(t_2 = 180s)}{IR(t_1 = 60s)} \tag{2.4}$$

$$\text{polarization index}: \quad PI = \frac{IR(t_2 = 600s)}{IR(t_1 = 60s)} \tag{2.5}$$

Impedance measurements

Impedance measurements, including inductance, capacitance and resistance, are made using a LCR meter at specific frequencies to verify the characteristics of the cable conductor, insulating material and the end device. Imbalances, mismatches or unexpectedly high or low impedances between the cable leads would indicate problems due to the degradation and ageing, faulty connections and splices, or physical damages [3].

Dissipation factor

A property that has shown changes with the ageing of the cable dielectric materials is the dielectric loss tangent, or dissipation factor $tan\,\delta$. Tan delta is a dimensionless property determined by insulator's structure, therefore affected by changes in it. This property is very sensitive to water ingress in cables [3].

$$tan\,\delta = \frac{\omega\varepsilon'' + \sigma}{\omega\varepsilon'} \tag{2.6}$$

Tan delta of an ideal insulation is 0, deviations from this value are indications of sample degradation. Measurements can be carried out at low voltages (e.g. 500 mV) at fixed frequency (50-60 Hz) or over a wide range of frequencies (e.g. 20 Hz to 500 kHz), using standard impedance bridge instruments. Tan delta of cable insulation is normally measured between conductors in adjacent cores or between single conductors and shielding. In some cases measurements can be carried out on jackets between shielding and an external ground plane. This technique does not require sample removal, but its disconnection.

In addition, other electrical properties, such as attenuation and/or signal propagation can be measured too.

2.2.4 Innovative techniques using electrical properties

Most of the mentioned electrical tests are effective as pass/fail indicators of functionality, but they seem to be not very sensitive to insulation degradation. However they can be sensitive to conductor integrity (e.g. loose connections, corrosion of connectors) [8].

Peculiarity of the electrical techniques is that they are capable to be performed *in-situ* and remote. In addition many of them can reveal characteristics along the whole length, measuring global properties, in contrast to those properties limited to providing data at the localized point where the sample is withdrawn (e.g. tensile testing and thermal analysis).

Starting from these advantages, innovative electrical techniques are being studied and developed [8, 4, 19]. Some of these will be now explained.

Space charge measurement

Space charge is the free charge accumulated in the insulation bulk due to traps present in the insulation matrix. This phenomenon is accentuated above all in high voltage direct current systems (HVDC), where during the continuous operation, a significant amount of electric charges (positive and negative) can be injected from the electrodes into the insulation bulk where chemical and physical traps are present. Electric charges can be trapped for a time correlated to trap depth (the deeper the trap depth, the longer the time needed for charges to escape) and this may lead to space charge accumulation in the insulation bulk, with an extent that depends on the density/depth of the traps. Since trap distirbution is correlated to material morphology/structure, ageing can be detected by means of measurements of space charge accumulation [8].

Space charge measurements can be carried out through several techniques. The pulsed electro-acoustic (PEA) technique is a non-destructive technique for profiling space charge accumulation in polymeric materials, providing a good spatial resolution of the space charge profile in the material bulk.

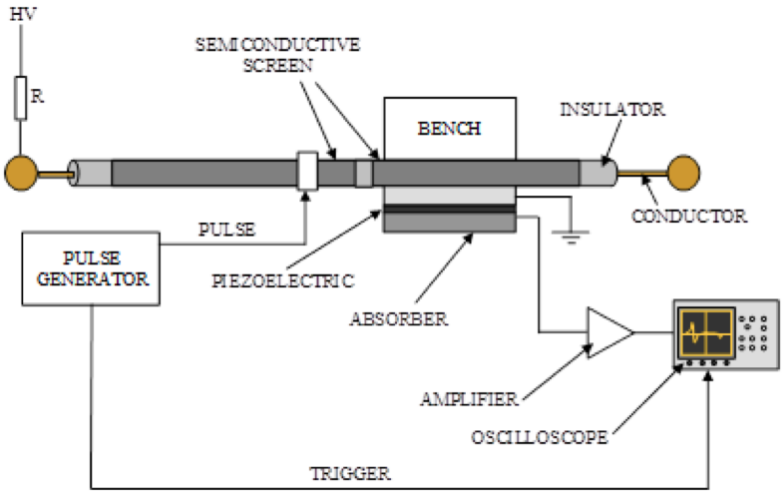

Figure 2.10: Schematic representation of PEA measurement experimental setup [8].

The specimen may consist of a small plaque of insulating material or a length of a cable. A sequence of high-voltage pulses of very short time length (5 - 40 ns) at repetition frequencies in the range $5 \cdot 10^{-2}$ Hz - 10 kHz is applied to the sample subjected to a DC field. Each generated pulse produces an electric force displacing internal charges and generating pulsed acoustic pressure waves in the correspondence of each charge layer in excess with respect to neutrality. The resultant pressure pulse is detected by a piezoelectric transducer, so that the charge distribution in the specimen under test is proportional to the output voltage profile provided by the transducer. The output signal is amplified and visualized by a digital oscilloscope.

Usually the analysis of space charge profiles is restricted to one dimension (fig. 2.11): this assumption imposes to consider that space charge density, electric field distribution and acoustic wave propagation can vary only along the specimen thickness.

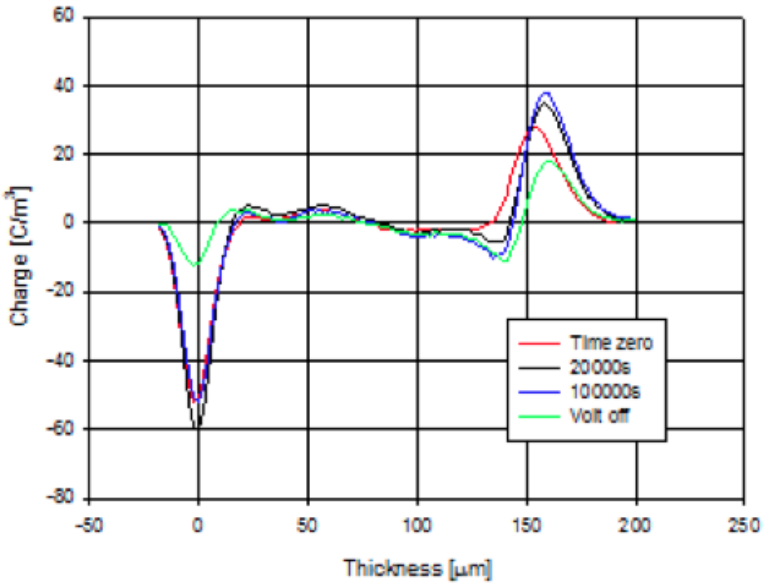

Figure 2.11: Example of space charge profiles recorded by PEA measurement [8].

The mean (absolute) space charge density $q(t, E_p)$ can be estimated from the charge density profile $q(x, t, E_p)$ through the following expression [8]:

$$q(t, E_p) = \frac{1}{x_l - x_0} \int_{x_0}^{x_l} |q(x, t, E_p)| dx \tag{2.7}$$

being x_0 and x_l the electrode position, t the time at which the measurement is performed and E_p the applied field (poling field). In order to calculate the value of $q(t, E_p)$, reference can be made properly with charge profiles observes during depolarization (the volt-off). For the sake of brevity, in the following, $q(t, E_p)$ and $q(x, t, E_p)$, will be referred as $q(t)$ and $q(x, t)$ respectively. Plotting the values of $q(t)$ in relative value with respect to $q_0 = q(t_0)$, being t_0 a reference time (generally 1-10 seconds after the volt-off), as function of the polarization time, the so-called depolarization characteristic can be obtained (fig. 2.12).

An estimate of the average trap-controlled mobility could be derived, in

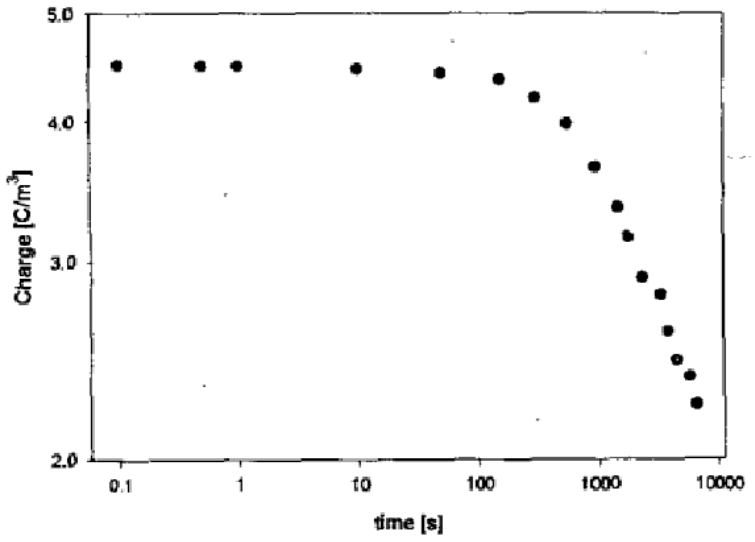

Figure 2.12: Example of depolarization characteristic [8].

principle, through appropriate processing of charge vs. time depolarization characteristic. Apparent trap-controlled mobility is only a very rough approximation of the mobility as usually defined, but, even if affected by significant

approximation, it can be useful for material characterization and aging diagnosis. The expression of the apparent trap-controlled mobility is the following [8]:

$$\mu = \frac{2\varepsilon}{q^2(t)} \frac{dq(t)}{dt} \tag{2.8}$$

where $\frac{dq(t)}{dt}$ is the slope of the depolarization curve at time t and ε is an average estimate coming from specific measurements of permittivity carried out on the specimens tested.

Once known apparent trap-controlled mobility, the trap depth could be estimated. This is a difficult problem, which has not been solved yet in a totally convincing way. An approximate method to obtain the trap depth distribution ΔU provides the following equation [8]:

$$\Delta U = kTln\left(\mu \frac{h}{eR^2}\right) \tag{2.9}$$

where R is the mean distance between localized states, e is the electron charge ($e = 1.6010^{-10}C$) and h is the Planck's constant ($h = 6.6310^{-34}J \cdot s$). Therefore, the values of the trap depth can be determined from the values previously calculated for μ.

Space charge measurements can be performed on every kind of solid insulating materials used in cables and accessories, but it is typically used for high and medium cable insulation which are usually subjected to a high field, where space charge accumulation is an important factor and can create electric field distortion in the insulation bulk. Space charge accumulation does not constitute a problem for the insulation of low voltage cables. Anyway, this technique can be used as a diagnostic tool to detect morphology modification of the material due to ageing. In fact, bulk degradation due to thermal and radiation stresses can be detected with this method since it is associated with modification of distribution of both chemical and physical traps. Chemical traps are characterized by chemical species present in the matrix different from the polymer, such as antioxidants, contaminants, cross-linking by-products. Physical traps can be associated with morpholoical non-homogeneities of the polymer chains, particularly at the interface between

the crystalline and the amorphous phase. As the polymer ages, phsical and chemical changes in the matrix occurr. Oxidation, bond breaking, free radicals and new chemical species formation are claimed to be the main effects of both thermal/electrical ageing of polymers. Such aging effects can alter trap density and depth, usually increasing the number or depth of charge traps [8].

Time Domain Spectroscopy (TDS)

Time Domain Spectroscopy (TDS), not to be confused with Time Domain Reflectometry (TDR), consists in the measurement of the polarization/depolarization current and it is an useful technique to investigate conductivity and dielectric response in time domain of polymeric dielectric materials, measuring material losses both in the polarization and depolarization phases [8, 19]. Depolarization losses are only dependant on the global ageing compared to the polarization losses, which can be dominated by a local insulation defect [19].

The measurement consists in two phases: the first consist of applying a DC voltage to the insulating material and acquire the value of current as a function of time; once this current has reached a steady state value, the polarization phase is complete (t_{pol} in fig. 2.13). The second phase starts switching off the voltage generator, specimen is instantly short-circuited and the value of the so-called depolarization current is recorded until it reaches negligible values (fig. 2.13).

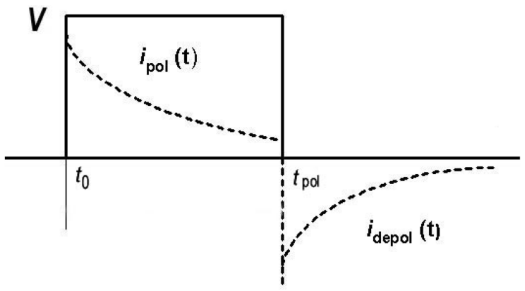

Figure 2.13: Principle of the TDS measurement; the dotted line represents the current in the two phases [19].

The expressions of the current in the two phases are respectively [19]:

$$i_{pol}(t) = i_{cap}(t) + i_{abs}(t) + i_{con}(t) \tag{2.10}$$

$$i_{depol}(t) = -i_{cap}(t) - i_{abs}(t) \tag{2.11}$$

The components contained in (2.11) and (2.10) can be defined as:

the capacitive current $i_{cap}(t)$**,** corresponding to the current charging the insulation like an ideal capacitor. It is a current with a high value at the beginning, which decreases quite rapidly and becomes negligible after few seconds or tens of seconds, depending on the capacitance of the sample;

the absorption current $i_{abs}(t)$**,** including different polarization effects but representing, at the time scale of our concern, the current generated by the alignment of polar molecules in the applied DC electric field and by the presence of heterogeneities in the dielectric. This component decreases slower than the capacitive current, requiring several minutes to reach a negligible value;

the conduction current $i_{con}(t)$**,** corresponding to the current (resistive or leakage) that continuously flows through the insulation. It gives the relevant information concerning the quality of the insulation. It is small

and stable in time for good insulations, large and may increase with time for poor insulations. The depolarization current, as seen in (2.11), lacks this component.

Time domain spectrometry evaluates bulk properties of the insulation. Changes in polarization/depolarization characteristics, which are caused by structural changes in the material due to the various modes of deterioration (such as water treeing, oxidation, presence of contaminants, and so on...), could be related to insulation ageing. A large change in the depolarization current could indicate advancing deterioration of the insulation and increasing probability of failure. Long-term ageing of miniature cables resulted in a significant increase in the area under the polarization current curve (fig. 2.13).

TDS can complete information from IR measurements. This technique is currently used for middle and high voltage cables. Because on-site tests can only be performed on de-energized cables, the tests have to be coordinated with the regular maintenance work schedule of the utility. The advantage of this technique is the very short time required to perform the measurements: few seconds is enough. Although, the commonly used techniques of the long-term depolarization current measurements require minutes or even hours [8]. Compared to the Frequency Domain Spectroscopy (FDS), the Time domain spectroscopy measures more rapidly the dielectric losses in the frequency range below 10^{-3} Hz, corresponding to interfacial polarization and charge trapping processes, predominant in insulating materials composed of different dielectric materials.

Dielectric Spectroscopy

Dielectric Spectroscopy measures the dielectric properties of a material as a function of frequency. To distinguish from the previously exposed Time Domain Spectroscopy, it can be called Frequency Domain Spectroscopy (FDS).

This technique is based on the interaction between an external applied

field and the electric dipole moment of the sample, namely electric polarization, previously present or field-induced. The main parameter which accounts for polarization is the complex permittivity [8]:

$$\varepsilon^*(\omega) = \varepsilon'(\omega) - i\varepsilon''(\omega) \tag{2.12}$$

This technique expects the measurement of impedance of system over a range of frequencies, and therefore the frequency response of the system. There are several tools for analysing the dielectric response of an insulation system in the frequency domain between 10^{-5} Hz and 10^{9} Hz, like the dielectric analyser and the network analyser.

The dielectric analyser can evaluate dielectric properties such as complex permittivity, capacitance, dissipation factor and conductivity, in the frequency range 10^{-2} - 10^{6} Hz. For this work a Novocontrol Alpha-A dielectric analyser, for analysis between $3{\cdot}10^{-6}$ and $20{\cdot}10^{6}$ Hz, shall be used.

The instrument consists of two major components:

- a frequency response analyser with a sine wave and DC-bias generator and two AC voltage input channels. Each input channel measures the AC voltage amplitude of an applied sine wave. In addition, the phase shift between the sine waves applied to the both inputs is detected. Generally only the fundamental harmonic is considered;

- a dielectric (or impedance) converter with a wide dynamic range current to voltage converter and a set of precision reference capacitors.

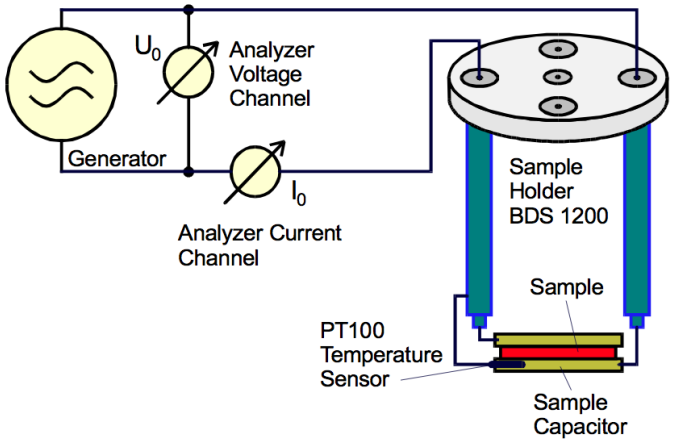

Figure 2.14: Schematic representation of the dielectric analyser (from Novocontrol manual).

A voltage with amplitude V_0 at fixed frequency $\omega/2\pi$ is applied to the sample capacitor. The result is a current of amplitude I_0 at the same frequency. The phase shift between current and voltage waveforms, φ, is measured.

Using the complex notation, the expression for voltage and current are respectively:

$$V(t) = V_0 sin(\omega t) = \Re e(V^* e^{i\omega t}) \tag{2.13}$$

$$I(t) = I_0 sin(\omega t + \phi) = \Re e(I^* e^{i\omega t}) \tag{2.14}$$

being

$$V^* = V_0 \tag{2.15}$$

and

$$I^* = I' + iI''; \quad I_0 = \sqrt{I'^2 + I''^2}; \quad tan\,\varphi = \frac{I''}{I'} \tag{2.16}$$

For a sample with linear electromagnetic response, the measured impedance of the capacitor is

$$Z^* = Z' + iZ'' = \frac{V^*}{I^*} \tag{2.17}$$

Therefore, instrument can measure sample capacitance and dissipation factor $tan\,\delta$, being $\delta = \frac{\pi}{2} - \varphi$.

Complex permittivity of the material is connected to impedance by the relation

$$\varepsilon^*(\omega) = \varepsilon' - i\varepsilon'' = \frac{-i}{\omega Z^*(\omega)} \frac{1}{C_0} \tag{2.18}$$

being C_0 the capacitance of the empty sample capacitor.

The specific conductivity σ^* is connected to complex permittivity by:

$$\sigma^* = \sigma' - i\sigma'' = i2\pi f \varepsilon_0 (\varepsilon^* - 1) \tag{2.19}$$

Like space charge measurements, dielectric spectroscopy can reveal bulk degradation due to thermal and radiation stresses. During ageing, insulating materials are subject to structural change because to oxidation, bond breaking, free radicals and new chemical species creation. This may change molecular mobility and dipole formation, changing relaxation phenomena and electric polarization.

Therefore physic-chemical changes modify the response of the material to an applied external field. This is the connection between the microscopical changes and the measured property, this explains why dielectric spectroscopy can reveal degradation changes in polymers.

In particular the imaginary part of permittivity, well correlated to oxidation and losses, exhibits a marked variation with ageing [8].

Within the extraordinarily broad dynamic study range, molecular and collective dipolar fluctuations, charge transport, and polarization effects at inner and outer boundaries take place, and determine the dielectric properties of the material under study.

Dielectric mechanisms can be divided into resonance and relaxation processes, at high and low frequencies, respectively. Dielectric spectroscopy provides a wealth of information on dipole relaxation arising from the reorentational motions of molecular dipoles, and electrical conduction arising from the translational motions of electric charges (ions, electrons).

The most common processes are four. Starting from the higher frequencies:

a) electronic polarization: a resonant process at 10^{15} Hz circa;

b) atomic polarization: a resonant process at 10^{13} Hz circa. It is found in ionic or partially ionic substances such as sodium chloride or carbon monoxide, whose molecules are formed by atoms having excess charges of opposite polarities;

c) dipolar relaxation: a relaxation process at frequencies highly depending on temperature, pressure, and chemical surrounding. The relaxation times range from several picoseconds to hours and even years. It is associated with dipoles intrinsic to molecules;

d) ionic relaxation: a relaxation process comprising ionic conductivity and interfacial or space-charge polarization. Ionic conductivity is dominant at low frequencies and high temperatures. Interfacial polarization occurs when charge carriers are trapped at interfaces in heterogeneous systems or when they are trapped by the electrode surface.

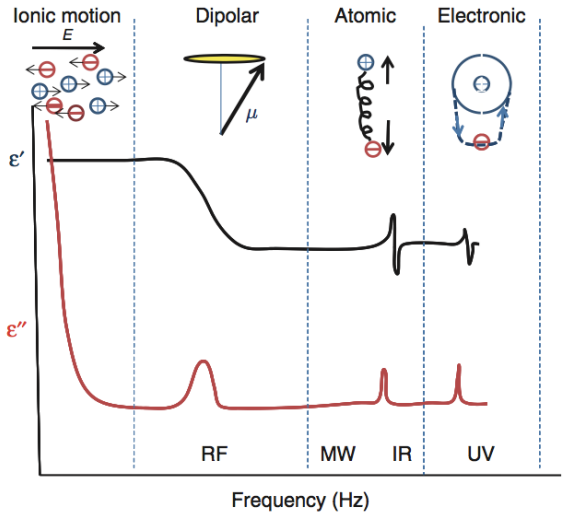

Figure 2.15: A schematic of the dielectric permittivity plotted over a broad range of requencies. The real ε' and imaginary ε'' parts are shown and the various processes are depicted [20].

Relaxation phenomena consist in the recovery of strain on removal of stress and it implies therefore a time dependence. This recovery is typically under sudden removal or sudden application of a steady stress, including the dielectric stress. The investigation of the dielectric response leads to information about different molecular motions and relaxation processes. Polymer relaxations are associated with thermally activated processes involving polymer morphology, degree of cristallinity, functional groups and dipoles resultant from oxidation. A relaxation is dielectrically active only when there is a reorientation of a dipole moment vector and also a release of space charges. For example, any presence of carbonyl dipole (C=O) and polar additives will introduce dipole moments in the polyethylene, wich may couple the molecular motions to the external field. It may be stated that dielectric relaxations of polyethylene owe their origin to the extraneous carbonyl group and/or other impurity dipoles [8].

As a general rule, studying other properties it is possible to analyse the spectrum and give physical explanation to the observed trends.

Dielectric spectroscopy is sensitive to a wide range of degradation mechanisms, related to electrical, thermal or radiation stresses. It can be performed o every kind of insulation system: solid and liquid. In particular it can be, and will be for this work, performed on cables, shielded or unshielded, multi-polar or mono-polar [8].

2.3 Previous Dielectric Spectroscopy results on PVC and EPR samples

The dielectric properties of the composite dielectric PVC/EPR samples should be, in theory, the composition of the dielectric properties of PVC and EPR. While composing the two spectra, one should make two considerations: i) that with the chosen approach, described in section 3.3.1, samples' dielectric behaviour should be mainly correlated to EPR behaviour; ii) that PVC has higher permittivity than EPR (between 3.5 and 6.5 for PVC and between 2.8 and 3.2 for EPR [24]). It is therefore interesting, while reviewing previous results, to make few considerations on the dielectric spectra of PVC and EPR. Analysis on experimental results in chapter 4 can be correlated to these results. Differences should arise because of the additives and the air-gaps.

2.3.1 Previous PVC results

Figure 2.16 shows dielectric permittivity of PVC/GTR (ground tire rubber) samples in relation to frequency, in the range 10^{-2} Hz to 10^{7} Hz, for various GTR concentrations (below 200 µm), at 30 °C [22].

Focusing on pristine or less-additived PVC, studying ε'' trend it is possible to observe a wide peak between 10^{4} and 10^{5} Hz. It is furthermore interesting to observe how this peak broadens with increasing values of ground tire rubber concentration.

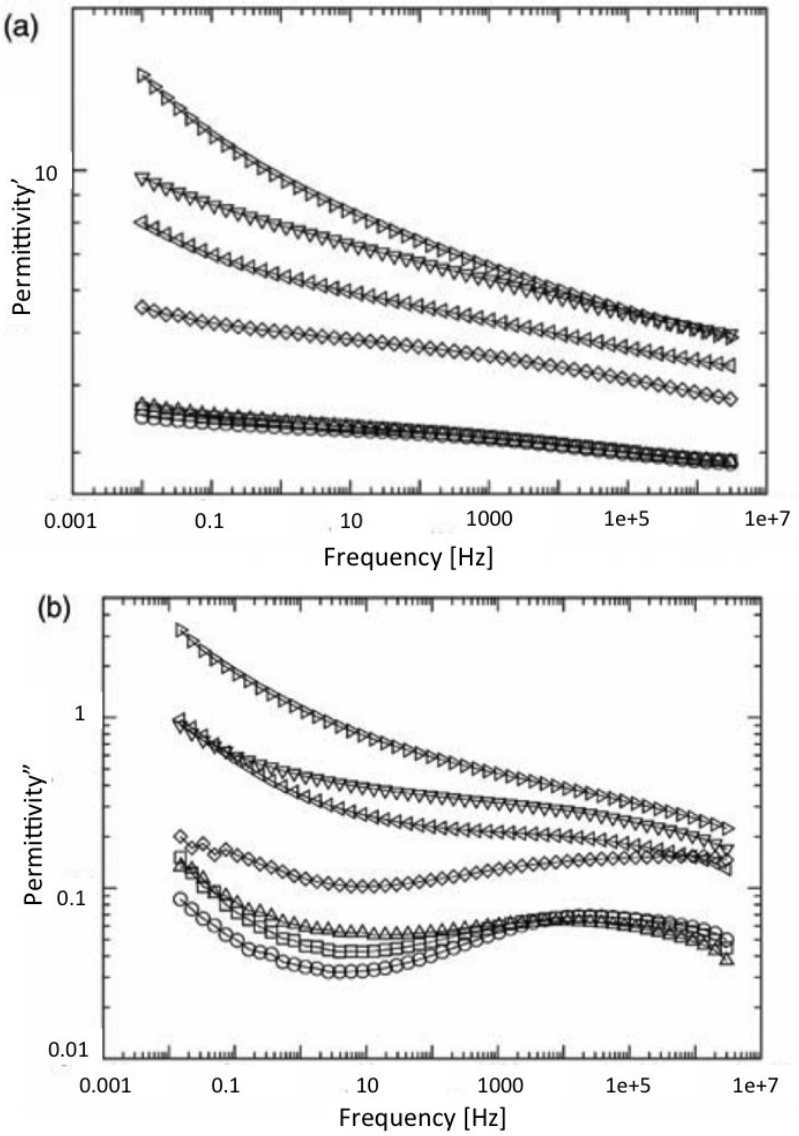

Figure 2.16: (a) Real and (b) imaginary dielectric permittivity of PVC/GTR (<200 µm) in relation to frequency. Legenda: ◯ pristine PVC; □ PVC +5% GTR; ◇ PVC +10% GTR; △ PVC +20% GTR; ◁ PVC +40% GTR; ▽ PVC +50% GTR; ▷ PVC +70% GTR [22].

2.3.2 Previous EPR results

In previous works [8], complex permittivity has shown a marked, monotonic trend with the stress levels (radiation and temperature) for polymers such as XLPE, EPR and EVA. This suggests to extend this methodology for the samples at issue.

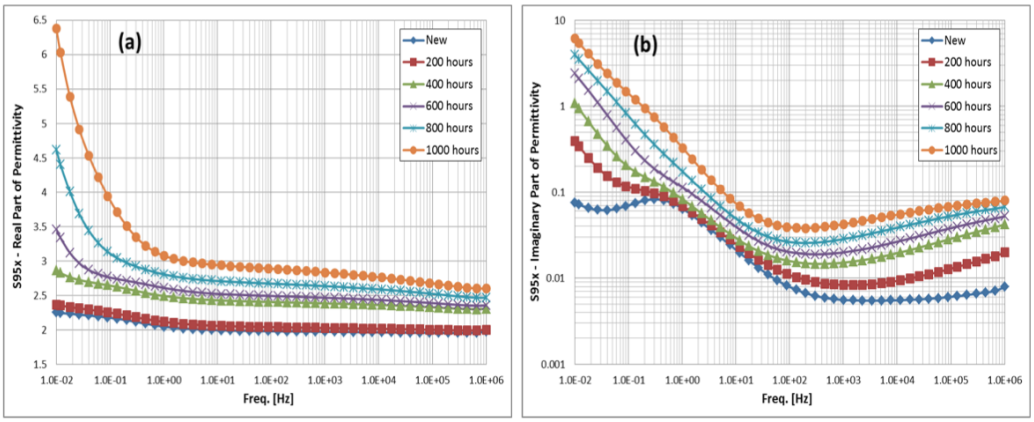

Figure 2.17: Real and imaginary part of permittivity as function of frequency for EPR samples aged at 85 °C with irradiation dose rate of 1.58 kGy/h, for different aging times [8].

Therefore, image 2.17 shows a previous result on and EPR sample, simultaneously aged with radiation and temperature.

One should research, on permittivity trends over the whole frequency range, two effects of the ageing:

1. how values change with the ageing time, for both the parts of permittivity;

2. how the shape of the polarization peak(s) of ε'' changes with the ageing time.

In these results it is possible to observe that ε' and ε'' increase over the whole frequency range. In addition, interesting information can be gathered

from the only polarization peak present in ε'' for this sample, in this frequency range. Peak broadens with increasing time until it disappears after 400 h. Probably this disappearance is because the polarization phenomenon is covered by the conductivity, as supported by the wide variations in ε' in correspondence of this region of the spectrum.

What we are researching is if a parameter, such as dielectric permittivity, can be correlated with ageing. Therefore it is interesting to study how real and imaginary permittivity, at chosen frequencies, vary with the ageing level.

In particular for this study, 0.1 Hz, 50 Hz, and 100 kHz, were selected as frequencies for, respectively, the low, the medium, and the high frequency region.

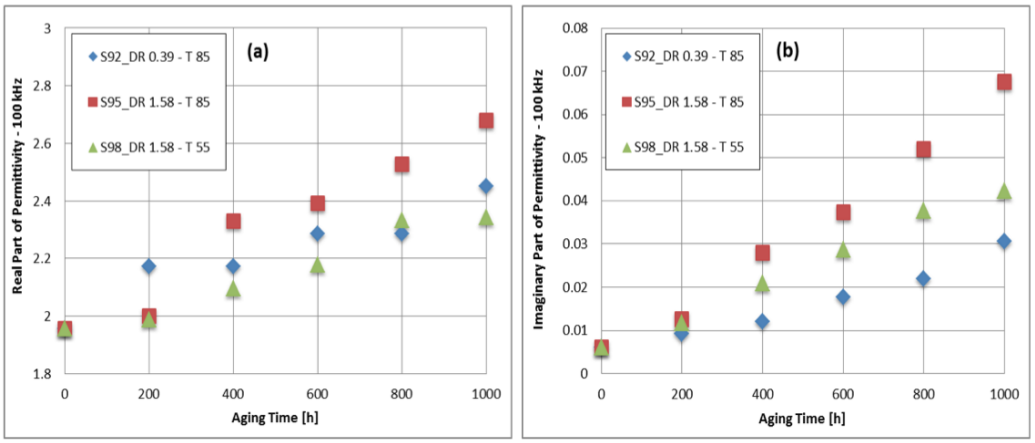

Figure 2.18: Real and imaginary part of permittivity at 100 kHz versus ageing time for EPR samples [8].

Image 2.18 shows the trends of permittivity parts at different ageing times, at 100 kHz, in a linear-linear plot. It is possible to observe that ε' and ε'' have monotonic trends, increasing linearly with the ageing time. Furthermore, the slope of the fitting line increases with temperature and with dose rate.

Finally, since one single diagnostic property is not sufficient to assess the state of the cable, the correlation curves (cross plots) between permittivity and another of the mentioned CM diagnostic properties should be studied.

Therefore one could study the cross plot of elongation at break and Young's modulus with imaginary part of permittivity at 100 kHz.

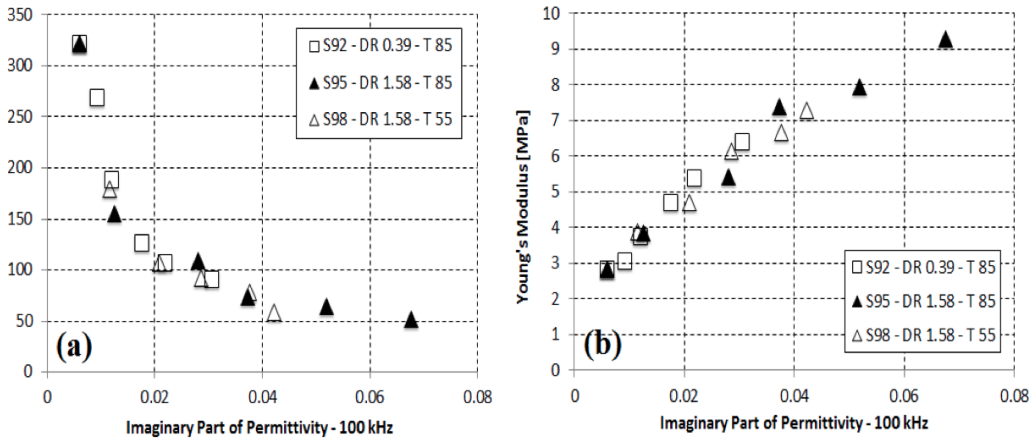

Figure 2.19: Crossplots of (a) EaB and (b) Young's modulus with ε'' at 100 kHz [8].

EPR samples are the one showing the best correlation with tensile testing, in the reported study. Results for different ageing conditions almost overlap and correlation curves can be found. This could be due to the absence of DLO, and should be verified with a specific analysis. In particular, observing 2.19a, it is possible to see that when EaB drops below 100%, ε'' shows a remarkably increase. In addition the correlation curve between Young's modulus and ε'' (2.19b) is almost linear: it is immediate to extend the Young's modulus end-of-life conditions to the ε'' end-of-life conditions.

These samples exhibit remarkable results and show how permittivity can work as a diagnostic marker for thermally and radiation aged EPR cables. In particular, the degradation of the EPR-based insulations can be reasonably well monitored through dielectric spectroscopy, using the imaginary part of permittivity at 100 kHz.

Chapter 3

Description of Samples and Methodology

A brief description of the samples, object of this study, as well as a description of the approach to measurements, will be hence given.

3.1 Description of the Samples

For this study, eighteen EPR/PVC cable samples have been provided by the Pacific Northwest National Laboratory (Washington). Cable samples are Okonite-FMR Okoseal, catalogue number 202-10-3203, rated for 600/100 V.

The structure of the samples, shown in fig. 3.1, as well as the dimensions[1] of the composing parts are:

- three copper conductors, stranded wire; total diameter: 1.84 mm;
- three EPR-based electrical insulators: black, blue, pink, thickness: 1.46 mm, total diameter of the insulated conductor: 3.40 mm;
- PVC-based outer jacket, average thickness: 1.56 mm (1.21 mm in the thinnest point, 1.92 mm in the thickest point);

[1]Those dimensions were measured on the unaged sample.

- other protectors and fillers: a film beneath the jacket, a braid beneath the jacket, a film between the conductors and the insulators.

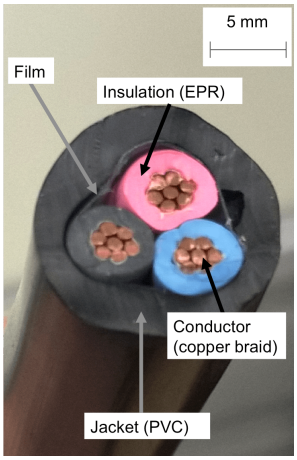

(a) Cable section

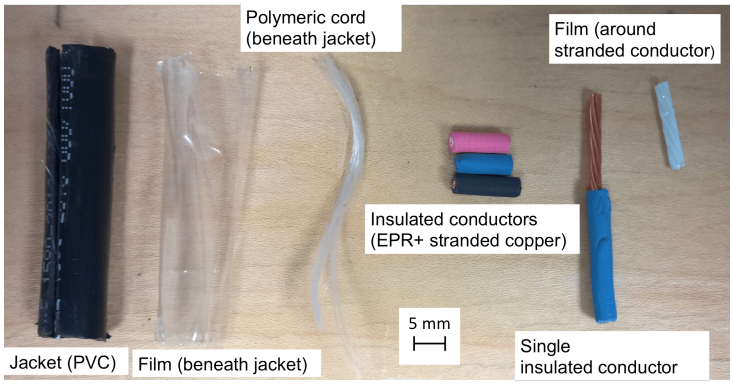

(b) Parts of the cable explicitly shown

Figure 3.1: Structure of Okonie-FMR Okoseal cable samples.

The length of each sample is around 45 cm.

These cables are suitable for power and control circuits, they're of common purpose inside a Nuclear Power Plant. As custom for cable used in NPPs, polymers are not pure but enriched with additives to enhance their electrical and physical properties.

3.2 Accelerated Thermal Ageing

To study property changes happening inside the NPP environment, to simulate, in a shorter time, physical changes happening during all the very long life time, accelerated ageing is required.

Accelerated ageing should follow as closely as possible the mechanism of long term degradation of the components of the cable during its lifetime.

As explained in section 1.3, a combination of radiation-induced degradation and thermal-induced degradation usually happens in the NPP environ-

ment. When considering synergistic effects in simultaneous ageing, it should be noted that generally radiation ageing will dominate at high dose rates wheareas thermal ageing will dominate at low dose rates [3].

Because in an operating NPP the maximum operating dose rate is about 0.1 Gy/h to 1 Gy/h, it makes sense to focus on thermal-induced degradation.

Therefore, since it would be not practical to age the cables for enormous time periods, the ageing time is accelerated by using oven temperatures higher than the expected service temperature. Typically the ageing oven temperatures are calculated based on the Arrhenius methodology using an estimated activation energy and a typical 40-year service life [9].

This methodology is widely applied and assumes that a single chemical reaction occurs under both actual and accelerated conditions.

According to the Arrhenius methodology, failure times or degradation rates are determined at elevated temperatures and these data are used to extrapolate material performance to lower temperatures.

Arrhenius extrapolations assume that a chemical degradation process (e.g. thermal oxidation) is controlled by a reaction rate k proportional to $exp(-E_a/RT)$, where E_a is the Arrhenius activation energy, R the gas constant ($R = 8.314 \quad J/molK$), T the absolute temperature and A the pre-exponential factor (eq. 3.1). Therefore, a log-plot of reaction rates (k) or degradation time ($1/k$) is expected to result in a straight line, allowing simple extrapolations to lower temperatures.

$$k = Aexp\frac{-E_a}{RT} \tag{3.1}$$

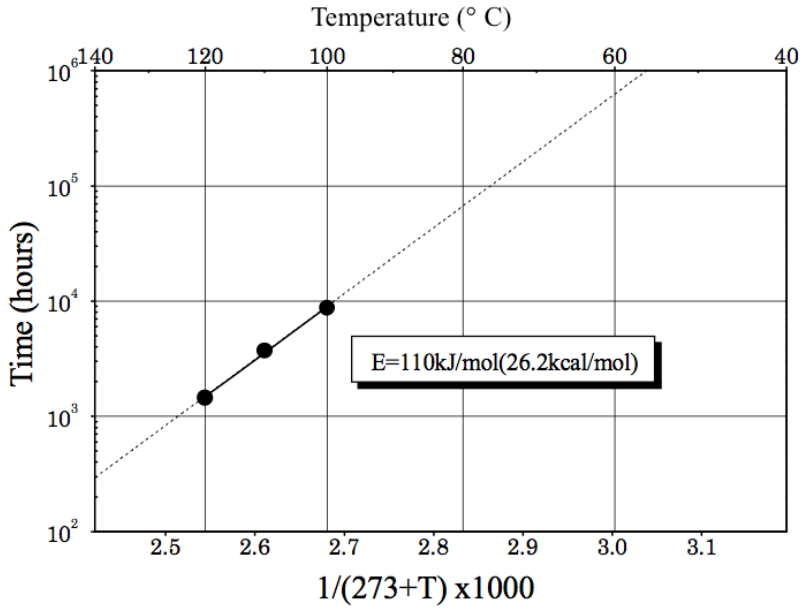

(a) Linear Arrhenius plot.

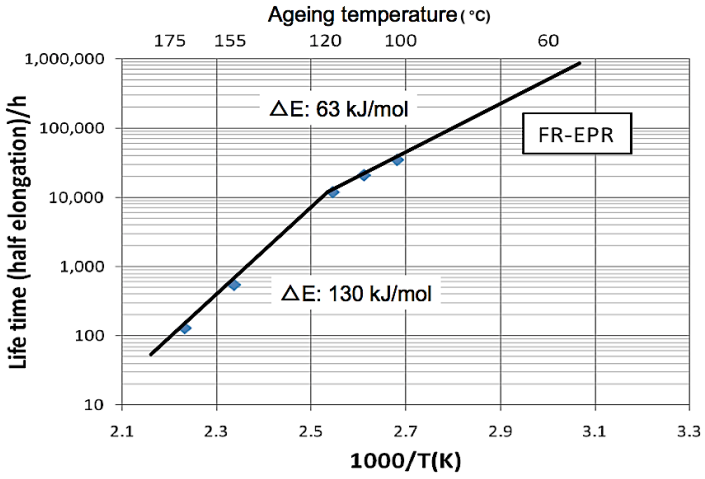

(b) Non-linear Arrhenius plot (two activation energies).

Figure 3.2: Two examples of Arrhenius plot for flame-retardant EPR from [25].

However this methodology has limitations. First, the assumption that a constant thermal environment exists in a nuclear power plant is erroneous:

temperature changes occur, both with time and location. Second, studies have shown that, for certain polymers, high temperature conditions may not induce the same single chemical reaction that occurs under actual plant conditions. This may happen in PVC materials, where plasticizer loss is the dominant mechanism at low temperatures but where hydrochloric acid (HCl) evolution nominates ad temperatures above 70 °C [3].

Also the elevated temperatures can sometimes cause multiple degradation mechanism which result in non-linear Arrhenius behaviour. This non-linear behaviour can lead to erroneous results if linear extrapolations are made.

Another concern with accelerated ageing is that it may cause heterogeneous degradation of the cable polymeric material.

One of the main degradation mechanisms for polymers is indeed reaction with oxygen. During cable service life, oxygen inside the bulk of the insulation material is consumed during oxidation, and is replenished by the diffusion process through the exterior surface. During accelerated ageing at higher temperature, if the polymer oxidation rate is higher than the oxygen diffusion rate, then the oxidation reaction in the interior of the polymer decreases because of the lack of oxygen. This results in heterogeneous degradation, with the surface of the material more degraded (oxidized or embrittled) than the interior. This is the Diffusion Limited Oxidation (DLO) and in other studies [8] showed itself with XLPE samples aged with high temperatures and gamma rays, causing the impossibility to compare dielectric diagnostic properties with the mechanical diagnostic properties.

The importance of DLO depends on geometry of the material as well as on temperature and radiation dose rate. An estimate of the sample thickness L at which DLO is significant can be made using the following equation, where p is the partial pressure of oxygen surrounding the sample, P_{ox} is the oxygen permeation rate and φ is the oxygen consumption rate in the material.

$$L \sim 2(pP_{ox}/\varphi)^{0.5} \tag{3.2}$$

Furthermore, particularly elevated oven temperatures are an additional concern with accelerated ageing because the Arrhenius equation cannot be

applied across a physical transition. Oven temperature of up to 150 °C have been used for cable testing. Most cables polymers have melting temperature ranging from 130 °C to 250 °C. Since the presence of a crystalline phase in the insulation renders the material sensitive to changes in temperature, oven condition well beyond these melting temperatures may bring large uncertainties compared to the linear extrapolation of chemical degradation behaviour at lower temperatures. Therefore oven temperatures that are too high can lead to erroneous extrapolation.

Another limitation with the use of the Arrhenius method is the estimated activation energy used in the calculations. Typically, the activation energy for a particular cable material is determined experimentally by obtaining e.g. three data points. These points are then used to estimate an activation energy for the material. However, if the actual behaviour of the material is non-linear, three data points may not be sufficient to identify this non-linearity and if linear extrapolations are made, the use of the Arrhenius methodology could produce erroneous results and underestimate or even overestimate the actual degradation in a real plant environment.

Summarizing, errors in using this approach arise when the effective curve moves away from the shape of a line. For example, in some instances DLO effects at high temperatures are responsible for curvature in Arrhenius plots and this results in longer ageing times than for non-DLO conditions.

Eventually the estimated qualified life of a polymer is very sensitive to the value used for the activation energy in the Arrhenius equation: a change from 0.1 to 0.3 eV increases the predicted qualified life from 12 to 87 years. A lower activation energy predicts a shorter life and vice versa (eq. 3.1).

The Arrhenius methodology has been studied extensively and has been shown to be a valid means of modelling thermal degradation in polymers. While the validity of Arrhenius has been proved, only limited work has been done to compare natural ageing with artificial ageing predictions for materials used in the construction of cables.

In examining the limitations of the Arrhenius method, it was found that

various materials show linear behaviour, while others do not. In studies on XLPO, chloroprene, Hypalon and nitrile rubber, these materials were found to exhibit linearity when the temperature dependence of their elongation loss is analyzed using the Arrhenius methodology. However, in studies on Ethylene-Propylene Rubber and Styrene-Butadiene Rubber (SBR) these materials were found to exhibit non-linear behaviour for elongation loss [9].

Therefore, utilizing this approach, the samples at issue have been put in an oven to be heated by a heat flow, in controlled and measured conditions. Oven temperature is chosen as 140 °C. Rated temperature of the cable is 90 C, continuous operation, wet or dry. Oven temperature has been chosen by PNNL for a matter of convenience, basing on previous results.

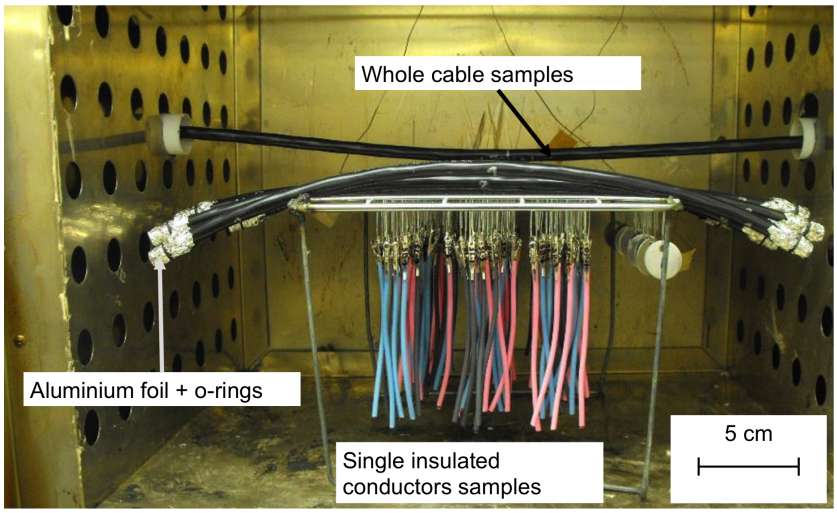

Figure 3.3: Inside the oven (photo provided by PNNL). The presence of aluminium foil and o-rings is to seal cables during accelerated ageing. The aged single insulated conductors have been used, by PNNL, to measure elongation at break.

Eventually, the table 3.1 reports the ageing conditions.

Sample #	Hours at 140 °C	Days at 140 °C
0	0	0
17	1960.60	8.2
1	205.66	8.6
2	317.66	13.2
16	326.30	13.6
3	472.66	19.7
15	479.10	20.0
4	629.06	26.2
14	640.07	26.7
5	790.03	32.9
13	796.47	33.2
6	942.83	39.3
12	951.47	39.6
11	1063.47	44.3
7	1072.53	44.7
8	1226.43	51.1
9	1269.13	52.9
10	1269.13	52.9

Table 3.1: Ageing conditions. Sample # is the number, placed on each sample by PNNL, characterizing each sample during the accelerated ageing procedure.

One of the first visual effects that has to be highlighted is that the thermal ageing has mainly damaged the outer PVC jacket of the cable causing no major damages to the insulation of the samples investigated. Effectively it is still possible to distinguish the colours of the cables (fig. 3.4).

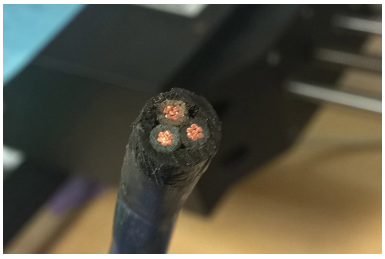

Figure 3.4: Sample #13, after 796.47 h at at 140 °C.

The eighteen samples can be divided into 3 categories on the basis of jacket integrity. For each category a different method of measurements should be taken.

100% intact : samples 0, 17, 1, 2, 16, 3, 15, 4, 14, 5, 13, 12, 11;

partially intact : samples 6 (26 cm intact), 7 (24 cm intact), 9 (11 cm intact), 10 (18.5 cm intact);

100% damaged : sample 8.

(a) Sample #16, intact.

(b) Sample #9, partially intact.

(c) Sample #8, completely damaged.

Figure 3.5: The three different condition of the samples.

For this work, measurements will be performed only on the 100% intact samples.

Even though it is possible to perform, with the same instrument, measurements on the single insulated conductors of the only 100% damaged cable (sample # 8) with a similar procedure to the one used by Verardi [8]: by measuring dielectric properties between cable conductor and an externally applied conductive sleeving, measurements on this cable will not be performed because it will not be possible to correlate the results to the results of the other seventeen samples, because of the different methodology.

The procedure for these measurements will be extensively explained successively in this chapter.

It is noteworthy to see how the outer diameter of the samples shows a monotone decrease with the increasing of the ageing hours: from 9.79 mm to 8.49 mm (nominal outer diameter is 10.2 mm), as seen in fig. 3.6.

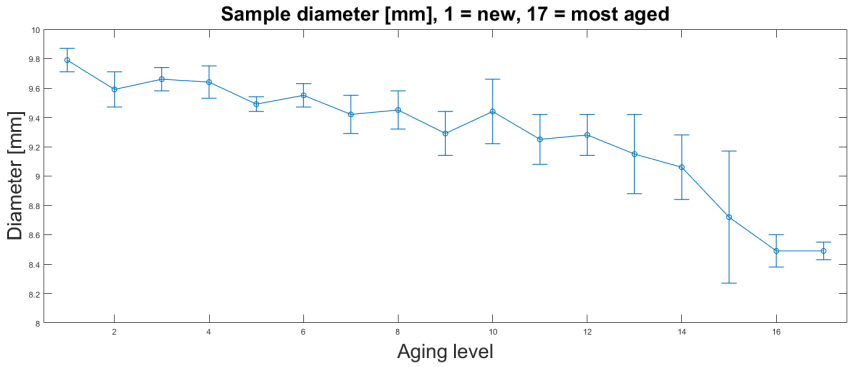

Figure 3.6: Samples diameter.

3.3 Description of the Methodology

As mentioned, Dielectric Spectroscopy has already proven [8] to be a good Condition Monitoring technique to assess the state of aged polymeric cables composed by one conductor. Holding in high regard the Non-Destructive aspect, this technique will therefore be applied on the whole, intact table, with the task of damaging and compromising samples as less as possible, in prevision of an hypothetical future reinsertion of the cables in heir original position inside the electrical system.

In fact, as seen in section 2.2, the non-destructivity and the non-intrusiveness are two essential properties a condition based diagnostic technique should have.

Ideally, not aim of this work, this technique can also be extended to an on-line measurement, with proper calibration, proper connections and proper instruments, by superimposing the measurement signal upon the work signal.

3.3.1 The approach to the sample

According to this philosophy, therefore, cable sample is seen as a capacitor with three electrodes (becoming four if one considers to apply a shielding conductive sleeving on the surface of the cable itself) which dielectric is heterogeneous and composed by, neglecting the fillers[2], three materials: PVC (jacket), EPR (insulation) and air (air-gaps).

The addition of a shielding sleeving around the cable could constitute an additional fourth electrode

Considering this it is possible to measure the impedance of the sample in seven different ways, as later described.

Then how to determine the best connection of the sample to the instrument? Which peculiarity should the chosen connection have? Answers to those questions will now be given.

[2]For this work the presence of the fillers seen in the fig. 3.1 will be neglected because of the expected small effect and the unknown composition of these.

Among the seven possible connections one should choose the one(s) in order that:

1. The measurements are well repeatable. A conductive surface surrounding the sample, connected to one of the electrodes, is expected to help having *always* the same electromagnetic structure, therefore *always* the same results of a measurement;

2. The measured capacitance of the sample is the highest possible among the configurations so that the instrument works in its highest accuracy range[3];

3. In the measured impedance, related to all the three dielectrics constituting the sample, the contribution given by the insulation is the highest possible. This has to be achieved because the degradation state of the insulation, having an important safety function, has to be held in the highest regard. While measuring a global property like the impedance of the intact cable sample, the price to pay is that the impedance is attributable to the other parts too: the jacket and the air gaps, both back-burner for this study. One should therefore choose the connection, among the possible ones, in which the contribution of the only insulation is the highest.

To help in this decision, 2D simulations with the finite element analysis software COMSOL Multiphysics have been made. A model resembling the actual samples has therefore been studied; while doing this one should pay particular attention to the jacket, which, as possible to see in fig.3.1a, does not fill all the parts but gives way to the presence of air gaps which have to be considered.

Therefore the jacket has been modelled as a cylinder which internal radius

[3]For the Novocontrol Dielectric Analyser the best performance will be reached with sample capacities from 50 pF to 200 pF (optimum performance around 100 pF), in the frequency range from 100 kHz to 10 MHz. At lower frequencies, higher capacitances up to 2 nF will yield good results too.

is lower in correspondence to the conductors, and higher in correspondence to the zone between two conductor.

Dimensions used in this model are the same reported in the section 3.1.

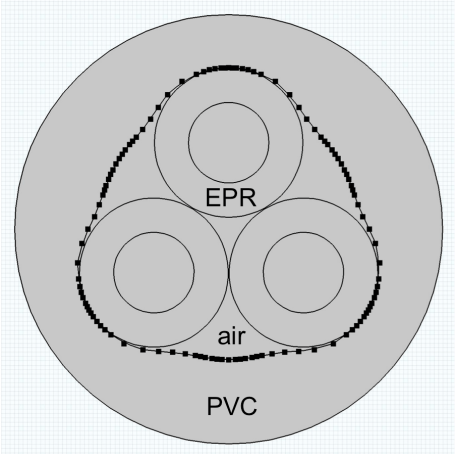

Figure 3.7: Model geometry in COMSOL Multiphysics software.

The electric permittivity of EPR and PVC based polymers strongly depend on the actual composition of the polymer; one can consider values between 3.5 and 6.5 for PVC and between 2.8 and 3.2 for EPR [24]. In the simulations, because of the unknown composition of the polymers, the value of these have been arbitrarily chosen as:

- $\varepsilon_r = 6.5$ for the PVC-based jacket;
- $\varepsilon_r = 3.2$ for the EPR-based insulation;
- $\varepsilon_r = 1$ for the air gaps.

These values have been chosen so that the simulated capacitance is as close as possible to the measured capacitance. In the actual cable, because of the potentially different values of the dielectric permittivities, it is possible that the values of capacitance and electric energy will be different from the simulated ones. But it is important to notice that for these materials it is always verified the condition $\varepsilon_{r,PVC} > \varepsilon_{r,EPR} > \varepsilon_{r,air}$, referring to the possible

values of the dielectric permittivity [24].

This means, e.g., that even though the values of the electric field E in the actual cable parts can be different from the values modelled using the software, it is always verified the condition $E_{r,air} > E_{r,EPR} > E_{r,PVC}$, which makes the method reasonable.

Therefore the seven possible configurations are, with or without the external conductive sleeving:

I) **Shielded configurations:**

10X(X): Conductor 0°: 1 V, conductor 120°: 0 V, conductor 240°: floating [4];

100(X): Conductor 0°: 1 V, conductor 120°: 0 V, conductor 240°: 0 V;

II) **Unshielded configurations:**

10X(S): Conductor 0°: 1 V, conductor 120°: 0 V, conductor 240°: floating;

100(S): Conductor 0°: 1 V, conductor 120°: 0 V, conductor 240°: 0 V;

011(S): Conductor 0°: 0 V, conductor 120°: 1 V, conductor 240°: 1 V;

1XX(S): Conductor 0°: 1 V, conductor 120°: floating, conductor 240°: floating;

111(S): Conductor 0°: 1 V, conductor 120°: 1 V, conductor 240°: 1 V.

For each one of the configurations, in electrostatic conditions, it has been possible to study and plot:

- The electric field magnitude E $[V/m]$
- The electric field lines;

[4]Note that using this symbology the sequence identifying the configuration represents the voltage of the three conductors clockwise, the letter between bracket represents the presence or not of shielding.

- The electric energy volumetric density $U = \frac{1}{2}\varepsilon E^2 \quad [J/m^3]$.

Furthermore it has been possible to evaluate:

- The capacitance C of the cable;
- The capacitance in the vacuum C_0 of the cable, needed to correlate impedance to permittivity;
- The integral of the electric energy volumetric density on selected surfaces: on the insulation only, on the whole cable, on the whole except the insulation, respectively defined as[5]:

$$w_{ins} = \iint_{ins} \frac{1}{2}\varepsilon E^2 \, dS \quad [J/m] \tag{3.3}$$

$$w_{tot} = \iint_{tot} \frac{1}{2}\varepsilon E^2 \, dS \quad [J/m] \tag{3.4}$$

$$w_{rest} = \iint_{rest} \frac{1}{2}\varepsilon E^2 \, dS \quad [J/m] \tag{3.5}$$

- the ratios between these quantities.

The results of the simulations can finally be shown in the following pages.

[5]While the electric energy density is a volumetric density, which dimension is an energy over a volume (J/m^3), the integral of the electric energy density on a surface is a linear density, which dimension is an energy over a length (J/m).

I) Unshielded configurations

a) 10X(X). Conductor 0°: 1 V, conductor 120°: 0 V, conductor 240°: floating.

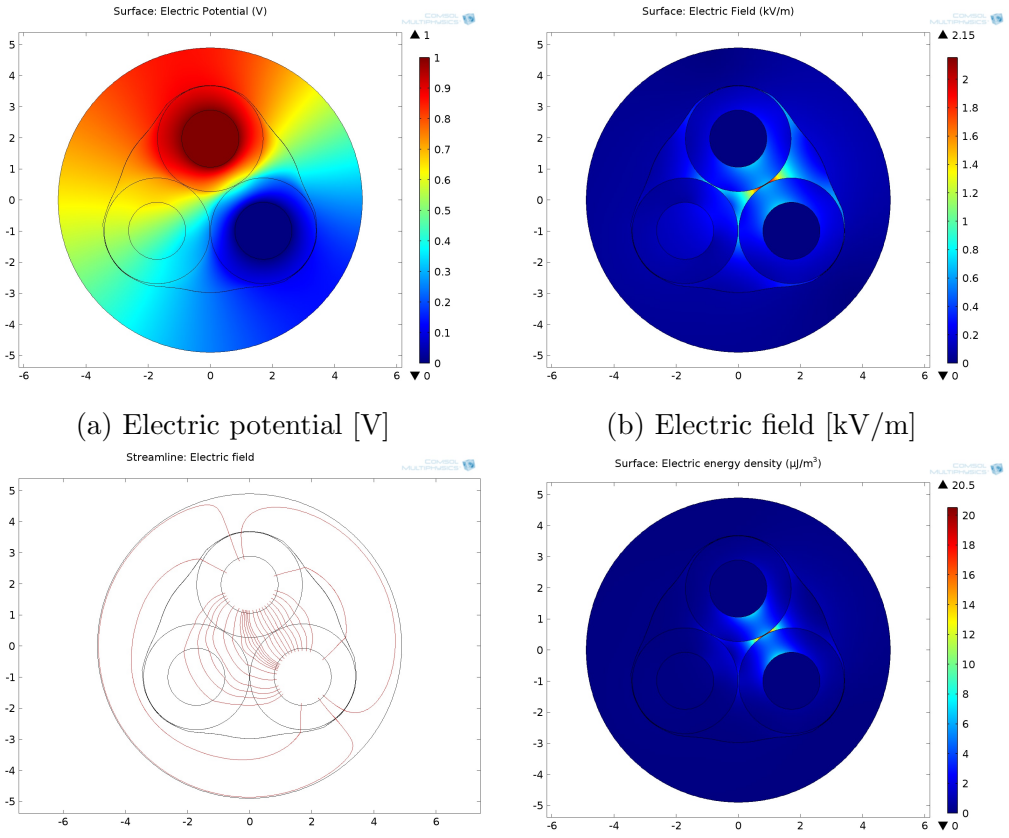

(a) Electric potential [V]

(b) Electric field [kV/m]

(c) Electric field lines

(d) Electric energy density [μJ/ m^3]

Figure 3.8: Configuration 10X(X)

C	26.35 pF	C_0	8.89 pF
C/C_0	2.96	w_{ins}	17.92 pJ/m
w_{tot}	29.25 pJ/m	w_{rest}	11.33 pJ/m
w_{ins}/w_{tot}	61.26 %	w_{ins}/w_{rest}	1.58 pF

Table 3.2: Properties for configuration 10X(X).

b) 100(X). Conductor 0°: 1 V, conductor 120°: 0 V, conductor 240°: 0 V.

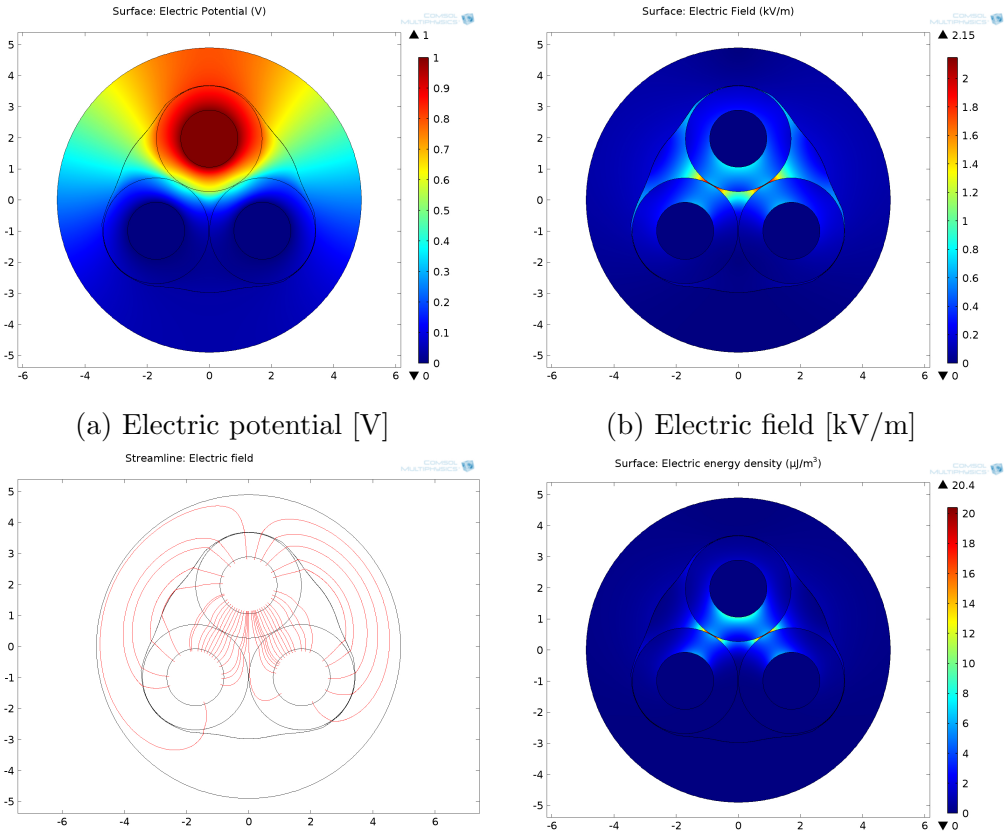

(a) Electric potential [V]

(b) Electric field [kV/m]

(c) Electric field lines

(d) Electric energy density [μJ/ m^3]

Figure 3.9: Configuration 100(X)

C	36.81 pF	C_0	12.35 pF
C/C_0	2.98	w_{ins}	25.62 pJ/m
w_{tot}	40.91 pJ/m	w_{rest}	15.28 pJ/m
w_{ins}/w_{tot}	62.63 %	w_{ins}/w_{rest}	1.68

Table 3.3: Properties for configuration 100(X).

One should highlight that electric field is highest in the air gaps, which absolutely cannot be neglected. Actually, supposing that the PVC jacket fill all the section of the cable, the behaviour of the model would be completely different.

However, even though electric field magnitude in the air gaps is about three times higher than in the insulation, the material composing the air gaps has a permittivity which is much lower (three times circa) than the one composing the insulation. This suggests to consider, as a parameter valid for the choice of the best connection, something involving the multiplication between those two properties. Therefore, the electric energy volumetric density $U = \frac{1}{2}\varepsilon E^2 \quad [J/m^3]$ is expected to be the best property to find the configuration so that the global measured property, the sample impedance, contains above all information about the insulation. For this reason images (d) show the map of the electric energy density.

One can visually see if the energy is more or less concentrated into the insulation, but at this point specific parameters, working as rankings for the various configurations, are needed. These parameters are the integral of the (volumetric) electric energy density over specific surfaces: w_{ins}, w_{tot}, w_{rest} and their ratios, previously introduced.

As one can expect, comparing 10X(X) and 100(X), in the latter capacitance is higher, because of the increased electrode surface.

It is instead surprising that both the ratios are higher in the latter as well, even if slightly. These ratios will display themselves as good properties to evaluate the best among the seven configurations, which will be chosen above all considering the highest values of these ratios (tab. 3.9).

II) Shielded configurations

a) 10X(S). Conductor 0°: 1 V, conductor 120°: 0 V, conductor 240°: floating.

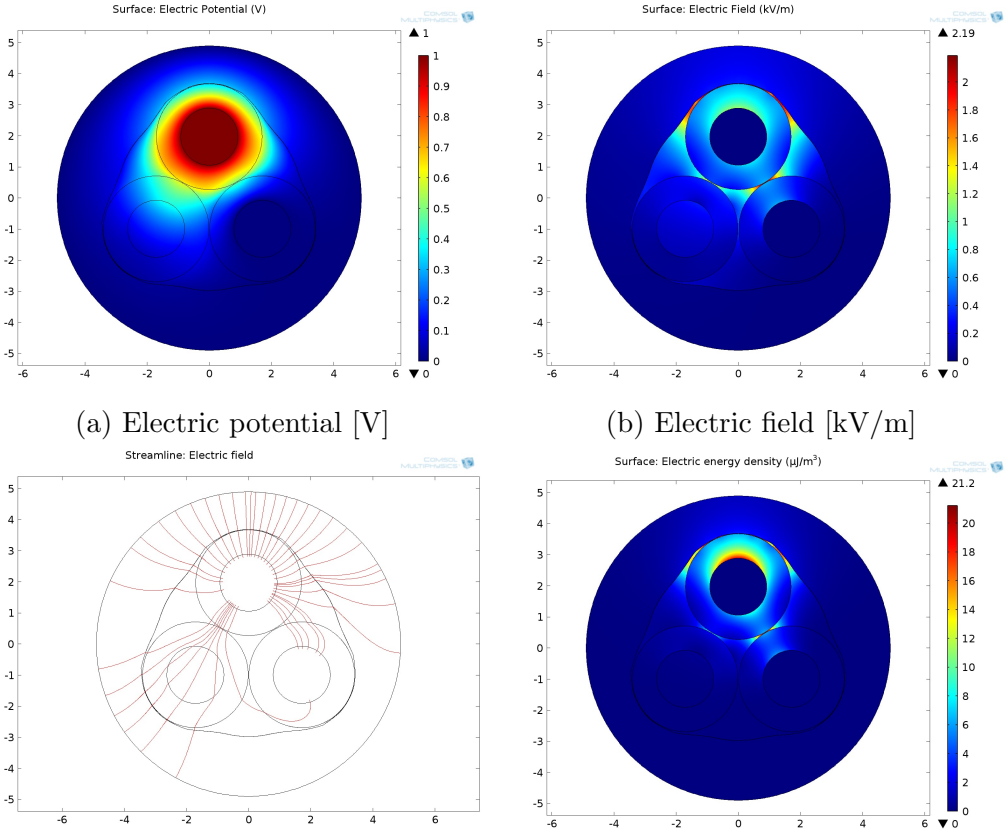

(a) Electric potential [V]

(b) Electric field [kV/m]

(c) Electric field lines

(d) Electric energy density [μJ/ m^3]

Figure 3.10: Configuration 10X(S)

C	61.89 pF	C_0	18.91 pF
C/C_0	3.27	w_{ins}	42.96 pJ/m
w_{tot}	68.77 pJ/m	w_{rest}	25.81 pJ/m
w_{ins}/w_{tot}	62.47 %	w_{ins}/w_{rest}	1.66

Table 3.4: Properties for configuration 10X(S).

b) 100(S). Conductor 0°: 1 V, conductor 120°: 0 V, conductor 240°: 0 V.

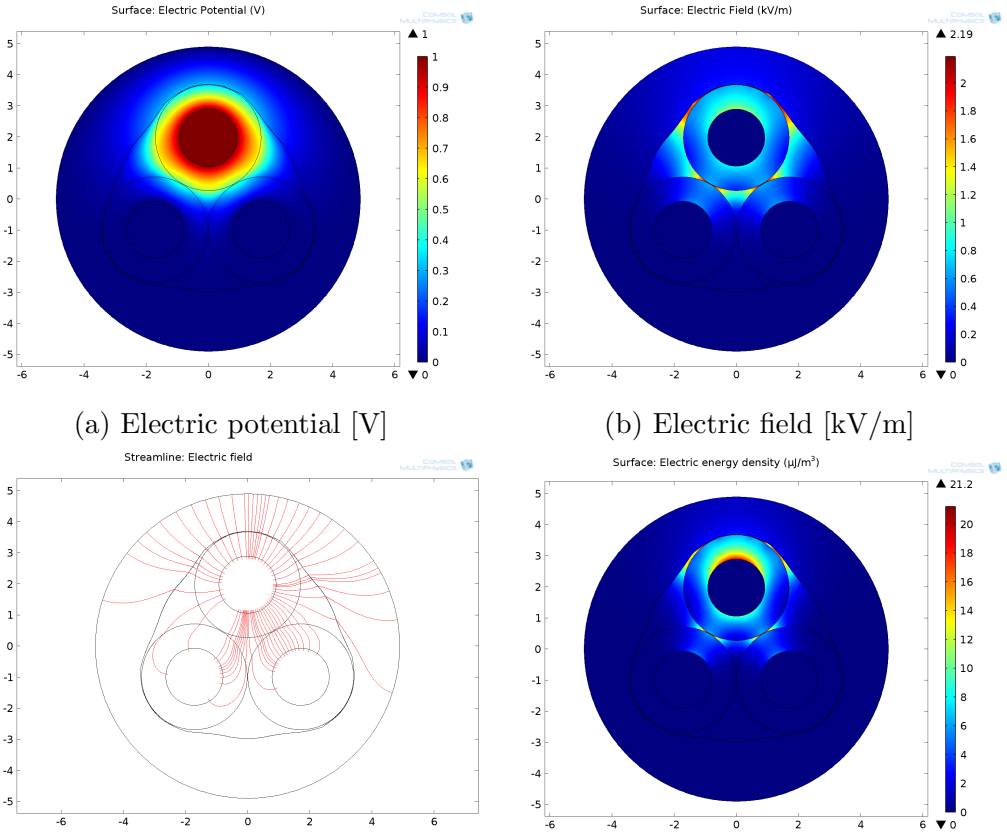

(a) Electric potential [V]

(b) Electric field [kV/m]

(c) Electric field lines

(d) Electric energy density [µJ/ m^3]

Figure 3.11: Configuration 100(S)

C	65.60 pF	C_0	20.29 pF
C/C_0	3.23	w_{ins}	47.28 pJ/m
w_{tot}	72.91 pJ/m	w_{rest}	25.63 pJ/m
w_{ins}/w_{tot}	64.85 %	w_{ins}/w_{rest}	1.84

Table 3.5: Properties for configuration 100(S).

c) 011(S). Conductor 0°: 0 V, conductor 120°: 1 V, conductor 240°: 1 V.

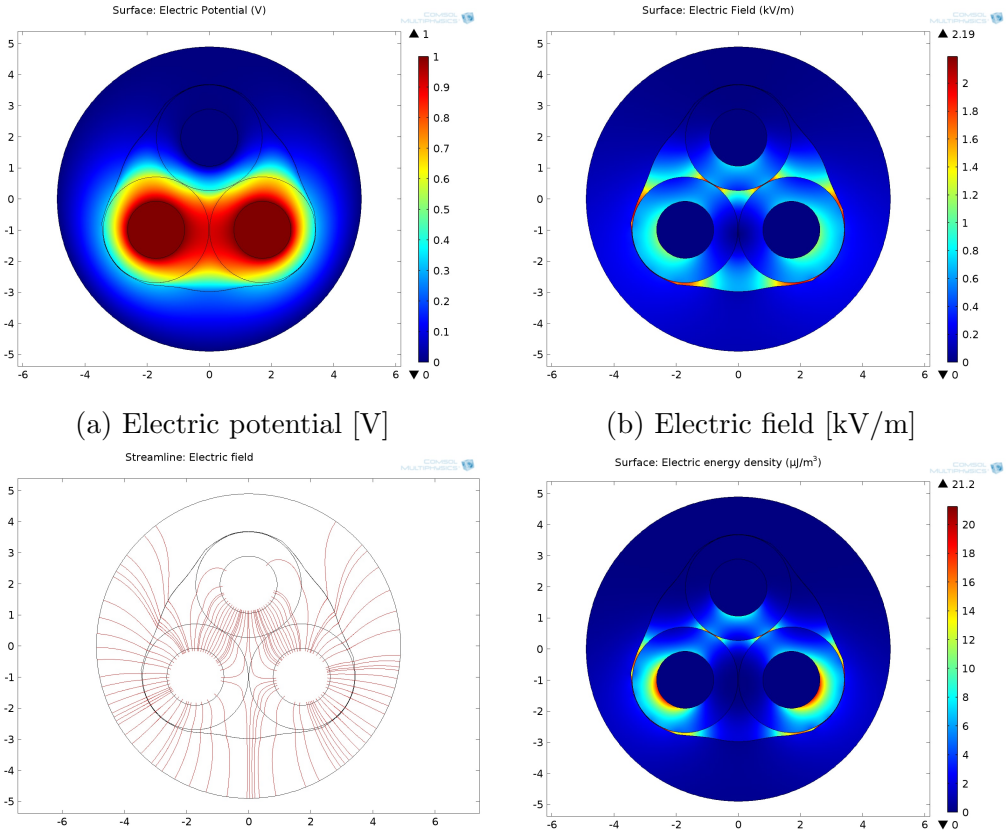

(a) Electric potential [V]

(b) Electric field [kV/m]

(c) Electric field lines

(d) Electric energy density [μJ/ m^3]

Figure 3.12: Configuration 011(S)

C	108.86 pF	C_0	31.73 pF
C/C_0	3.43	w_{ins}	73.06 pJ/m
w_{tot}	120.96 pJ/m	w_{rest}	47.90 pJ/m
w_{ins}/w_{tot}	60.40 %	w_{ins}/w_{rest}	1.53

Table 3.6: Properties for configuration 011(S).

d) 1XX(S). Conductor 0°: 1 V, conductor 120°: floating, conductor 240°: floating.

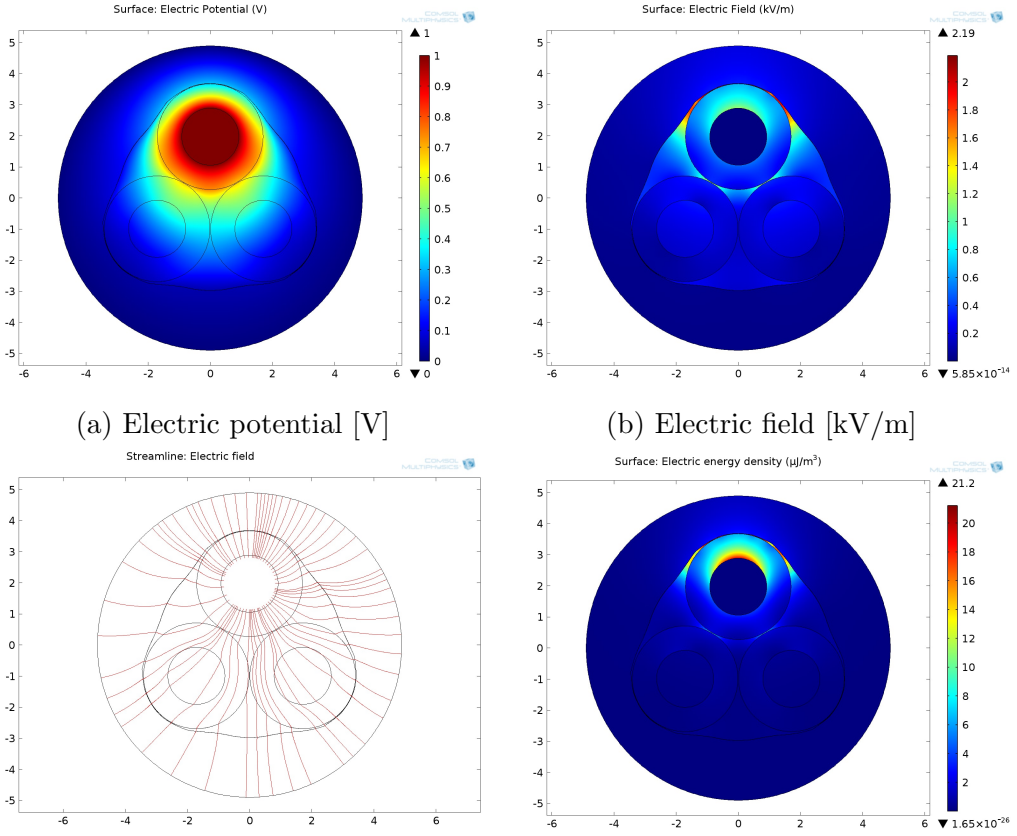

(a) Electric potential [V]

(b) Electric field [kV/m]

(c) Electric field lines

(d) Electric energy density [µJ/ m^3]

Figure 3.13: Configuration 1XX(S)

C	56.41 pF	C_0	16.84 pF
C/C_0	3.35	w_{ins}	36.34 pJ/m
w_{tot}	62.68 pJ/m	w_{rest}	26.33 pJ/m
w_{ins}/w_{tot}	57.98 %	w_{ins}/w_{rest}	1.38

Table 3.7: Properties for configuration 1XX(S).

e) 111(S). Conductor 0°1 V, conductor 120°: 1 V, conductor 240°: 1 V.

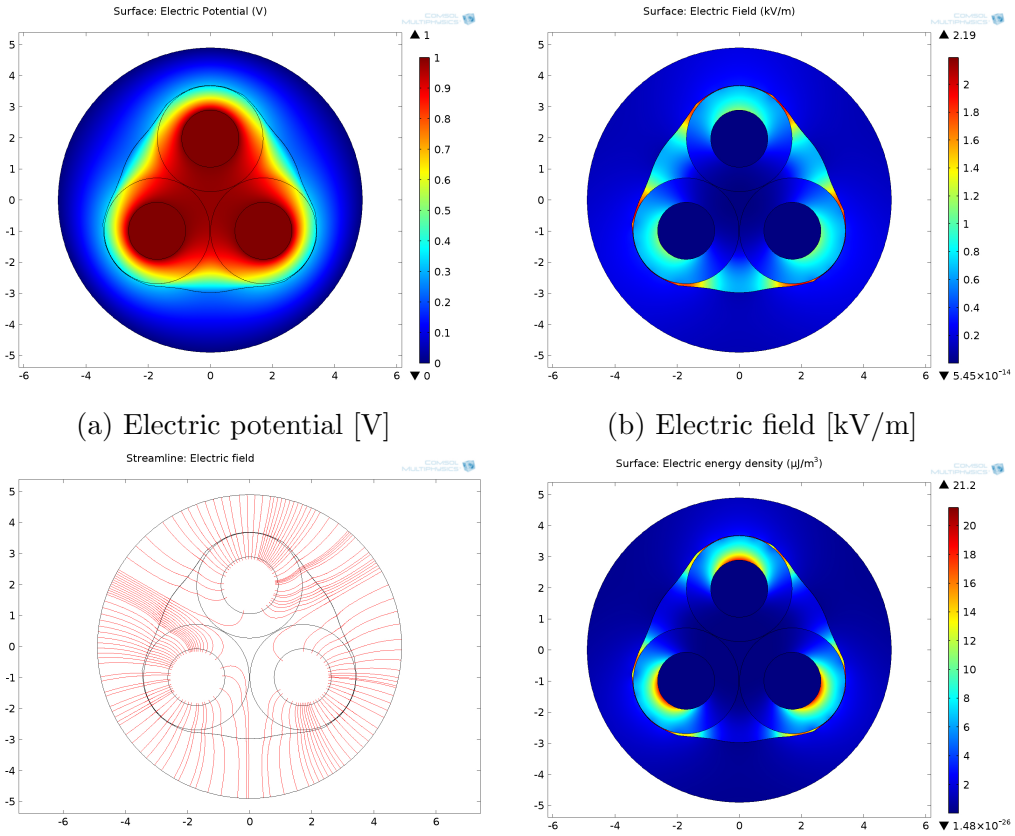

(a) Electric potential [V]

(b) Electric field [kV/m]

(c) Electric field lines

(d) Electric energy density [μJ/ m^3]

Figure 3.14: Configuration 111(S)

C	129.53 pF	C_0	34.3 pF
C/C_0	3.78	w_{ins}	77.08 pJ/m
w_{tot}	143.92 pJ/m	w_{rest}	66.84 pJ/m
w_{ins}/w_{tot}	53.56 %	w_{ins}/w_{rest}	1.15

Table 3.8: Properties for configuration 111(S).

One should highlight that in this last configuration, even though the capacitance is the highest among the seven, energy dispersion is the highest as well. This is obviously because the three central conductor are equipotential and the electric field is almost absent in the zone among the conductors.

To choose the best configuration among the seven the following table 3.9 will be very useful:

Configuration	w_{ins}/w_{tot} [%]	w_{ins}/w_{rest}	C [pF]	C_0 [pF]
Unshielded Configurations				
10X(X)	61.26	1.58	26.35	8.89
100(X)	62.63	1.68	36.81	12.35
Shielded Configurations				
10X(S)	62.47	1.66	61.89	18.91
100(S)	64.85	1.84	65.60	20.29
011(S)	60.40	1.53	108.86	31.73
1XX(S)	57.98	1.38	56.41	16.84
111(S)	53.56	1.15	129.53	34.30

Table 3.9: Summary of simulated properties.

It is immediately possible to draw the main differences between the unshielded and shielded configurations:

1. in the shielded configurations capacitance is always higher. This is because the conductive sleeving acts as an additional, wide, electrode, missing in the unshielded configurations. In these configurations capacitance can be also 5 times higher than the one in the unshielded configurations, e.g. comparing 111(S) with 10X(X). This could be particularly useful with short cable samples;

2. in the real application, the unshielded configurations should highly depend from the surrounding electromagnetic environment. In the shielded

configurations, being all the four conductive parts *always* at known potential, the electromagnetic behaviour of the sample is expected to be *always* the same, for the good of an higher repeatability.

On the basis of those considerations one should indicate the shielded configurations as the most appropriate for the designed purpose. Among the shielded configurations the ones without floating conductors (100(S), 011(S) and 111(S)) appear to be the most appropriate because the potential of all the electrodes is always at known value.

On the basis of all those considerations the chosen configuration is the 100(S), namely the conductor 0 °constitutes the electrode at high potential and the two conductors 120 °and 240 °, together with the sleeving, constitute the electrode at low potential (fig. 3.15).

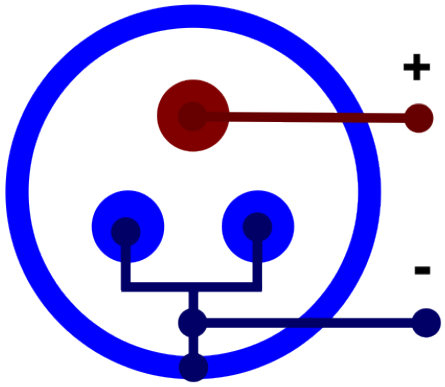

Figure 3.15: A schematic representation of configuration 100(S): the high potential electrode (+) is constituted by one conductor, the low potential electrode (-) is constituted by the other two conductors, together with the conductive external sleeving.

In these simulations, configuration 100(S) has the highest ratio energy density insulating/total over all the configurations: 64.85 %, meaning that, theoretically, almost 2/3 of the measured impedance is correlated to the insulating properties.

Lastly, among the seven configurations, capacitance of configuration 100(S) is enough high: the third highest, after the 111(S) and the 011(S).

This value of capacitance should allow the instrument to work in his best accuracy region, which is, as mentioned in subsection , between 50 and 100 picofarads. For lower sample lengths, one could favour connections with high capacitance, instead of high energy in the insulating.

In brief, configuration 100(S) has all the peculiarities searched at the beginning of this section, and it is therefore reasonable to be used.

3.3.2 The connection of the sample

The previous considerations upon the choice of the connection led us discover a method to perform measurements on intact three-phase cables, without the need to separate the three insulated conductors. To continue on this direction, the connection of the samples to the instrument can be researched so that the cable terminations are damaged as less as possible. This leads to conceive a connector, inserted on the sample using three pins, and connected to the instrument and the sleeving.

Furthermore, with this connector it is not needed to bend cables during measurements and, to place it on the sample, only few millimetres of jacket and insulator at only one termination shall be cut away.

In addition such a connector, a solid interface between the two electrodes of the cable and the instrument, leads to the possibility of having *always* the same connection conditions, aspect which contributes to having *always* the same conditions during the measurements.

The three pins have to be chosen according to the specific structure of the conductors of the cable. Each of the three conductors, which total diameter is 1.84 mm, is a stranded wire composed by seven solid conductors: a central one surrounded by six. The diameter of each one is around 0.61 mm.

The best way to connect the dielectric analyser with the stranded conductor is using three ferrules: cylinders which nominal internal diameter is

(a) Ferrules photography (from Newark website).

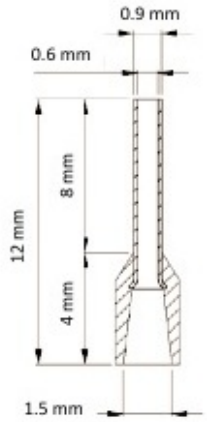

(b) Ferrule dimensions (from producer Weidmuller catalogue).

Figure 3.16: Chosen ferrules.

0.6 mm, as the one shown in the fig.3.16. Each ferrule goes around the central conductor of each braid.

The unwanted grey polypropylene insulating (fig. 3.16a) has been removed.

The idea is that a low impedance connection is achieved by means of the contact between the ferrule and the central conductor, and the contact between the ferrule and the surrounding six conductors. The conductive sleeving is connected to the low electrode through an alligator clip. All the connection cables are shielded. Preliminary measurements have showed the absence of the spikes typical of the bad connections, which makes reasonable this connection.

To give robustness to the connector, the active parts are inserted into an epoxy potting compound, as shown in figure 3.17.

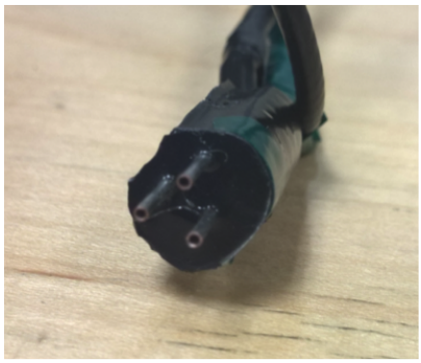

Figure 3.17: Ferrules cast in epoxy resin, constituting the head of the connector, going inside the sample. The green tape marks the two ferrules connected together.

The final appearance of the connector is like a plug, connected to *all* the samples *always* in the same way. The influence of the connector is excluded through proper instrument calibration.

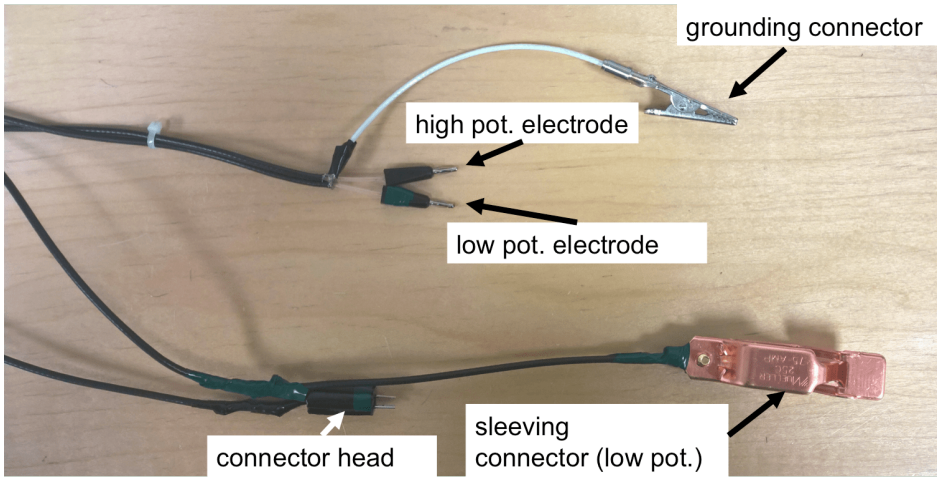

Figure 3.18: The finished connector, with the two edges highlighted. The cable is connected to the instrument using two 2 mm pins, the white cable connects the shielding of the cables to the instrument. The copper alligator clip connects the sleeving to the lower electrode. The colour green marks the low-potential electrode.

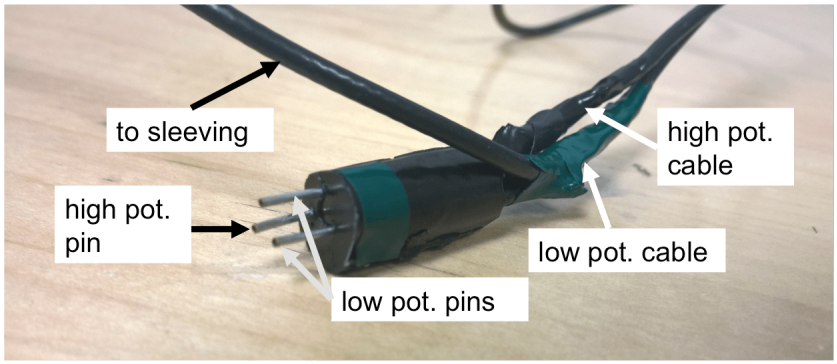

Figure 3.19: A particular of the finished connector head. The two shorted pins used for the low potential connection are marked by a green tape.

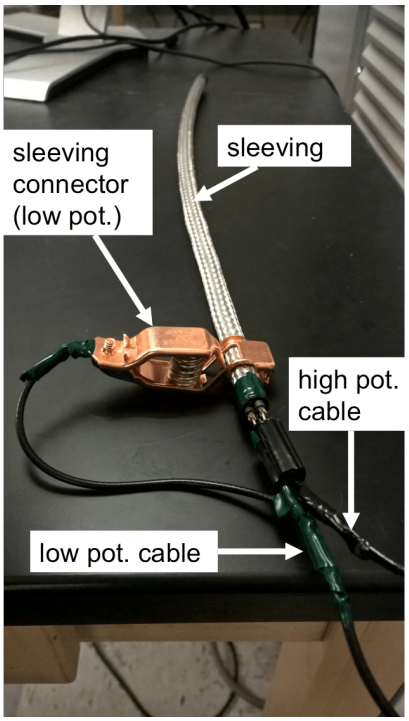

Figure 3.20: The connector attached to the sample, all the connections realized. It is possible to notice that cable does not need to be bent, and that sleeving can be applied and removed without damaging the sample.

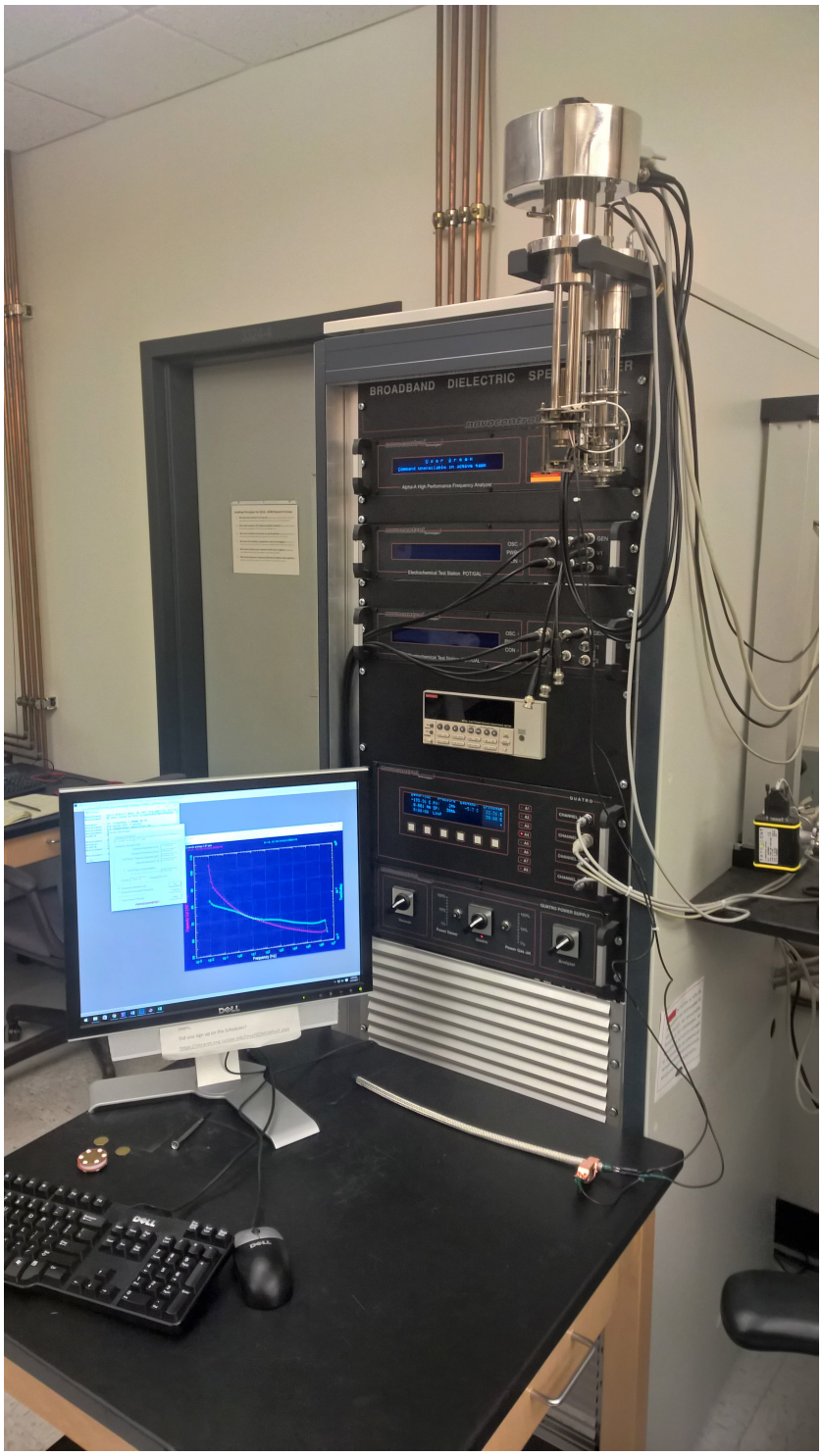

Figure 3.21: The complete measurement system.

3.3.3 A non-destructive technique?

It is interesting to analyse the modifies to the cable necessary to make this measurement possible.

Figure 3.22 shows the two edges of the cable sample before the measurement, new and intact. To perform this measurements, about 5 mm of jacket and 3 mm of insulating have to be cut off. The sleeving can be attached and removed from the cable leaving no damages. Cable does not need to be bent, which could constitute a severe mechanical stress for the most aged, embrittled, samples.

Therefore, after the measurement the only irreversible modify is the small amount of material removed to only one of the edges, while the other is not modified at all. Figures 3.23 and 3.24 show the cable edge facing the connector, after the modifies needed for the connection.

(a) Left edge of the sample, before the measurement.

(b) Right edge of the sample, before the measurement.

Figure 3.22: Sample before the measurement.

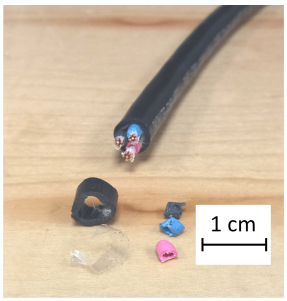

(a) Left edge of the sample, after the measurement.

(b) Right edge of the sample, after the measurement.

Figure 3.23: Sample after the measurement.

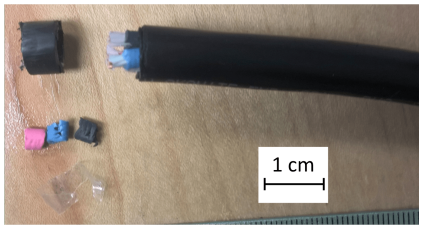

Figure 3.24: A particular of the quantity of material lost by the left edge of the sample to make the connection possible.

Chapter 4

Experimental Results and Discussion

This work started from the theoretical basis to proceed and apply those principles to the samples at issue. It is now time to study the experimental results and discuss whether the preset purposes have been achieved or not.

Among the eighteen samples, measurements were made on eight samples. These eight samples have been chosen to fulfil two requirements: i) for this sample elongation at break (EaB) results have been provided so that a comparison is possible, ii) sample is intact or slightly damaged, iii) ageing conditions of that sample are different enough from the one of the others.

Elongation at break results were performed by PNNL on the samples # 0, 1, 2, 3, 4, 5, 6, 7, 8. Among these, sample # 7 is intact for only 24 centimetres and sample # 8 is too damaged to be used: its complete jacket is destroyed (see figure 3.5c); these two samples haven't been tested. Besides those samples, it is useful, to study even the most aged samples, to consider also the intact sample # 12, and the intact part of the sample # 11, after the damaged part is cut away.

Summarizing, the following table exhibits the characteristics of the eight samples chosen to perform the measurements:

Sample #	Hours at 140 °C	EaB results?	Intact?	Length [cm]
0	0	✓	✓	45
1	205.66	✓	✓	42.5
2	317.66	✓	✓	44
3	472.66	✓	✓	44
4	629.06	✓	✓	44
5	790.03	✓	✓	45
12	951.47		✓	45
11	1063.47		in part	36.2[1]

Table 4.1: Characteristics of the chosen samples.

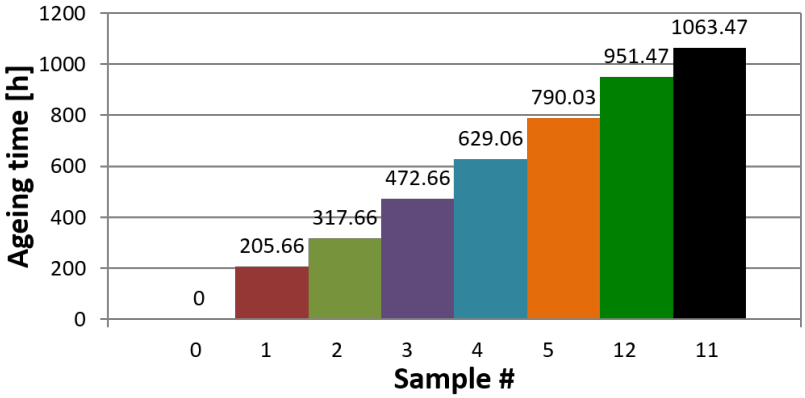

Figure 4.1: Schematic representation of the ageing conditions of the eight chosen samples.

[1]Length of the intact part.

Measurements were performed according on the methodology exhibited in chapter 3. The applied voltage is 3 V_{rms}, the studied frequency range is 10^{-2} - 10^{6} Hz. For each frequency, three measurements were performed by the analyser and the average of these displayed. To evaluate how the different dyes effect the behaviour of the insulation, for each samples three measurements were performed: one connecting the black cable at the high potential, one connecting the blue cable at the high potential, one connecting the pink cable at high potential; as exposed the two remaining cables, and the conductive outer sleeving, are connected to the low potential.

Referring to the COMSOL simulations of chapter 3, the integral of the electric energy density on the surface of the insulation corresponding to the conductor at high potential is 38.79 pJ/m, being 42.28 pJ/m the one on the surface of all the three insulation and being 72.91 pJ/m the one on the total surface of the cable section. This means that, while putting a particular colour at high potential, the energy in the insulation is 91.75 % correlated to the fed colour. Therefore each of the three measurements on the sample carries information about the colour at high potential and the effects of the different dyes can be accounted.

Referring to the equivalent parallel circuit of a real dielectric, the real part of capacitance C'_p and dissipation factor $tan(\delta)$ will be studied in the following analysis.

The error bars of these parameters are not included in the following plots because their width is smaller than the marker width. In facts, in the studied range, samples capacitance is between 45 and 115 pF, always close to the maximum accuracy range 50-200 pF, and the corresponding uncertainty is between 0.01 % and 0.1 %. Measurements were performed in room ambient, at a temperature 22 °C and at relative humidity of 26 %.

Figures 4.2 - 4.9 show capacitance and dissipation factor of each of the studied samples, as function of logarithm of frequency.

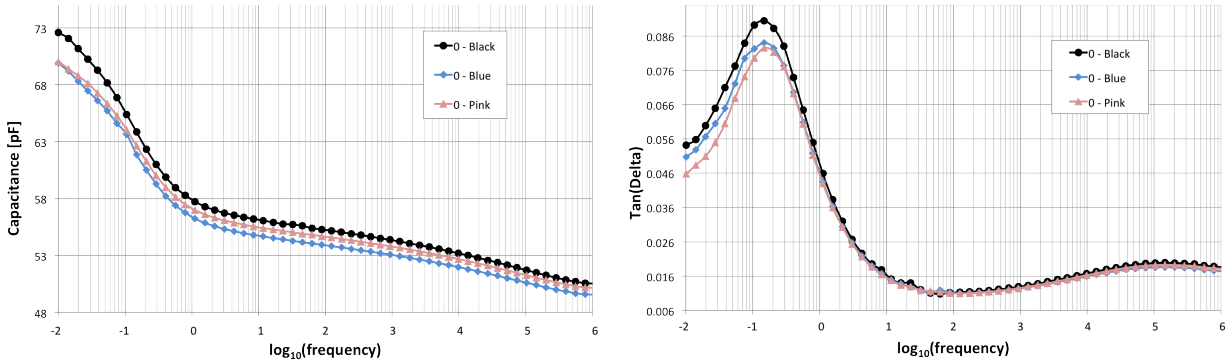

Figure 4.2: Spectra of sample # 0, unaged.

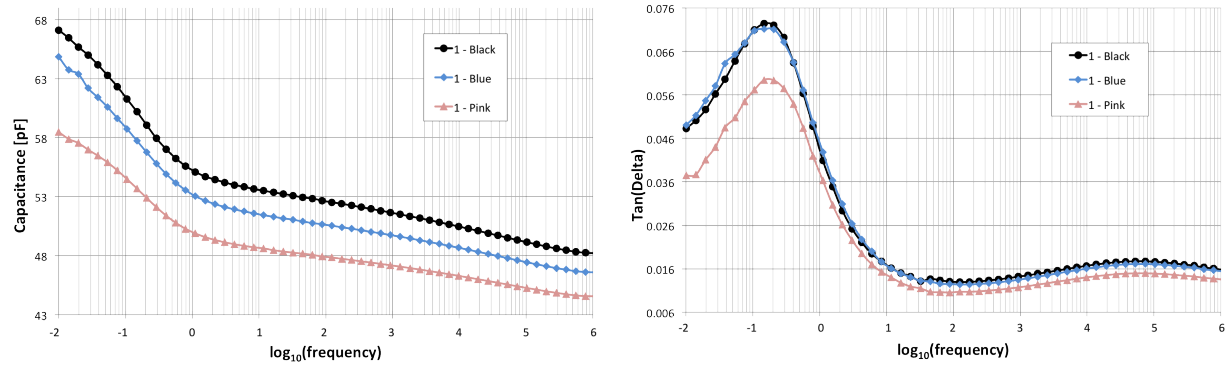

Figure 4.3: Spectra of sample # 1, aged for 205.66 hours at 140 °C.

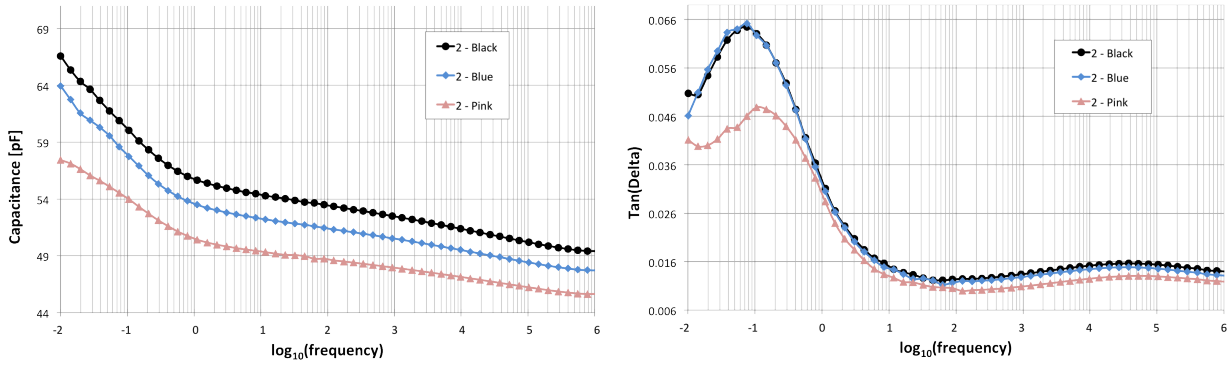

Figure 4.4: Spectra of sample # 2, aged for 317.66 hours at 140 °C.

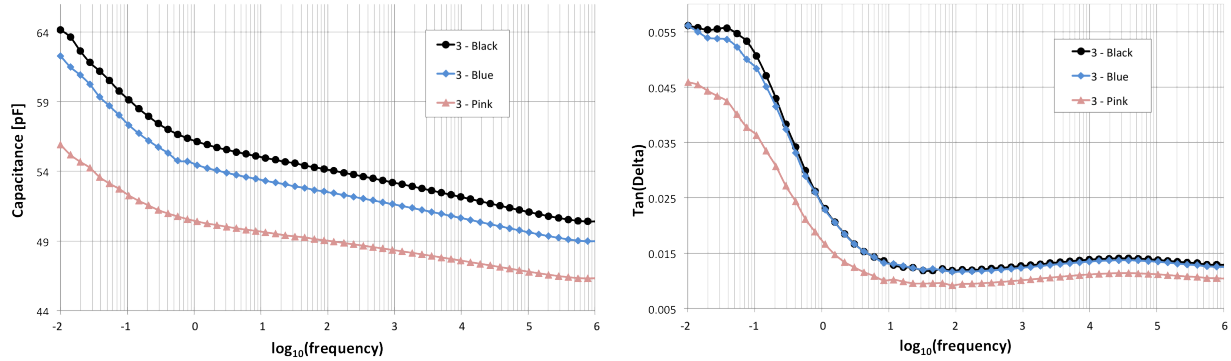

Figure 4.5: Spectra of sample # 3, aged for 472.66 hours at 140 °C.

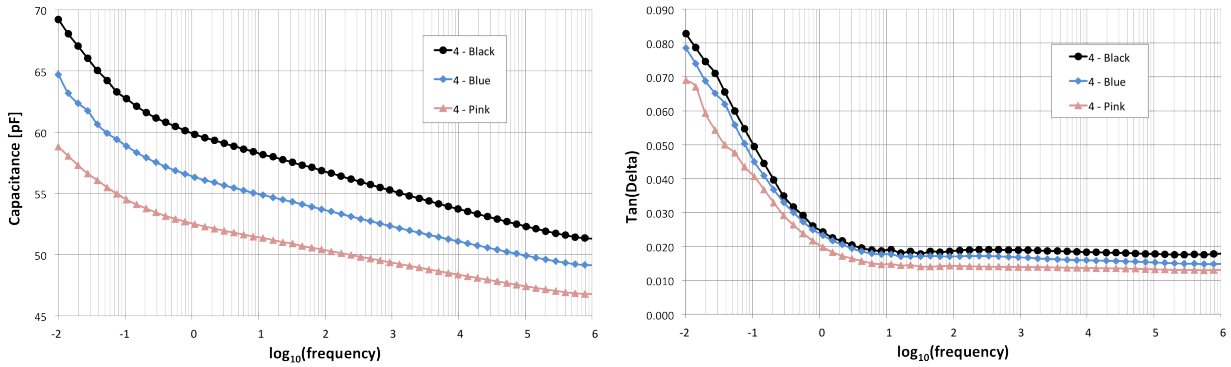

Figure 4.6: Spectra of sample # 4, aged for 629.06 hours at 140 °C.

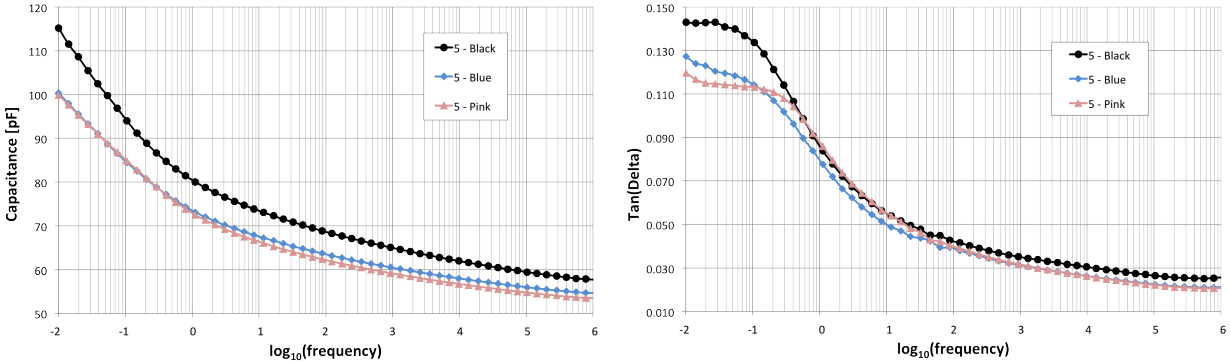

Figure 4.7: Spectra of sample # 5, aged for 790.03 hours at 140 °C.

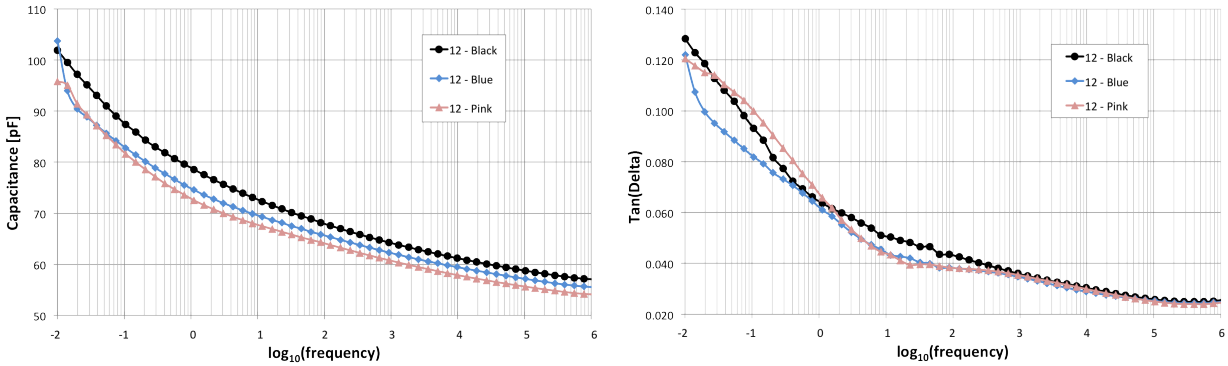

Figure 4.8: Spectra of sample # 12, aged for 951.47 hours at 140 °C.

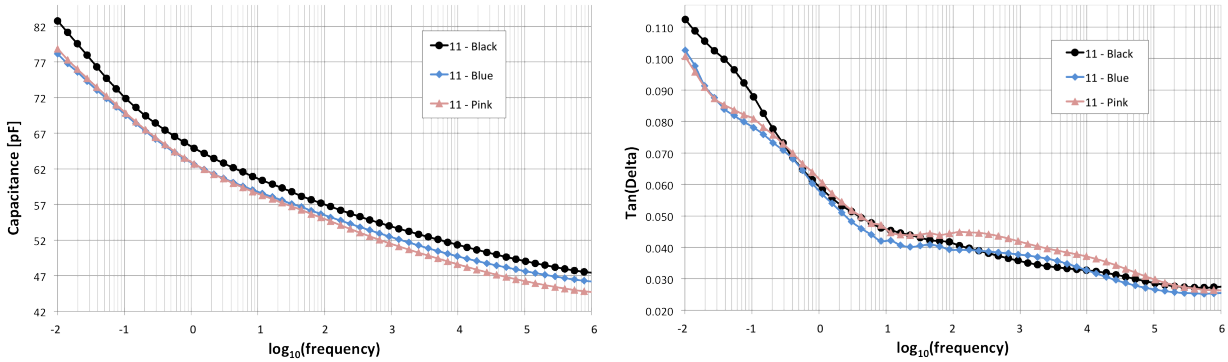

Figure 4.9: Spectra of sample # 11, aged for 1063.47 hours at 140 °C.

It is interesting to see that the dielectric properties of the black series are always greater than the one of the blue series, which are always greater than the one of the pink series, except for the unaged sample. The effects of the different dyes are clear. Furthermore, for most of the samples, the black and blue behaviours seems to be similar. This makes sense because of the similar aspect of these two colours.

It is furthermore interesting to observe that the the $tan(\delta)$ spectra exhibits two polarization peaks: one corresponding to a frequency of around 10^{-1} Hz and one corresponding to a frequency of around 10^{5} Hz. These two peaks tend

to disappear as the degradation exhibits, constituting a first visual difference between the ageing conditions.

4.1 Comparison with previous results

Referring to the previously mentioned PVC and EPR results, exposed in section 2.3, it is interesting to compare the spectra of PVC and EPR, and the obtained spectrum of the composite PVC/EPR sample cables. Observing fig. 2.16b it is possible to see that PVC has a broad peak around 10^5 Hz, while, observing fig. 2.18b, it is possible to see that EPR has a pronounced peak around 10^{-1} Hz. Observing fig. 4.2b it is clearly possible to find these two peaks in the $tan(\delta)$ spectrum of the unaged sample. The $tan(\delta)$ spectrum of the samples at issue seems to be the superimposition of the separate spectra of the two materials. Furthermore the EPR-related peak is much greater than the PVC-related one, which gives credit to the preset purpose of having a measurement above all related to the EPR insulation.

4.2 Relationship between dielectric properties and ageing

What we are going to assess is if capacitance and $tan(\delta)$ can constitute two diagnostic markers for the samples at issue. Consequently it is necessary to study how these properties vary with the ageing conditions of the samples, namely the ageing time. To compare different samples, specific capacitance (capacitance divided per sample length, listed in table 4.1) and $tan(\delta)$ are studied. The following images show these parameters of different samples, of the same colour series, plotted together.

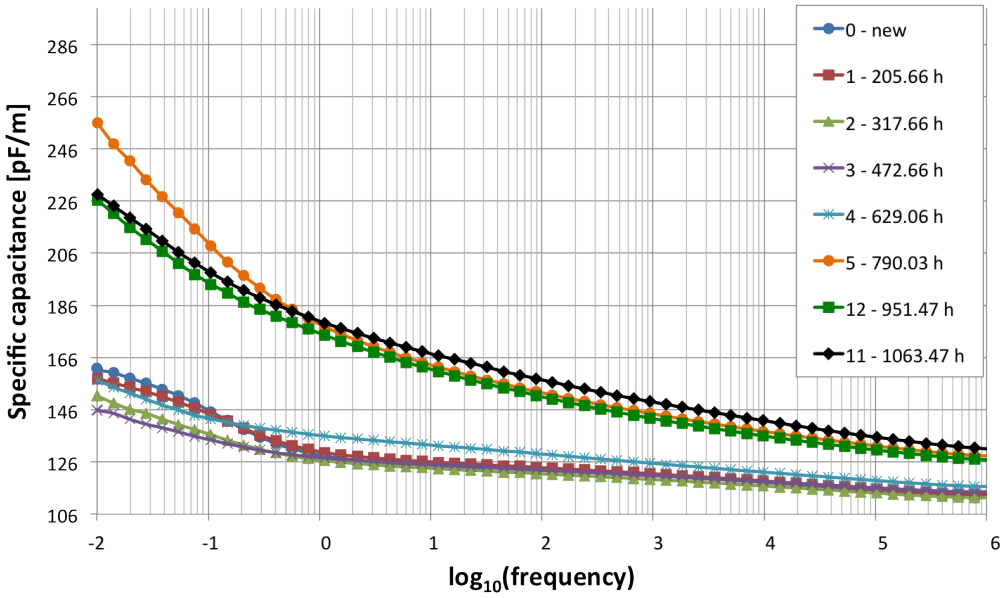

Figure 4.10: Specific capacitance of the black series over the frequency range.

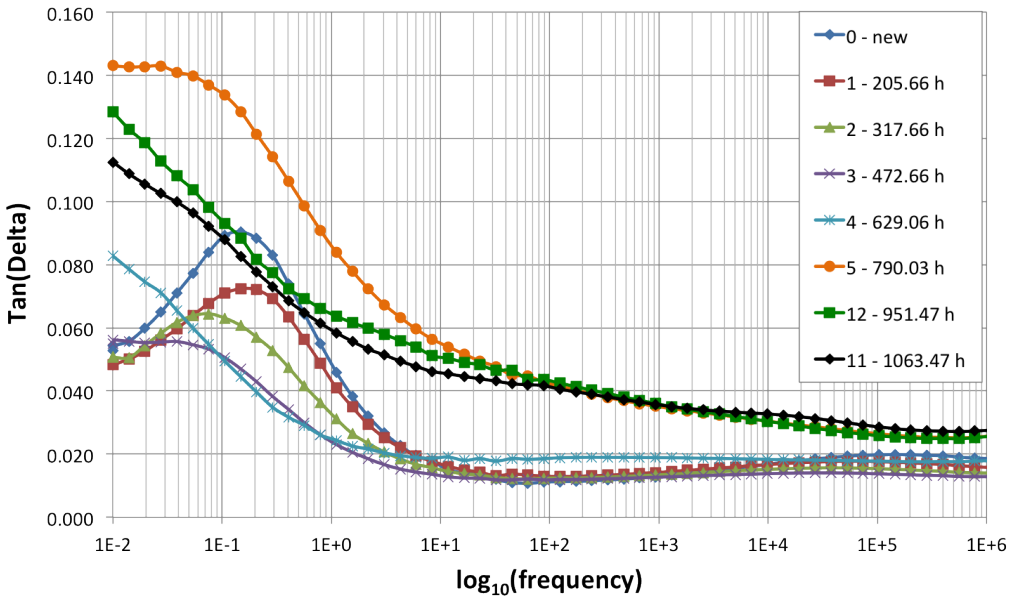

Figure 4.11: Dissipation factor of the black series over the frequency range.

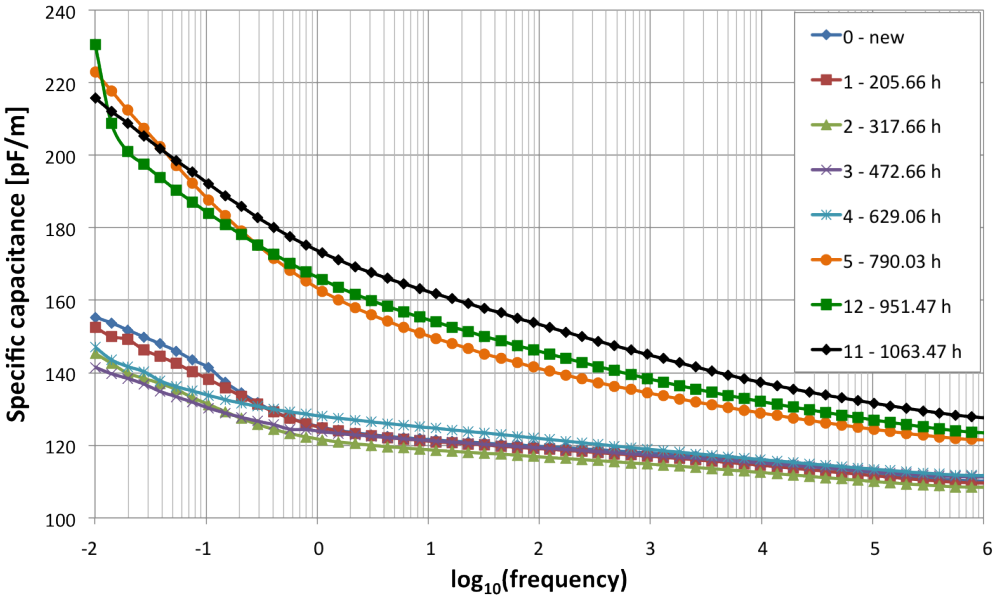

Figure 4.12: Specific capacitance of the blue series over the frequency range.

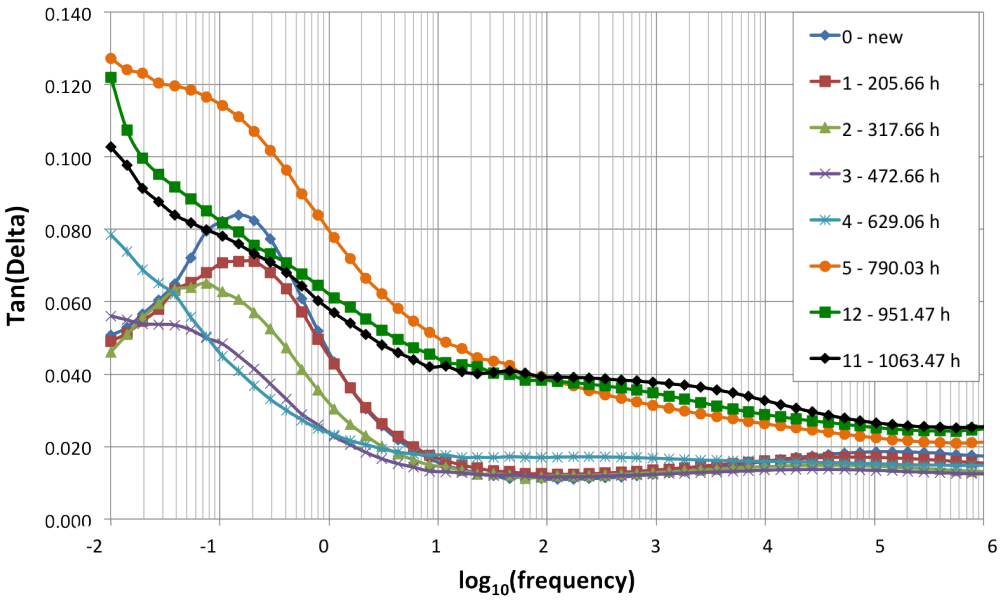

Figure 4.13: Dissipation factor of the blue series over the frequency range.

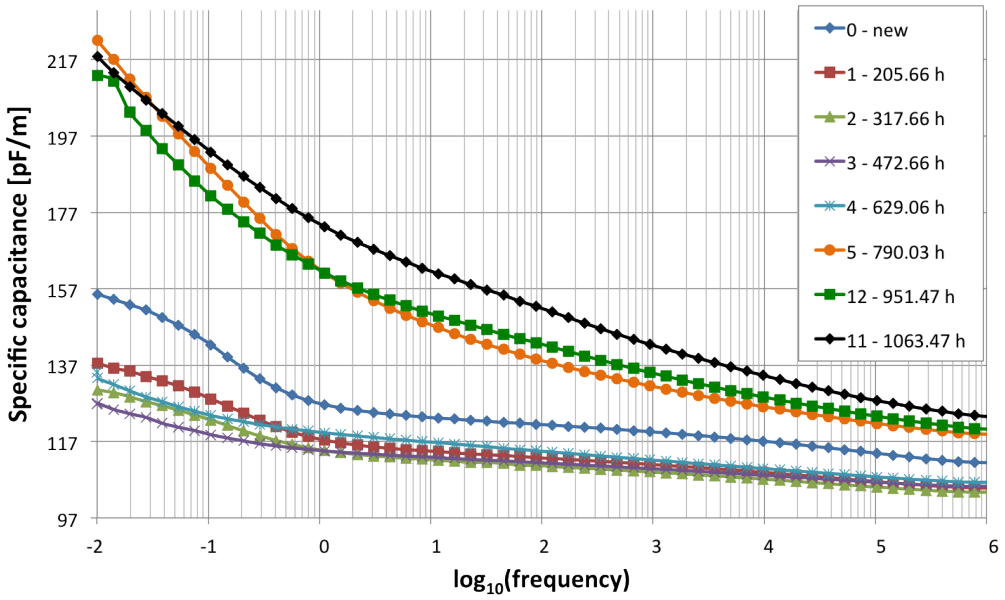

Figure 4.14: Specific capacitance of the pink series over the frequency range.

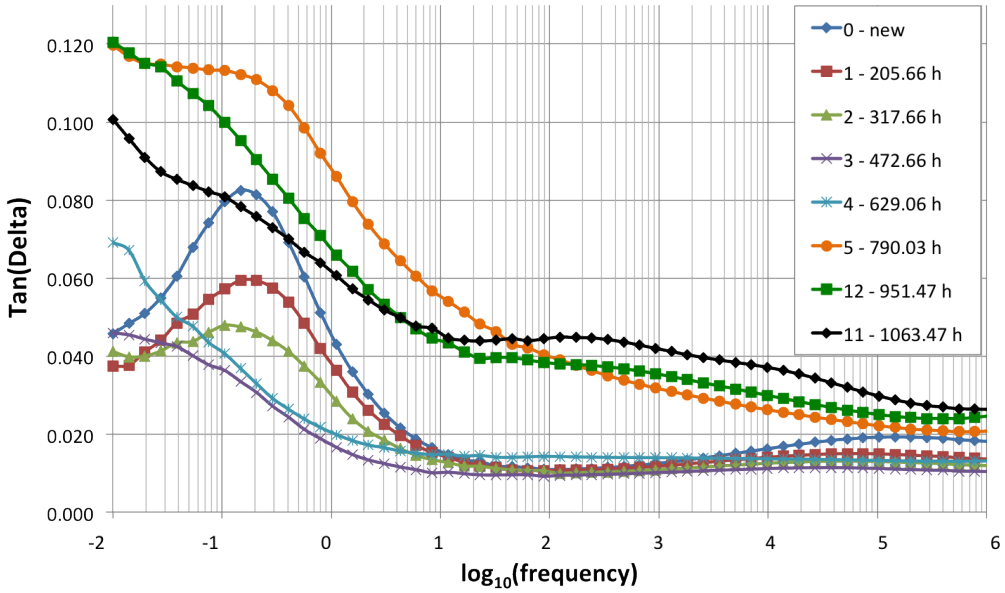

Figure 4.15: Dissipation factor of the pink series over the frequency range.

What we are looking for is a measured property, or more properties, which show a significant, marked, variation with the ageing condition, namely the ageing time. The following analysis will discuss if specific capacitance and $tan(\delta)$ can fulfil this purpose. For this aim four frequency values will be studied: 0.1 Hz, 10 Hz, 1 kHz, and 100 kHz, constituting four "slices" in the spectra so that it is possible, for each colour, to study capacitance and $tan(\delta)$ as a function of the ageing time, as shown by the images 4.16 - 4.19.

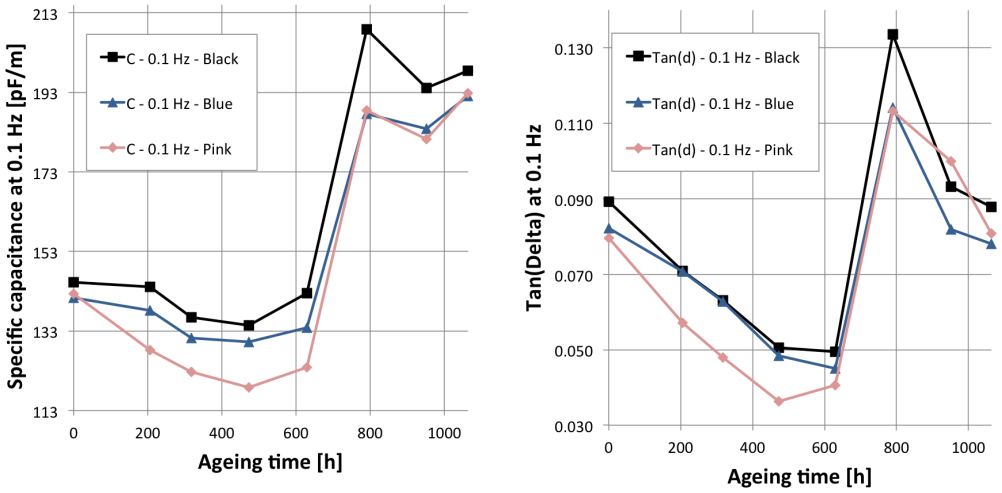

Figure 4.16: Specific capacitance (a) and $tan(\delta)$ (b) at 0.1 Hz, as function of the ageing time.

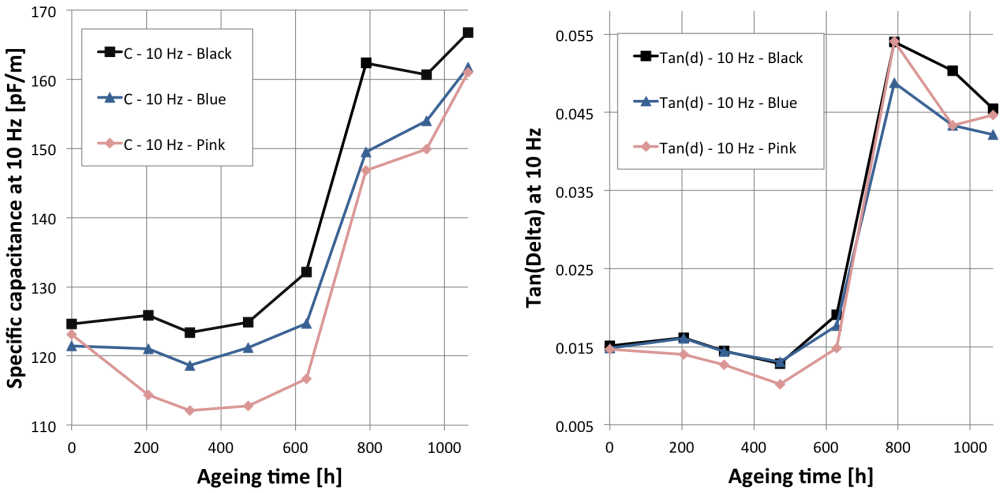

Figure 4.17: Specific capacitance (a) and $tan(\delta)$ (b) at 10 Hz, as function of the ageing time.

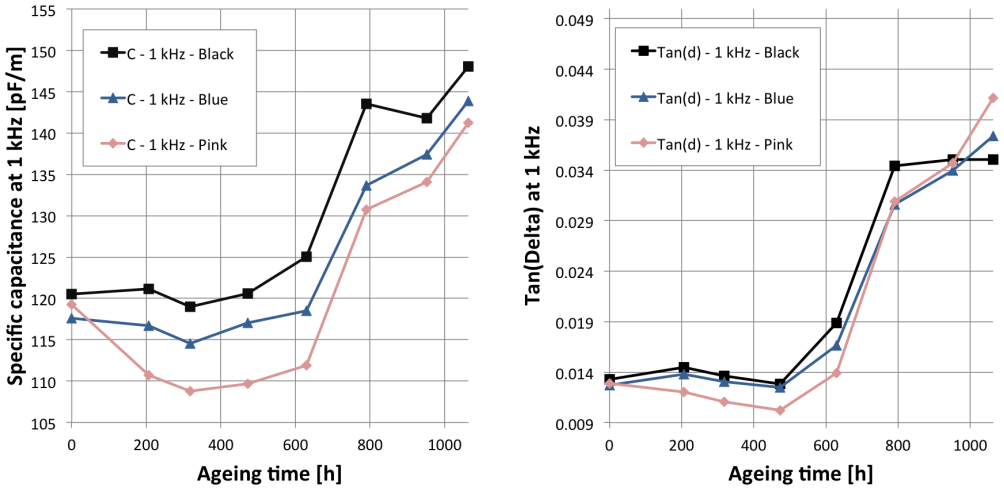

Figure 4.18: Specific capacitance (a) and $tan(\delta)$ (b) at 1 kHz, as function of the ageing time.

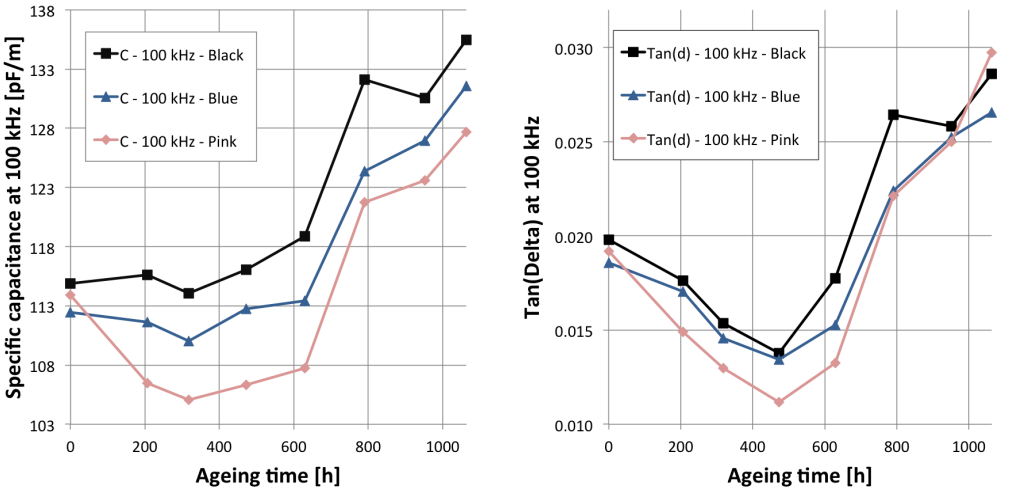

Figure 4.19: Specific capacitance (a) and $tan(\delta)$ (b) at 100 kHz, as function of the ageing time.

4.2.1 Analysis of capacitance

As possible to see, specific capacitance always show a clear, mostly monotonic, increase with ageing time. This increase is less marked at low ageing hours (below 500 hours) and at low frequency (e.g. 0.1 Hz, see fig. 4.16a). Trends become more marked, above all for the black and blue series, for properties measured at the higher frequencies. As possible to see, for the unaged sample the three colours seem to overlap but after few hours the pink series shows a drop and becomes different from the others two; this difference is less pronounced for high ageing hours.

Summarizing, in these study capacitance at 10 Hz, 1 kHz and 100 kHz is a good diagnostic marker, showing a clear increase with the ageing time.

4.2.2 Analysis of dissipation factor

Dissipation factor increases appear more confused than the capacitance ones: $tan(\delta)$ at 0.1 Hz (fig. 4.16b) does not show a monotonic trend but fluctuates around 0.08. Instead $tan(\delta)$ at 10 Hz and at 1 kHz show an excellent, marked monotonic increase. As for capacitance these trends are almost monotonic and become more marked for the most aged samples. Dissipation factor at 100 kHz shows a monotonic increase, only after 500 hours. Comparing to capacitance, the three colours almost overlap, above all for $tan(\delta)$ at 10 Hz. As for capacitance, the $tan(\delta)$ of the pink series at 0.1 Hz and 100 kHz moves away from the black and blue one, for middle values of the ageing time. The best diagnostic markers are $tan(\delta)$ at 10 Hz and 1 kHz, proving that the middle frequencies are the most appropriate for this evaluation. Furthermore, $tan(\delta)$ at 10 Hz and 1 kHz trends for the three different colours are almost overlapping.

4.3 Comparison with elongation at break

Together with the samples, the Pacific Northwest National Laboratory provided results of elongation at break (fig. 4.20). These tests have been performed on the aged single insulated conductors which can be seen in fig. 3.3. It is important to compare the dielectric properties with this mechanical property, to highlight common points as well as differences.

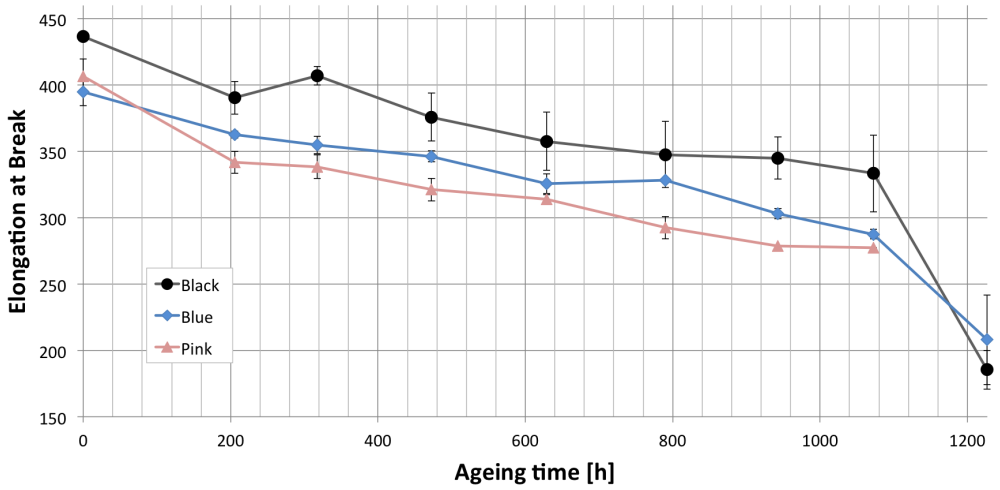

Figure 4.20: Elongation at break results.

As possible to see in fig. 4.20, this property has a slow, continuous decrease with the ageing time, showing a sudden drop after 1100 hours. It is interesting to study if the same behaviour is showed by the dielectric properties and in which case the variation is the highest. Therefore the following figures 4.21 - 4.28 show three axis plots. In each of these, the X axis is the ageing time (hours) and the left Y axis is the relative elongation at break in percentage, defined as the ratio between the elongation at break at a given ageing time and the elongation at break of the unaged sample; multiplied 100 times. The right Y axis is the specific capacitance, or the dissipation factor divided per the corresponding property of the unaged sample and multiplied times 100. The numeric values of the properties of the unaged sample, used to normalize EaB, capacitance and $tan(\delta)$ are shown in the table 4.2.

	Black series	**Blue series**	**Pink series**
	Elongation at break		
	406.67 ± 12.84	436.45 ± 3.43	394.69 ± 10.19
Frequency [Hz]	**Specific capacitance [pF/m]**		
10^{-1}	145.29	141.42	142.33
10^{1}	124.60	121.49	123.12
10^{3}	120.49	117.62	119.26
10^{5}	114.89	112.43	113.91
Frequency [Hz]	**Dissipation factor**		
10^{-1}	$8.92{\cdot}10^{-2}$	$8.23{\cdot}10^{-2}$	$7.95\ {\cdot}10^{-2}$
10^{1}	$1.51{\cdot}10^{-2}$	$1.48{\cdot}10^{-2}$	$1.47\ {\cdot}10^{-2}$
10^{3}	$1.33{\cdot}10^{-2}$	$1.27{\cdot}10^{-2}$	$1.29\ {\cdot}10^{-2}$
10^{5}	$1.98{\cdot}10^{-2}$	$1.86{\cdot}10^{-2}$	$1.92\ {\cdot}10^{-2}$

Table 4.2: Elongation at break, specific capacitance, and dissipation factor for the unaged sample (sample # 0).

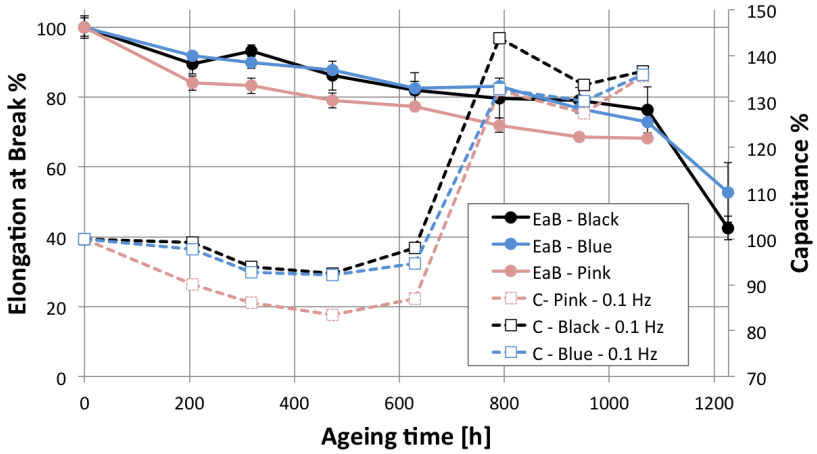

Figure 4.21: Comparison between elongation at break and capacitance at 0.1 Hz.

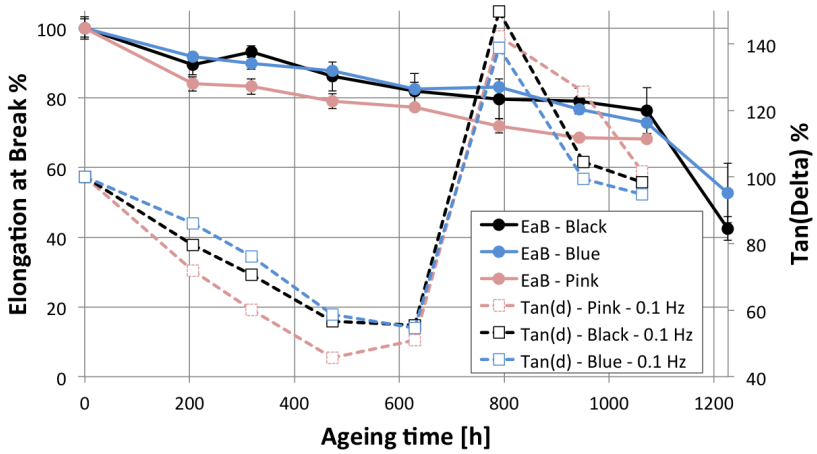

Figure 4.22: Comparison between elongation at break and $tan(\delta)$ at 0.1 Hz.

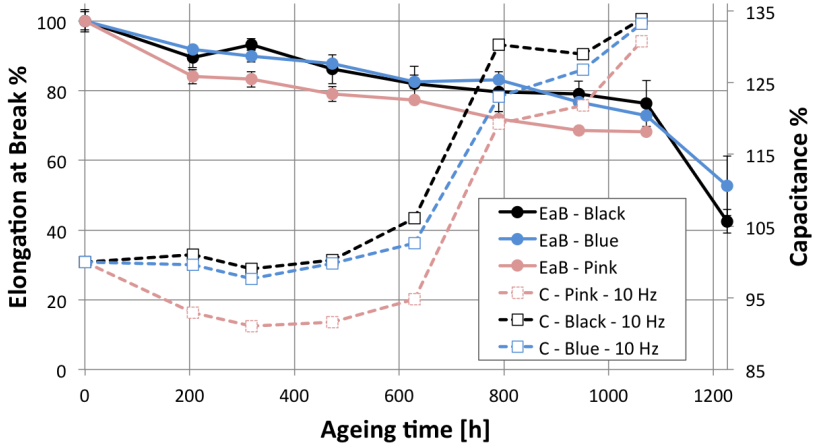

Figure 4.23: Comparison between elongation at break and specific capacitance at 10 Hz.

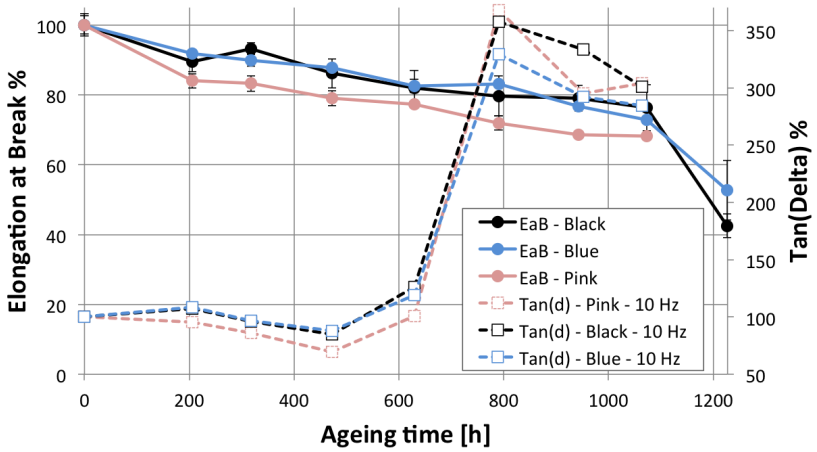

Figure 4.24: Comparison between elongation at break and $tan(\delta)$ at 10 Hz.

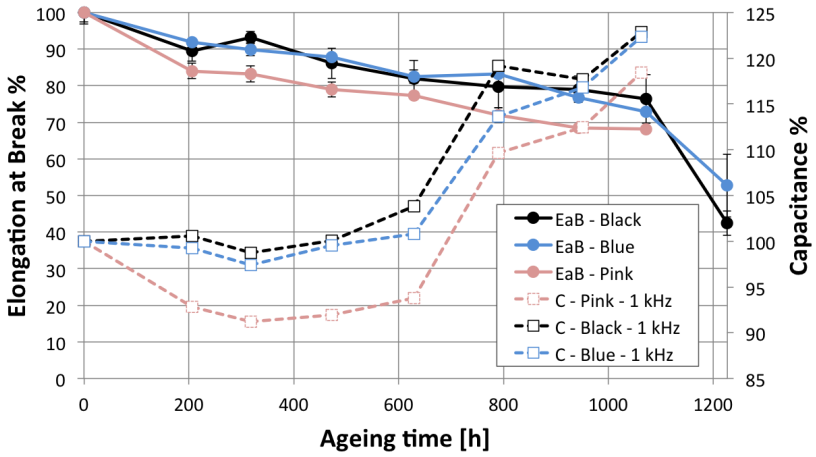

Figure 4.25: Comparison between elongation at break and specific capacitance at 1 kHz.

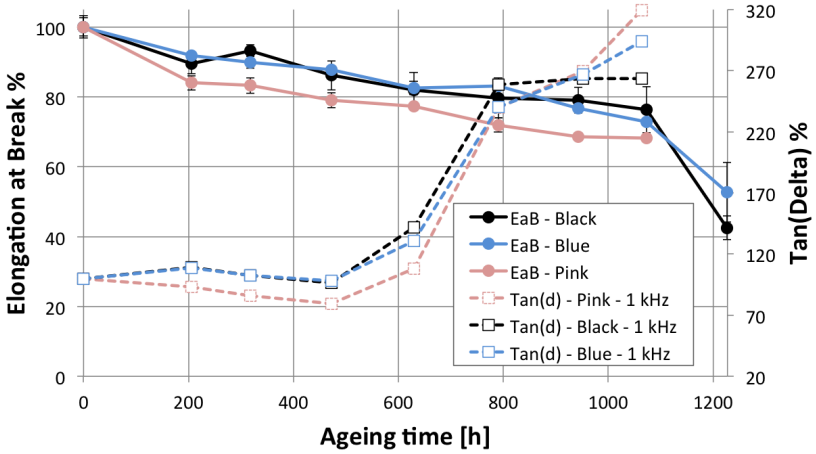

Figure 4.26: Comparison between elongation at break and $tan(\delta)$ at 1 kHz.

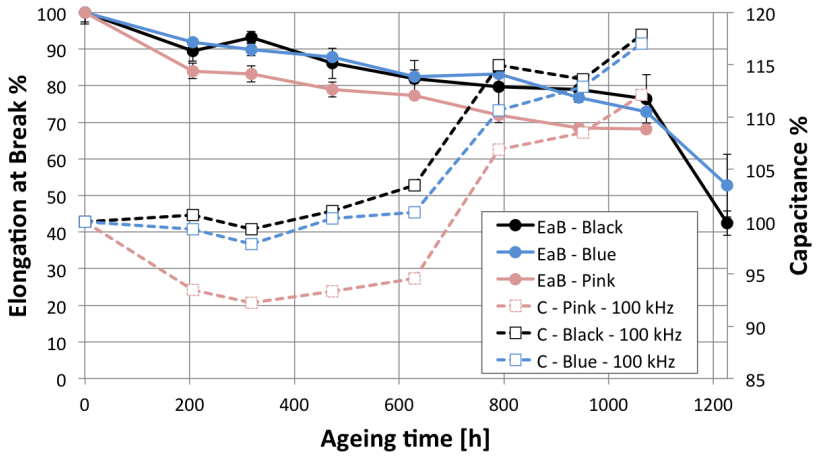

Figure 4.27: Comparison between elongation at break and specific capacitance at 100 kHz.

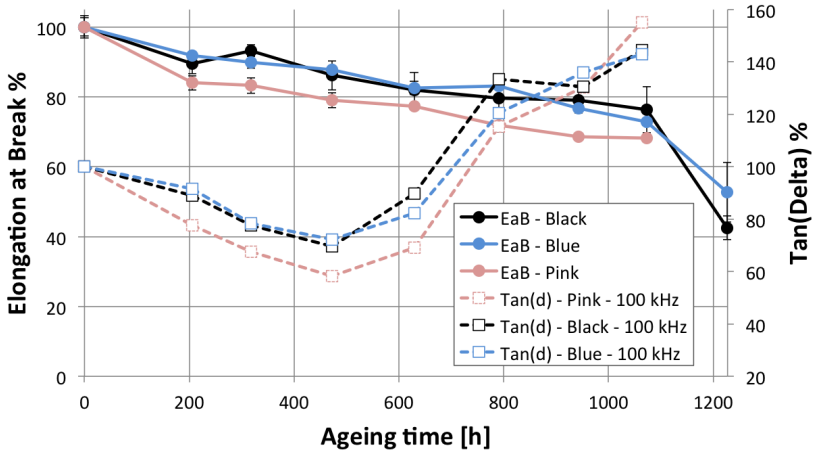

Figure 4.28: Comparison between elongation at break and $tan(\delta)$ at 100 kHz.

It is remarkable that the increases of the dielectric properties begins always much prior than the decrease of the elongation at break: capacitance or $tan(\delta)$ shows a marked increase after 600 hours, while EaB shows a marked decrease after 1100 hours. This has a very interesting benefit: dielectric properties are the first wake-up call, they're the leading indicator for the studied samples.

It is furthermore interesting to study which property has the largest variation with ageing. To do this, the difference between the relative (percentage) property of last (most aged) and the first (unaged) samples will be commented. Therefore table 4.3 shows these differences (with sign).

	Black series	**Blue series**	**Pink series**	**Average**
	Variation of EaB [%]			
	-57.52	-47.30		-52.41
Frequency [Hz]	**Variation of specific capacitance [%]**			
10^{-1}	+36.60	+35.80	+35.47	+35.96
10^{1}	+33.82	+33.13	+30.73	+32.56
10^{3}	+22.89	+22.33	+18.39	+21.20
10^{5}	+17.89	+17.03	+12.10	+15.69
Frequency [Hz]	**Variation of dissipation factor [%]**			
10^{-1}	-1.47	-5.1	+1.63	-1.65
10^{1}	+201.11	+184.54	+203.92	+196.52
10^{3}	+163.62	+193.68	+219.36	+192.22
10^{5}	+44.46	+43.00	+55.06	+47.51

Table 4.3: Variation of EaB %, specific capacitance % and tan(δ) %, previously defined, as ageing occurs. Each value is the difference between the value of the last (most aged) sample and the first (unaged) sample. A positive value means an increment, a negative value means a decrement. The values of the black, blue and pink series, as well as the average among those three, are displayed.

EaB decrease is 52.41 % on average. Capacitance shows a small increase: on average this is between 15.69 % (100 kHz) and 35.96 % (0.1 Hz); this value increases from high to low frequencies. Capacitance increases are smaller than EaB decreases.

Dissipation factor fluctuates at 0.1 Hz, showing an average decrease of 1.65 %; this property has large increases at 10 Hz and 1 kHz: on average 196.52 % and 192.22 % respectively. These increases are way higher than decreases of elongation at break. Dissipation factor at 100 kHz has a less marked increase: 47.51 % on average.

Summarizing, the variations of EaB are higher than the variations of capacitance, but smaller than variations of $tan(\delta)$.

The best diagnostic marker for this study seems to be $tan(\delta)$ measured at 1 kHz (fig. 4.18b and fig. 4.26), having a marked variation of 192.22 %, which becomes steeper after only 600 hours.

It is, eventually, interesting to analyse the correlation plots (crossplots) between EaB and the dielectric properties. For this purpose the following images 4.29 - 4.31 show as X axis the relative EaB and as Y axis relative capacitance or $tan(\delta)$, as previously defined. Each crossplot contains, for that property, all the four studied frequencies.

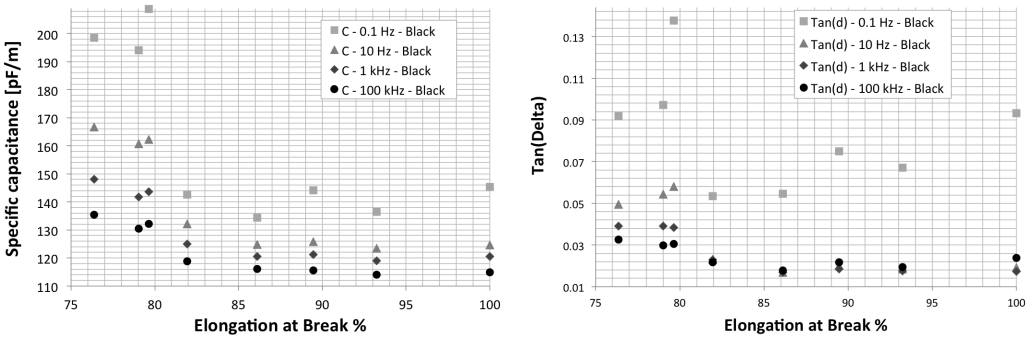

Figure 4.29: Crossplots of the black series between EaB % and specific capacitance (a) and between EaB % and $tan(\delta)$ (b).

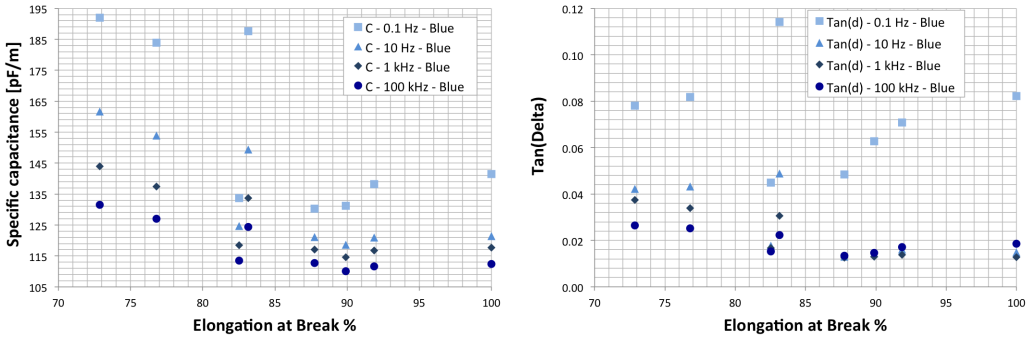

Figure 4.30: Crossplots of the blue series between EaB % and specific capacitance (a) and between EaB % and $tan(\delta)$ (b).

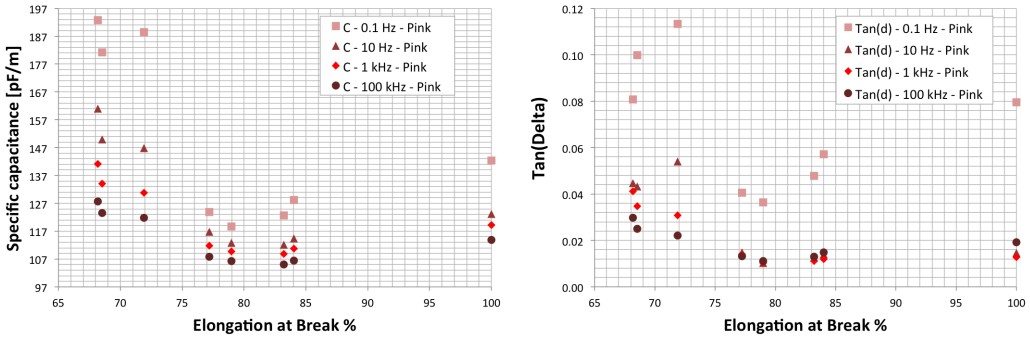

Figure 4.31: Crossplots of the pink series between EaB % and specific capacitance (a) and between EaB % and $tan(\delta)$ (b).

Observing the points representative of a certain single frequency, for most of the crossplots, the trend is clear: high values of specific capacitance (or $tan(\delta)$) correspond to low values of EaB %.

While considering the complete crossplots, capacitance and $tan(\delta)$ crossplots show more concentrated points in correspondence of low values of EaB.

Capacitance points, even if don't overlap, show similar trends; higher differences are found for the pink series. Consistently with what previously seen, furthermore, $tan(\delta)$ points at 10 Hz and 1 kHz almost overlap.

Conclusions

Concluding, the focal points of this thesis work are three: i) the theoretical background, showing how and why dielectric spectroscopy, among the other condition monitoring diagnostic techniques, can be used to effectively assess the ageing condition of electrical cables; ii) the application of this technique to the samples at issue: the study of the best connection *ad hoc* for the given samples; iii) the realisation of the measurements and the elaboration of the experimental data.

The aim of this work was to find a measurable property that could be effectively related to the ageing condition of the PVC/EPR samples, holding in high regard the non destructive aspect. This technique can reasonably be considered non destructive because about 3 millimetres of insulation and about 5 millimetres of jacket have to be cut off. The application/removal of the conductive sleeving leaves no damages on the sample surface. The cable after the measurement is not significantly damaged and can be, hypothetically, reinserted in its original position.

Furthermore this opens to a possible future development which is performing on-line and *in situ* measurements without the need of disconnecting the cable section. To make this possible, the specific configuration should be studied in detail, inquiring the capability, through a specific joint and with a specific instrument, of superimposing a measurement signal on the normal work signal of that cable. Some of the NPP cables are already shielded, some aren't. To perform this on unshielded cables one should consider, if possible, to apply an external sleeving; if this is not possible one should acknowledge

that the shielding is recommended for this technique, but not necessary: it is indeed possible to perform this measurements without a shielding sleeving, but measurements are expected to be largely imprecise.

Both specific capacitance and dissipation factor show a marked increase way before the elongation at break decrease: these dielectric properties are the leading indicators of ageing, for the studied samples. Specific capacitance shows a marked monotonic trend if measured at 10 Hz, 1 kHz and 100 kHz, although increases are limited. Dissipation factor shows large increases, greater than EaB decreases. Dissipation factor trends are not well defined at 0.1 Hz and 100 kHz, but this property shows a clear, monotonic trend when measured at 10 Hz and at 1 kHz.

On the basis of these considerations, $tan(\delta)$ at 1 kHz, with its marked and timely increase, can be accounted as the best diagnostic marker for the studied samples.

Although being the strong point of this method, performing measurements on intact samples, that show inevitable differences, has contributed to the confusion of some of the trends, which can be accounted as the biggest disadvantage of this technique.

Besides the effective capability of a correlation with the ageing in a non destructive way, it has to be pointed out an other advantage of this technique: its adaptability. The application of this methodology to other samples, bigger or smaller, shielded or unshielded, monopolar or multipolar with a different number of conductors, is immediate. The extension of this method to different cable samples can be made repeating the same considerations: modelling the electromagnetic behaviour of that cable, choosing the best connection, and building the connector most suitable to that sample. Metallic sleeving and ferrules are available in different sizes.

This Conclusions chapter summarizes the aspects of this study, which contributes to the subject of the Condition Monitoring diagnostics for low voltage cables for nuclear power plants, focusing on advantages and disadvantages, as well possible extension and future applications of this very flexible

methodology.

Bibliography

[1] L. Verardi, D. Fabiani, G.C. Montanari, U.W. Gedde, E.Linde, "Aging investigation of low-voltage cable insulation used in nuclear power plants", Electrical Insulation and Dielectric Phenomena (CEIDP), 2012 Annual Report Conference on Electrical Insulation and Dielectric Phenomena.

[2] Electrical Power Research Institute, "Aging management guideline for commercial nuclear power plants - electrical cable and terminations", 1996.

[3] International Atomic Energy Agency Technical Report, "Assessing and Managing Cable Ageing in Nuclear Power Plants", 2012.

[4] International Atomic Energy Agency Coordinated Research Project, "Condition monitoring and Management of Ageing of Low Voltage Cables in Nuclear Power Plants, 2016.

[5] United States Nuclear Regulatory Commission, Glossary, https://www.nrc.gov/reading-rm/basic-ref/glossary.htmlH.

[6] United States Nuclear Regulatory Commission, "Pressurized water reactor main steam line break (MSLB) benchmark", 1999.

[7] Electrical Power Research Institute Report, "Low Voltage Environmentally-Qualified Cable License Renewal Industry Report", 1994.

[8] L. Verardi, "Aging of Nuclear Power Plant Cables: in search of non-destructive diagnostic quantities", PhD Thesis, University of Bologna, 2012-2013.

[9] U.S. Nuclear Regulatory Commission, "Literature Review of Environmental Qualification of Safety-Related Electric Cables", 1996.

[10] C. Kröhnke, Polymer Science: A Comprehensive Reference. Elsevier, 2012, vol-8.14-Polymer Additives.

[11] U.S. Department of Energy, Office of Nuclear Energy, "Light Water Reactor Sustainability Program: Evaluation of Localized Cable Test Methods for Nuclear Power Plant Cable Agin Management Programs", 2016.

[12] Electrical Power Research Institute, "Integrated cable system aging management guidance - low voltage cables", 2003.

[13] International Atomic Energy Agiency, "Assessment and management of ageing of major nuclear power plants components important to safety: in-containment instrumentation and control cables", 2000.

[14] H. Kudo, A. Shimada, A. Idesaki, T. Ohshima, K. Tamura, T. Seguchi, "Degradation mechanisms of cable insulation materials during radiation-terhaml aging in radiation environment", in *Proceedings of the International Symposium on the Ageing Management and Maintenance of Nuclear Power Plants*, 2010, pp. 84-91.

[15] K.L. Simmons, L.S. Fifield, M.P. Westman, P. Ramuhalli, A.F. Pardini. J.R. Tedeschi, A.M. Jones, from Pacific Northwest National Laboratory, "Determining remaining useful life of aging cables in nuclear power plants", Interim Study FY13 for the U.S. Department of Energy, 2013.

[16] G.C. Montanari, D. Fabiani, P. Morshuis, L. Dissado, "Why residual life estimation and maintenance strategies for electrical insulation systems have to rely upon condition monitoring", on *IEEE Transactions*

on Dielectrics and Electrical Insulation, Vol. 23, No. 3, pp. 1375-1385, 2016.

[17] International Atomic Energy Agency, "Pilot study on the management of ageing of instrumentation and control cables", 1995.

[18] M. Villaran and R. Lofaro for the Office of Nuclear Regulatory Research of the Nuclear Regulatory Commission, "Condition monitoring of cables, task 3 report: condition monitoring techniques for electric cables", 2009.

[19] S Bernier, J. L. Parpal, E. David, D. Jean and D. Lalancette, "Dielectric response of laboratory aged PE cables", in *Conference Record of the 2008 IEEE International Symposium on Electrical Insulation*, 2008, pp. 83-86.

[20] C. Kröhnke, Polymer Science: A Comprehensive Reference. Elsevier, 2012, vol-2.32-Dielectric spectroscopy.

[21] A. K. Jonscher, "Dielectric relaxation in solids", in *Journal of Physics, D: applied physics* number 32, 1999, pp. R57-R70.

[22] J. Orrit-Prat, R. Mujal-Rosas, A. Rahhali, M. Marin-Genesca, X. Colom-Fajula, and J. Belana-Punseti,"Dielectric and mechanical characterization of PVC composites with ground tire rubber", in *Journal of composite materials* 45(11), 2010, pp. 1233-1243.

[23] M. Celina, K.T. Gillen, R.A. Assink, "Accelerated aging and lifetime prediction: Review of non-Arrhenius behaviour due to two competing precesses", in *Polymer Degradation and Stability*, vol. 90, pp. 395-404, 2005.

[24] Anixter Technical Information Handbook: Wire and Cable, 2013.

[25] Japan Nuclear Energy Safety Organization, Nuclear Energy System Safety Division, "The final report of the project of *Assessment of Cable Aging for Nuclear Power Plants*", 2009.